

AN ABSTRACT OF THE THESIS OF

Claude Steward Lindquist for the Ph.D. in Electrical Engineering
(Name) (Degree) (Major)

presented on Nov 21, 1968

Title: ANALYSIS AND SYNTHESIS OF ACTIVE TRANSMISSION LINES

Abstract approved: Redacted for Privacy
(Major Professor)

Active transmission lines, a generalization of classical transmission lines, are useful electrical devices. They can be utilized to realize distributed amplifiers and to obtain other electrical characteristics unattainable with passive lines. Active lines have historical significance and model many physical processes including heat conduction in an internally heated material, a vibrating string, pressure waves in gas, neutron diffusion and fission, and semiconductor photodetection. This paper fully develops the analysis and synthesis of active transmission lines using a network theory approach.

An active line is characterized by distributed series voltage and shunt current sources in addition to the passive line parameters. These sources may be of independent and/or dependent type.

It is shown that independent sources may be removed from the line if appropriate modifications in port conditions are made. Extraction integrals are formulated for this purpose. Examples of independent sources include initial condition generators; they also occur in devices exhibiting active coupling such as the traveling-wave transistor.

Dependent sources however change the two-port parameters of the

active line. These sources have their outputs controlled by either line voltage or current (a source at position x has an output which depends on either voltage or current at position x). Two basic types of lines are therefore possible.

The uniform active line having dependent distributed sources is completely analyzed. Its traveling-wave characteristics including characteristic impedances and propagation functions are presented. Laplace transformation techniques are used to analyze the driving-point and transfer admittances, gain, bandwidth, step response, rise and delay time, and sensitivity of uniform rcg active lines.

The general nature of the pole-zero patterns of nonuniform active lines having distributed dependent sources are investigated using several results from differential equation theory. Their two-port parameters are readily expressed using the basic set notation and self-adjoint properties of the active line equations. Lack of pole-zero cancellation is noted utilizing the Wronskian of the basic set solutions. Sturm-Liouville theory establishes the general pole-zero locations. Many of the powerful theorems concerning lumped passive networks are seen to parallel those of active lines.

Active transmission lines are readily synthesized directly in the time or frequency domain using variational calculus techniques. The parameter distributions required to produce specified port response for arbitrary excitations and loadings (consistent with parameter bounds, etc.) are generated by expressions involving voltage and current along the original line and a so-called adjoint line. The method is readily implemented by digital and hybrid computers.

At the present time, active transmission lines cannot be realized because of the inability to distribute dependent sources along a passive line. Therefore artificial active lines are presently utilized. The topology and two-port parameter requirements of the iterative two-port are discussed.

Future advances in solid-state electronics and thin-film technology should overcome this difficulty. Several current research studies involving semiconductor bulk effects and solid-state traveling-wave amplifiers are cited.

Although this thesis is concerned with the class of active distributed network having an active transmission line equivalent, the various considerations are readily extendable to networks having other differential models. More generally then, this investigation is concerned with developing methods for analyzing and synthesizing active distributed networks.

ANALYSIS AND SYNTHESIS OF ACTIVE TRANSMISSION LINES

by

CLAUDE STEWARD LINDQUIST

A THESIS

submitted to

OREGON STATE UNIVERSITY

in partial fulfillment of
the requirements for the
degree of

DOCTOR OF PHILOSOPHY

June, 1969

APPROVED:

Redacted for Privacy

~~Professor of Electrical Engineering~~
~~In Charge of Major~~

Redacted for Privacy

~~Head of Department of Electrical Engineering~~

Redacted for Privacy

~~Dean of Graduate School~~

Date thesis is presented November 21, 1968

Typed by Diana M. Lindquist

ACKNOWLEDGEMENT

This thesis arose from a study of semiconductor photodetection undertaken in the Network Theory Seminar directed by Professors J.H. Mulligan, Jr., S.S. Shamis, and M.S. Ghausi of New York University. Special thanks is given to Dr. Mulligan for his unique instruction and aid during two years of graduate study.

I am extremely grateful to Professors L.C. Jensen and P.C. Magnusson of Oregon State University. Professor Jensen has advised the author during two years of study. His careful review and constructive criticism has improved the thesis manuscript. Impromptu discussions with Dr. Magnusson have been of considerable value. The funds granted by the Research Council making computer use available are appreciated.

Warmest thanks are extended to my wife Diana for her continual enthusiasm and encouragement, and for her typing of the thesis.

TABLE OF CONTENTS

I.	Introduction	1
	Active Transmission Lines	1
	Iterated Networks and Distributed Amplifiers	3
	Active Transmission Line Analogs	8
	Heat Conduction with Internal Heating	9
	Small Transverse Vibrations of a Horizontal String	11
	Small Longitudinal Pressure Waves in Gas	12
	Neutron Diffusion and Fission	13
	Photodetection Process	14
	Summary	18
II.	Transmission Lines Having Independent Distributed Sources	20
	Independent Distributed Sources	20
	Two-Port Theory of Linear Networks	22
	Extraction Integrals for Active Transmission Lines	25
	Applications of the Extraction Integral	30
III.	Uniform Transmission Lines Having Dependent Distributed Sources	35
	Dependent Distributed Sources	35
	Active Transmission Line Equations	37
	Traveling-Wave Analysis	38
	Characteristic Impedance	41
	Propagation Constant	43
	Laplace Transform Analysis and Two-Port Parameters	45
	Driving-Point Admittance—Type 1-3 RCG Active Lines	48
	Transfer Admittance, Gain, and Bandwidth— Type 1-3 RCG Active Lines	51
	Step Response, Stability, Rise and Delay Time— Type 1-3 Active Lines	54
	Sensitivity—Type 1-3 RCG Active Lines	61
	Driving-Point Admittance—Type 2-4 RCG Active Lines	64
	Transfer Admittance, Gain, and Bandwidth— Type 2-4 RCG Active Lines	71
	Step Response, Stability, Rise and Delay Time— Type 2-4 RCG Active Lines	75

	Sensitivity—Type 2-4 RCG Active Lines	77
	Mixed-Type Lines	77
IV.	Nonuniform Transmission Lines Having Dependent Distributed Sources	79
	Two-Port Parameters	79
	The Basic Set	82
	The Wronskian and Self-Adjoint Systems	88
	Sturm-Liouville Theory	92
	Driving-Point Admittance—Type 1-3 Active Lines	96
	Transfer Admittance and Gain—Type 1-3 Active Lines	103
	Driving-Point Admittance—Type 2-4 Active Lines	106
	Transfer Admittance and Gain—Type 2-4 Active Lines	108
	Active Transmission Line Analysis—Concluding Remarks	109
V.	Synthesis of Active Transmission Lines	111
	Synthesis Using Variational Calculus	111
	Time Domain Synthesis—Type 1-3 Active Lines	112
	Frequency Domain Synthesis—Type 1-3 Active Lines	124
	Time Domain Synthesis—Type 2-4 Active Lines	128
	Frequency Domain Synthesis—Type 2-4 Active Lines	133
	Variational Synthesis in Retrospect	135
VI.	Realizations of Active Transmission Lines	138
	Summary	138
	Artificial Type 1-3 Active Lines	139
	Artificial Type 2-4 Active Lines	143
	Conclusion	147
	Bibliography	149

LIST OF FIGURES

<u>Figure</u>	<u>Page</u>
1 Approximation of an active line of length Δx	2
2 Differential section of an active transmission line	2
3 Π representation of any linear two-port	3
4 Cascaded Π networks	3
5 Analogous L section of the iterated structure	4
6 The artificial active line resulting from a particular choice of y_{12} and Y	4
7 Artificial distributed amplifier	5
8 Equivalent circuit of the artificial distributed amplifier	6
9 The traveling-wave transistor.	7
10 The differential model of the traveling-wave transistor	7
11 Heat conduction analog including initial condition impulse generator	10
12 Vertically vibrating horizontal string analog	12
13 Small longitudinal pressure waves in gas analog	12
14 Neutron diffusion and fission analog	13
15 Semiconductor photodetection analog	18
16 Actively and passively coupled transmission line	21
17 Coupled line equivalent circuit using distributed dependent sources	21
18 Various characterizations of two-ports containing independent sources	23
19 Voltage contributions $\Delta V_{1z}(x)$ and $\Delta V_{2z}(x)$ due to independent sources $E(x)\Delta x$ and $J(x)\Delta x$ acting alone at x	28
20 Type 1-3 active line differential section	36
21 Equivalent differential section of a type 1-3 active line	36

22	Type 2-4 active line differential section	36
23	Domain of propagation constant values when $r^*, g^* > 0$. . .	44
24	Domain of propagation constant values when $r^*, g^* < 0$. . .	44
25	Domain of propagation constant values when $r^* < 0, g^* > 0$ or $g^* < 0, r^* > 0$	44
26	Domain of propagation constant values	45
27	Port conventions of an active line	46
28	Normalized pole-zero pattern of y_{11} and y_{22}	49
29	Bode plots of driving-point admittance y_{11} and y_{22}	50
30	Normalized pole-zero pattern of gain T	52
31	Bode plots of gain T	53
32	Normalized root locus for poles of T_v as Y_L varies from 0 to ∞	53
33	Normalized pole-zero pattern of S_K^T	62
34	Normalized pole-zero pattern of S_L^T	62
35	Bode magnitude plot of sensitivity S_K^T	62
36	Bode magnitude plot of sensitivity S_L^T	63
37	Graphical construction yielding the imaginary zeros of eq. 3.119 (excluding the first pair for $k < -1$)	66
38	Graphical construction yielding the real zero pair of eq. 3.119 for $k \leq -1$	66
39	Root locus for $N(f)$ as k varies from $-\infty$ to $+\infty$	67
40	Normalized root locus of zeros of y_{11} as $(L-K)$ varies from $-\infty$ to $+\infty$ (or y_{22} reversing the arrow direction). . .	69
41	Conditions under which the zeros and poles of y_{11} are determined	94
42	The root locus of eq. 4.58 as λ varies from 0 to ∞	99
43	Conditions under which the zeros and poles of y_{12} are determined	104

44	General active line embedded between voltage sources and loads	112
45	Time domain variational synthesis requires time domain solution of the original active line and the adjoint line shown. Their constraints are labelled on the (x,t)-plane .	118
46	Flow chart of time domain calculations to determine optimum parameter distributions for type 1-3 active lines .	123
47	Frequency domain synthesis requires frequency domain solution of the original active line and the adjoint line shown. Their constraints are labelled on the (x,w)-plane .	127
48	Time domain synthesis requires time domain solution of the original line and the adjoint line shown. Their constraints are labelled on the (x,t)-plane	132
49	Frequency domain synthesis requires frequency domain solution of the original active line and the adjoint line shown. Their constraints are labelled on the (x,w)-plane .	136
50	Lumped approximation of the type 1-3 active line of length D	139
51	First realization of the artificial type 1-3 active line .	140
52	Second realization of the artificial type 1-3 active line .	140
53	Two-port equivalent of the first realization	141
54	Two-port equivalent of the second realization	142
55	Lumped approximation of the type 2-4 active line of length D	143
56	First realization of the artificial type 2-4 active line .	144
57	Second realization of the artificial type 2-4 active line .	144
58	Two-port equivalent of the first realization	145
59	Two-port equivalent of the second realization	146

LIST OF TABLES

<u>Table</u>		<u>Page</u>
1	Relationships between the various pairs of independent sources in Fig. 18	26
2	Extraction integrals for an active transmission line	29
3	Extraction integrals for a uniform active transmission line	31
4	Two-port parameters for the type 1-3 active transmission line expressed in terms of the basic set voltage solution at $x=d$	84
5	Two-port parameters for the type 2-4 active transmission line expressed in terms of the basic set voltage solution at $x=d$	85

LIST OF SYMBOLS

Symbol

A,B,C,D	chain parameters
a,b,c,d	inverse chain parameters
a	local series time constant of transmission line ($a=1/r$)
b	local shunt time constant of transmission line ($b=c/g$)
C^n	function is n times continuously differentiable
c	shunt capacitance/unit length (f/m)
D	approximation network length (m)
D^s	open domain $D^s = \{(x,s): 0 < x < d, s < \infty\}$
D^t	open domain $D^t = \{(x,t): 0 < x < d, t \geq 0\}$
D^w	open domain $D^w = \{(x,w): 0 < x < d, w < \infty\}$
$\underline{D}^s, \underline{D}^t, \underline{D}^w$	corresponding closed domains, e.g. $\underline{D}^s = \{(x,s): 0 \leq x \leq d, s < \infty\}$
d	active transmission line length (m)
E	Laplace transformed distributed series voltage/unit length (volt-sec/m); error integral
E*	augmented error integral
e	distributed series voltage/unit length (volt/m)
F	arbitrary Laplace transformed function ($F=F(x,s)$)

f arbitrary complex function ($f=u+jv$); Hertzian frequency (Hertz)
 g shunt conductance/unit length (mhos/m)
 g^* effective shunt conductance/unit length of type 1-3 active line (mhos/m) ($g^*=g+L$)
 g_m transconductance/unit length (amps/volt)
 $g_{11}, g_{12}, g_{21}, g_{22}$ inverse hybrid parameters
 $h_{11}, h_{12}, h_{21}, h_{22}$ hybrid parameters
 I Laplace transformed current (amp-sec)
 i current (amps)
 i_1, i_2 independent basic set current solutions
 J Laplace transformed distributed shunt current/unit length (amp-sec/m)
 j distributed shunt current/unit length (amps/m); imaginary unit ($j=\sqrt{-1}$)
 K distributed series voltage source strength (volts/volt or volts/amp)
 L distributed shunt current source strength (amps/amp or amps/volt)
 l series inductance/unit length (h/m)
 m_p excess phase function associated with effective dominant pole p_e
 m_z excess phase function associated with effective dominant zero z_e
 \underline{P} parameter column matrix
 p coefficient in Sturm equation
 p_e effective dominant pole
 Q partial differential operator of Sturm equation
 q coefficient in Sturm equation
 R_1, R_2 load resistances
 r series resistance/unit length (ohms/m); coefficient in Sturm equation
 r^* effective series resistance/unit length of type 1-3 active line (ohms/m) ($r^*=r+K$)
 S_x^y sensitivity of y with respect to x
 s complex frequency (1/sec) ($s=\sigma + j\omega$)

s_N normalized complex frequency (1/sec) ($s_N = \sigma_N + j\omega_N$)
 s_p, s_z complex frequency pole and zero, respectively
 T gain function; transpose
 T_V, T_I voltage and current gain functions, respectively
 t time (sec)
 t_d delay time (sec)
 t_r rise time (sec)
 u real part of arbitrary function f
 V Laplace transformed voltage (volt-sec)
 v voltage (volts); imaginary part of arbitrary function f
 v_a, v_b arbitrary independent voltage solutions
 v_1, v_2 independent basic set voltage solutions
 W Wronskian
 W_1, W_2 weighting functions
 x position along line (m)
 Y shunt admittance/unit length of transmission line (mhos/m) ($Y = g + sc$)
 Y^* effective shunt admittance/unit length of type 1-3 active line (mhos/m) ($Y^* = g^* + sc$)
 Y' modified shunt admittance/unit length of transmission line (mhos/m)
 $Y_{11}, Y_{12}, Y_{21}, Y_{22}$ admittance parameters
 Z series impedance/unit length of transmission line (ohms/m) ($Z = r + sl$)
 Z^* effective series impedance/unit length of type 1-3 active line (ohms/m) ($Z^* = r^* + sl$)
 Z' modified series impedance/unit length of transmission line (ohms/m)
 Z_0 characteristic impedance of transmission line (ohms) ($Z_0 = \sqrt{Z/Y}$)
 Z_1, Z_2 load impedances
 $Z_{11}, Z_{12}, Z_{21}, Z_{22}$ impedance parameters
 z_e effective dominant zero

α attenuation function of transmission line (nepers/m)
 α_1, α_2 attenuation function of type 2-4 active line (nepers/m)
 β phase function of transmission line (radians/m)
 β^P, β^Z imaginary part of complex frequency of pole and zero, respectively
 β_1, β_2 phase function of type 2-4 active line (radians/m)
 δE first variation of error integral
 δy_i first variation of the i^{th} arbitrary function y_i
 $\delta^2 E$ second variation of error integral
 $\Gamma_\alpha, \Gamma_\beta$ complex functions of type 2-4 active line
 γ complex propagation function of transmission line
 (1/m) ($\gamma = \sqrt{ZY}$)
 λ eigenvalue of Sturm equation
 $\lambda^r, \lambda^g, \lambda^l, \lambda^c, \lambda^K, \lambda^L$ Lagrange multipliers of time and frequency invariance constraints on r, g, l, c, K, and L, respectively
 λ_n n^{th} eigenvalue of Sturm equation
 λ_n^P, λ_n^Z n^{th} eigenvalue corresponding to a pole and zero, respectively
 φ, θ Lagrange multipliers of active transmission line equations
 σ real part of complex frequency s (1/sec)
 σ_N normalized real part of complex frequency s
 ω imaginary part of complex frequency s (radians/sec)
 (radian frequency)
 ω_N normalized imaginary part of complex frequency s

ANALYSIS AND SYNTHESIS OF ACTIVE TRANSMISSION LINES

I. INTRODUCTION

Active Transmission Lines

The active transmission line is a generalization of the classical transmission line. By introducing distributed voltage and current sources along a transmission line, the line may be made active and capable of delivering energy from its ports. Active lines can be utilized to realize distributed amplifiers and to obtain other electrical characteristics unattainable with passive lines.

The active transmission line is characterized by the parameters:

r , the series resistance/unit length (ohms/m),

l , the series inductance/unit length (henries/m),

e , the distributed series voltage/unit length (volts/m),

g , the shunt conductance/unit length (mhos/m),

c , the shunt capacitance/unit length (farads/m),

j , the distributed shunt current/unit length (amperes/m).

Parameters r , l , c , and g are time-invariant and may be functions of distance. The distributed voltage and current sources are independent or dependent sources, or a combination of both which have time and spacial dependences. This is explicitly denoted by writing $e = e(x,t)$ and $j = j(x,t)$.

Kirchhoff's equations relate port voltage and current of the active line element of length Δx in Fig. 1 as

$$v(x+\frac{1}{2}\Delta x,t) = v(x-\frac{1}{2}\Delta x,t) - e(x,t)\Delta x - r(x)\Delta x i(x,t) - l(x)\Delta x \frac{\partial i(x,t)}{\partial t} \quad (1.1)$$

$$i(x+\frac{1}{2}\Delta x,t) = i(x-\frac{1}{2}\Delta x,t) - j(x,t)\Delta x - g(x)\Delta x v(x,t) - c(x)\Delta x \frac{\partial v(x,t)}{\partial t} \quad (1.2)$$

for $\Delta x \rightarrow 0$ where v and i are assumed continuously differentiable in x and t . This implies that r and g are nonzero, l and c are continuous, and r , g , e , and j are continuously differentiable in x and t along the line. Dividing each side of eqs. 1.1 and 1.2 by Δx and letting $\Delta x \rightarrow 0$, the active transmission line equations become

$$-\frac{\partial v(x,t)}{\partial t} = e(x,t) + r(x)i(x,t) + l(x) \frac{\partial i(x,t)}{\partial t} \quad (1.3)$$

$$-\frac{\partial i(x,t)}{\partial x} = j(x,t) + g(x)v(x,t) + c(x) \frac{\partial v(x,t)}{\partial t} \quad (1.4)$$

where the differential section is shown in Fig. 2. Active transmission lines have historical significance and current importance as shall be seen in the discussion that follows.

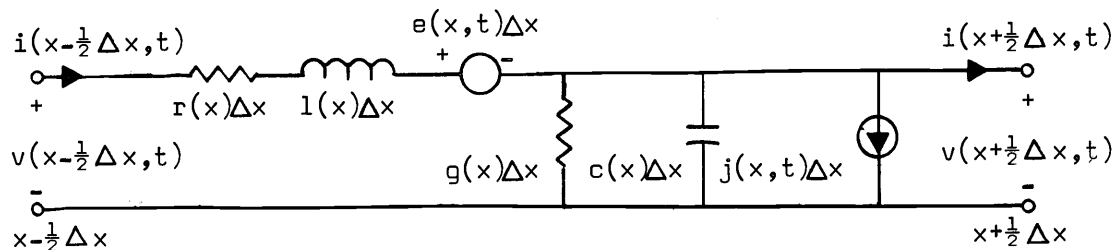


Fig. 1. Approximation of an active transmission line of length Δx .

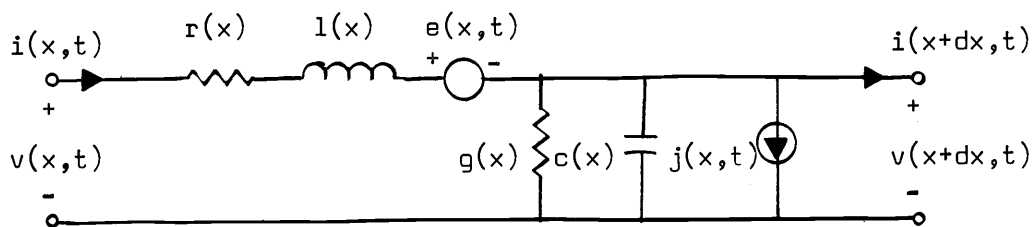


Fig. 2. Differential section of an active transmission line.

Iterated Networks and Distributed Amplifiers

Any linear active or passive two-port defined by an admittance matrix may be represented as the Π network shown in Fig. 3. An iterated structure composed of such cascaded Π 's is shown in Fig. 4 where for brevity we let $Y = y_{11} + y_{22} + 2y_{12}$ and $g_m = y_{21} - y_{12}$. The structure may alternatively be viewed as composed of L sections shown in Fig. 5 (with impedance $y_{11} + y_{12}$ at the input port). For systems which are adequately described with $-y_{12}$ as a series resistance and inductance, and Y a shunt conductance and capacitance as shown in Fig. 6, the structure becomes artificial or lumped "equivalent" of a section of active transmission line. Nonuniform structures have $-y_{12n}$, g_{mn} , and Y_n dependent upon ladder location n . This corresponds to spatially dependent $-y_{12}(x)$, $g_m(x)$, and $Y(x)$ along the active line.

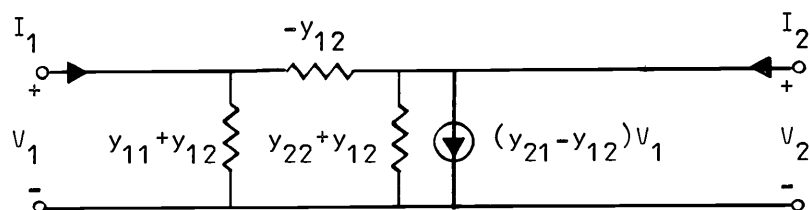


Fig. 3. Π representation of any linear two-port.

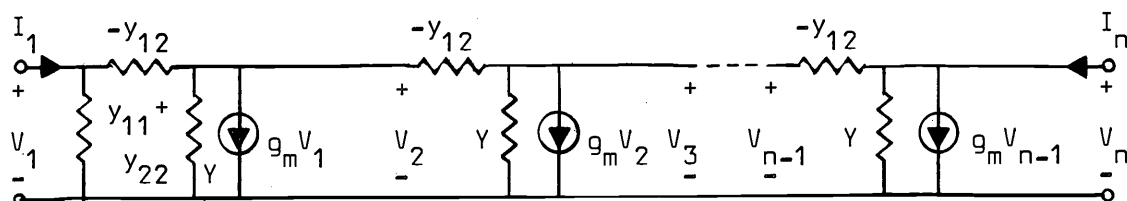


Fig. 4. Cascaded Π networks.

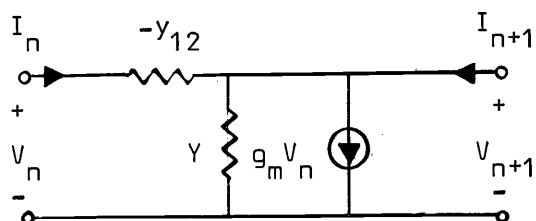


Fig. 5. Analogous L section of the iterated structure.

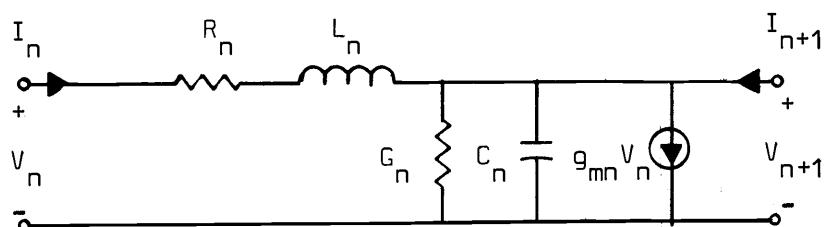


Fig. 6. The artificial active line resulting from a particular choice of y_{12} and Y .

The loss-pass electrical behavior of an n -section artificial line approximates that of an active line d units in length. Since active distributed networks were not available in the past, iterated structures were fully exploited. To achieve an overall voltage gain exceeding unity in such cascaded systems having identical stages, each section must have a gain greater than unity. For a given active network and interstage, there is a fixed upper frequency limit f_0 where the gain becomes less than one.

Historically, many factors made large cascaded amplifier systems impractical. With a large number of sections, unavoidable introduction of parasitic inductance and capacitance deteriorated system performance at high frequencies. Insufficient redundancy and high failure rates of electronic tubes made proper operation largely dependent upon optimum performance of each stage (18). In an effort to overcome these basic limitations and obtain amplifiers which would

operate at frequencies greater than f_o , additive amplifiers were conceived. In these systems, outputs from each stage are added rather than multiplied. By paralleling more stages, greater than unity gain is possible at frequencies above f_o .

An artificial distributed amplifier is an additive amplifier system.¹ It has the form shown in Fig. 7 with its equivalent circuit in Fig. 8. The pentodes actively couple the input line to the output line via transconductance g_m (amperes/volt). Grid and plate capacitances are absorbed in the artificial lines. Design requirements include equal phase velocities in input and output lines and matched terminating impedances to prevent reflections. Such systems are cascaded by connecting the properly matched output line to the input line of the next stage thereby increasing the overall gain. Improved frequency response is derived by introducing mutual coupling between adjacent inductors on both lines.

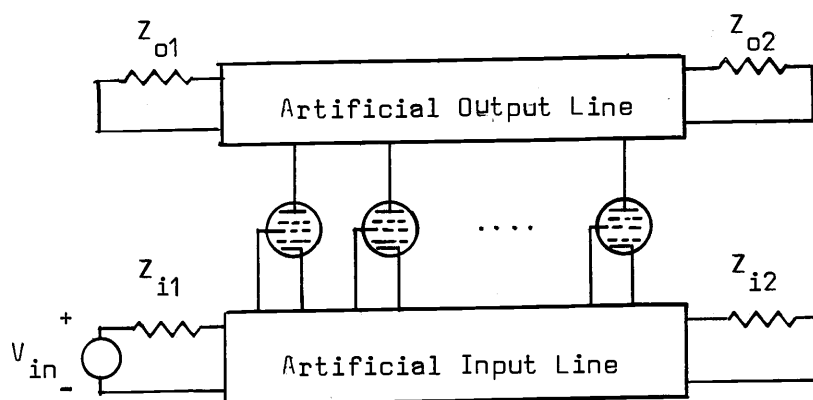


Fig. 7. Artificial distributed amplifier.

¹W.S. Percival holds a British patent dated July 24, 1936 for (artificial) distributed amplifiers using pentodes.

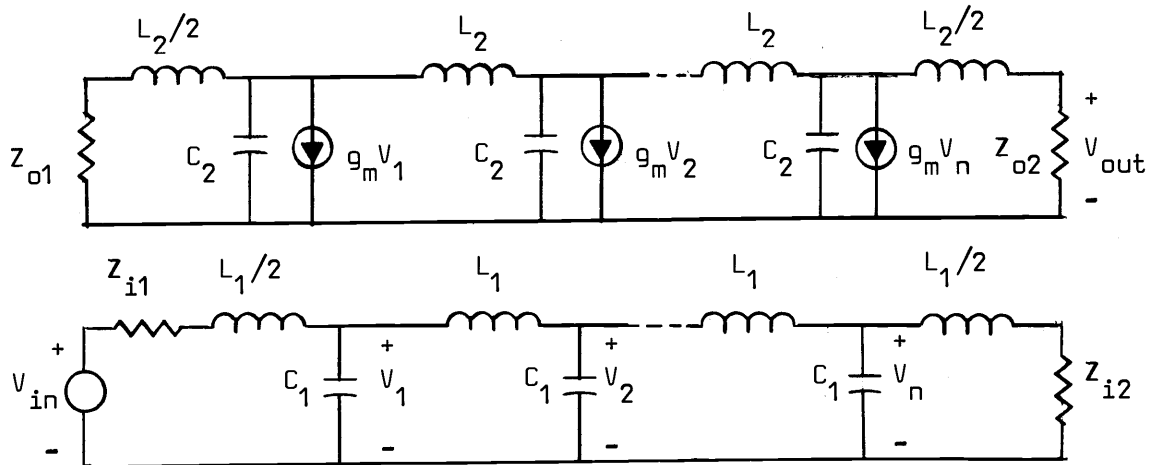


Fig. 8. Equivalent circuit of the artificial distributed amplifier.

Transistor artificial distributed amplifiers have also been investigated (25), but with less successful results due to the differing characteristics between pentodes and transistors. These include significant base-collector capacitive coupling and low input and output impedances. FET or MOS transistors may be employed to advantage because of small gate-drain capacitive coupling and high input and output impedances.²

In an effort to realize true distributed amplifiers and thereby realize higher frequency amplifiers, McIver has proposed the traveling-wave transistor (22), shown in Fig. 9 with its equivalent circuit in Fig. 10. Essentially an insulated-gate FET, strip-type transmission lines deposited on uniformly doped semiconductors form the gate and drain channels. Again phase velocities and terminating impedances are matched. g_m is to be maximized and the device length made long enough to achieve usable gain. Others have considered the effect of capaci-

²E.g. see P.G. Jessel and J.S. Thorp. An amplifier design using MOS transistors. Proceedings of the IEEE 54(11):1581-1582. 1966.

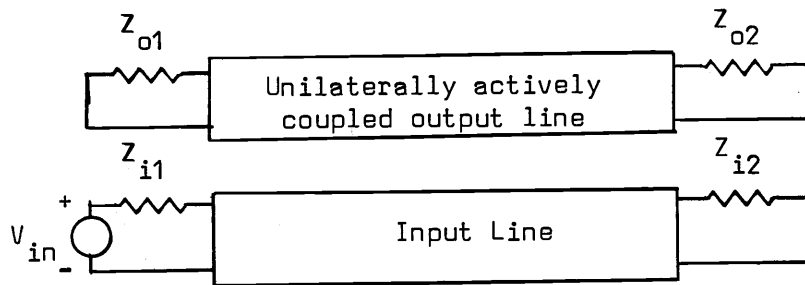


Fig. 9. The traveling-wave transistor.

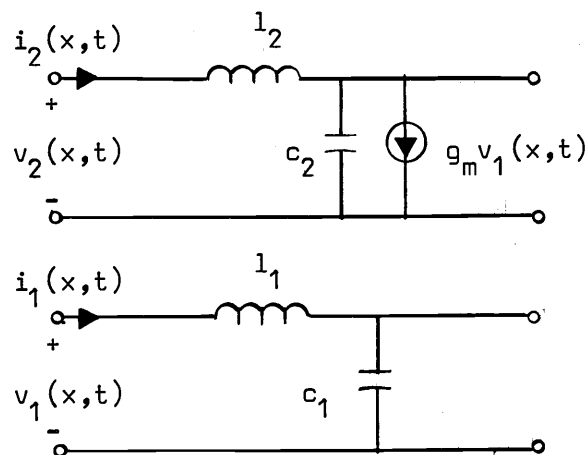


Fig. 10. The differential model of the traveling-wave transistor.

tive coupling between lines on gain (12, 17).

The requirement of equal phase velocities and presence of capacitive coupling may be eliminated if single line distributed amplifiers could be realized, where for example in the active line of Fig. 2, $e(x,t)$ and $j(x,t)$ are dependent sources controlled by either $v(x,t)$ or $i(x,t)$. This thesis is concerned with the general analysis and synthesis of such networks. The results may be extended directly for networks having differential models other than Fig. 2.

Much current attention is being directed toward realizing single line distributed amplifiers. We should note, however, that many of the

problems encountered with cascaded amplifiers may today be circumvented due to the advent of integrated-circuit technology. Iterative structures having sufficient redundancy to insure their two-port characteristics (10) may be fabricated with great precision. Currently power capabilities appear to be the major limitation of integrated circuits. Due to their microscopic size, when particular networks are iterated to form systems, their approximation by a distributed network may lead to more ready analysis and synthesis results than by using, for example, chain matrix products.

Active Transmission Line Analogs

Active transmission lines can be used to model many physical processes and thus form an important analog to process studies and simulation. In the illustrative examples that follow, pertinent equations describing the process are expressed in active transmission line equation form. By associating appropriate quantities with the active line parameters, two differential analogs may be formed. These analogs are duals and one is readily drawn from the other. Therefore, only one is drawn, the choice being determined by the "driving functions" of the process and familiarity with a given differential section type. To indicate how initial and boundary conditions are incorporated into the model, the heat conduction problem is analyzed in more detail to serve as an example. By applying the results of this thesis to processes not modeled by active lines, similar conclusions concerning their nature may be made.

Heat Conduction with Internal Heating (29)

One-dimensional heat conduction in a homogeneous material, internally heated, for example, by radioactive decay or absorption or by thermochemical reactions, has a uniform rc or lg transmission line analog. Nonhomogeneous materials have nonuniform analogs.

Consider heat conduction along an insulated internally-heated rod. The diffusion and continuity equations relate heat flow density q (cal/sec-m²) and temperature T (°C) as

$$-q = k \frac{\partial T}{\partial x} \quad (1.5)$$

$$-\frac{\partial T}{\partial t} = \frac{1}{\rho c} \left(\frac{\partial q}{\partial x} + j \right) \quad (1.6)$$

where k is the thermal conductivity (cal/sec-m²-C°), ρ the density (kg/m³), c the specific heat (cal/kg-C°), and j represents the heating due to the internal heat generators (cal/sec-m³). Comparing eqs. 1.5 and 1.6 with the active transmission line equations (eqs. 1.3 and 1.4), they are made identical by setting $v=T$, $i=q$, $r=1/k$, and $c=\rho c$. This results in an rc active line analog. An lg active line could equally well be used. Depending on the process involved, j may be an independent or dependent source. In some cases of interest $j(x,t) = a(x)T(x,t)$. Here then, j is a distributed source whose output at point x is dependent upon the temperature at point x for all time.

The boundary conditions fix the port terminations. For example, if a material L units long has temperatures $T(0,t) = T_1$ and $T(L,t) = T_2$ maintained at the ends, then voltage sources of T_1 and T_2 volts are placed at the respective ports of the equivalent line. If on the other hand the material is insulated at $x = L$, there is no heat

conduction through the output port and the line is open-circuited at that end. Heat may also be transferred by convection or radiation of energy. It is found that for practical calculations, the heat flow density is proportional to the difference in temperatures between the convective or radiative mediums or

$$q = h(T_a - T_b) \quad (1.7)$$

where h is the convective or radiative coefficient ($\text{cal}/\text{sec}\cdot\text{m}^2\cdot\text{C}^\circ$) and T_a and T_b the "driving" temperatures of the process (23, 24). Thus, terminating resistors of $1/h_1$ and $1/h_2$ ohms form the convective or radiative heat analog; they relate the port current densities q_1 and q_2 to the voltage differences $T_1 - T(0,t)$ and $T_2 - T(L,t)$ across their terminals.

For nonzero initial temperature distribution throughout the material, initial condition impulse generators must be introduced. Thus when the initial temperature $T(x,0)$ is specified, the source distribution required to establish this initial condition is known. The differential section of the heat conduction analog including the initial condition generator is shown in Fig. 11.

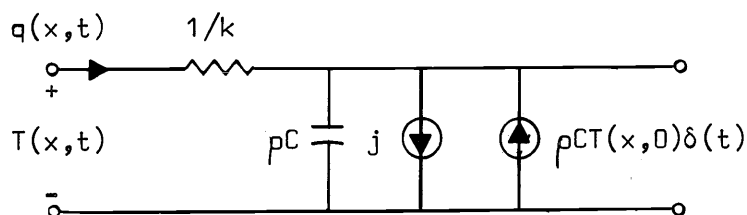


Fig. 11. Heat conduction analog including initial condition impulse generator.

Small Transverse Vibrations of a Horizontal String (24, 29)

Consider a horizontal, possibly nonuniform string under uniform tension T experiencing small vertical vibrations. When the string's stiffness is neglected (i.e. assuming perfect elasticity), the equations relating transverse momentum P (n-sec) and small transverse displacements y (m) are related by Newton's force equation and the momentum equation as

$$- T \frac{\partial y}{\partial x} = \frac{\partial P}{\partial t} \quad (1.8)$$

$$- \frac{\partial P}{\partial x} = \rho \frac{\partial y}{\partial t} + By + \rho g t - p_e \quad (1.9)$$

where ρ is the mass/unit length of the string (kg/m), B the viscous friction of medium surrounding string (n-sec/m²), g the gravitational constant, and p_e the upward distributed momentum along the string (n-sec/m) where the external force density applied along the string is $f_e = \partial p_e / \partial t$. The right hand terms of eq. 1.9 account for inertial, damping, gravitational, and external force effects. If in addition the spring is placed in an elastic medium, the term $K \int_0^d y dt$ is added to the right side. The differential analog model is shown in Fig. 12. Here $\rho g t$ and p_e represent independent distributed sources while $K \int_0^d y dt$ is a dependent distributed source.

Longitudinal vibrations in an elastic bar and (one-dimensional) transverse vibrations of a thin membrane are described by equations somewhat similar to eqs. 1.8 and 1.9. However transverse bar vibrations are described by higher order equations and cannot be identified as active transmission lines.

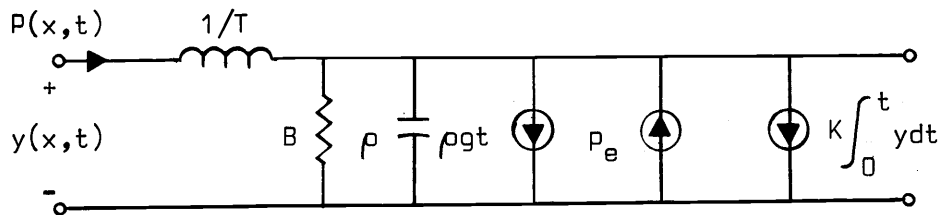


Fig. 12. Vertically vibrating horizontal string analog.

Small Longitudinal Pressure Waves in Gas (32)

One-dimensional propagation of sound waves in gas neglecting viscosity effects exemplify many fluid and gas flow problems. Newton's force equation and the continuity equation relates the pressure P (n/m^2) and the longitudinal displacement velocity of the medium v (m/sec) as

$$- A \frac{\partial P}{\partial x} = \rho_0 \frac{\partial v}{\partial t} - \rho_0 F_e \tag{1.10}$$

$$- \frac{\partial P}{\partial t} = B_0 \frac{\partial v}{\partial x} \tag{1.11}$$

where ρ_0 is the equilibrium mass density (kg/m), B the bulk modulus of the medium where $B_0 = \rho_0 \left(\frac{\partial P}{\partial \rho_0} \right)$ (n/m^2), A the channel area (m^2), and F_e the body force/unit mass due to external forces (n/kg). The differential section of the analog is shown in Fig. 13.

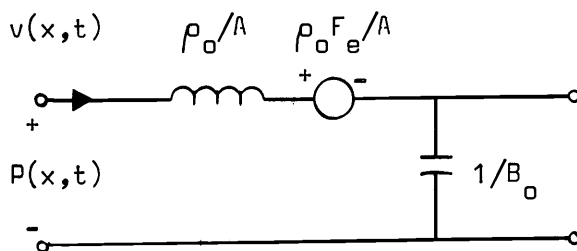


Fig. 13: Small longitudinal pressure waves in gas analog.

Neutron Diffusion and Fission (24)

One-dimensional nuclear reaction problems involving absorption and generation by fission of neutrons have active transmission line analogs.

The diffusion and continuity equations for neutrons capable of producing fission (having speeds less than some critical velocity v_c) relate neutron current density j (neutrons/m²-sec) and neutron n (neutrons/m³) as

$$- j = D \frac{\partial n}{\partial x} \quad (1.12)$$

$$- \frac{\partial n}{\partial t} = \frac{\partial j}{\partial x} + Xn - Rn - q \quad (1.13)$$

where D is the neutron diffusion constant (m²/sec), X the absorption constant (sec⁻¹), R the reproduction factor (sec⁻¹), and q the applied neutron current density arising from sources other than fission. The differential section of the analog is shown in Fig. 14. q is an independent distributed source while Rn is a dependent distributed source.

Sometimes analysis must include the fact that the new neutrons arising from the fission process are not emitted immediately but in a delayed manner where T_d is the mean delay emission time. The reproduction term $Rn(x,t)$ is here replaced by $Rn(x,t-T_d)$.

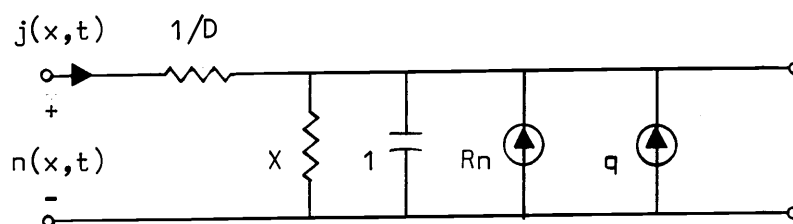


Fig. 14. Neutron diffusion and fission analog.

Photodetection Process

Semiconductor detection of optical frequency (or less) signals make use of the photoelectric effect and may be readily characterized by active transmission lines. Ettenberg and Nadan have found analogous but simplified results when analyzing gain in solid-state traveling-wave amplifiers (8). Kawamura and Morishita have presented more involved analysis (14). Problems in physical chemistry involving diffusion of solutes undergoing ionization and deionization in a solvent have similar analogs.

According to quantum theory, an apparently continuous electromagnetic wave of frequency f is quantized and consists of discrete quanta or photons which have energy $E = hf$ joules/photon where h is Planck's constant. When a photon is absorbed by an atom in a material, its entire energy is transferred to an electron. This electron may be free and so experiences an increased velocity, or more likely the electron may be excited from the valence band into the conduction band (assuming the photon has sufficient energy to do so). Generally then additional hole-electron current carriers are created, the spectral distribution of which is determined by the absorption spectrum of the material (31).

To determine the carrier generation rates, consider a uniform semiconductor rod of length L with coherent radiation of frequency f directed longitudinally upon its end. If I_0 is the radiation intensity (photons/sec-cm²) just beneath the surface, the intensity at depth x is

$$I(x) = I_0 \exp(-kx) \quad (1.14)$$

where $k = k(f)$ is the absorption constant of the material. Since, in the photoelectric effect, a photon is annihilated and a hole-electron pair created, the generation rate of holes and electrons is

$$G(x) = -n(\text{div } I(x)) = nkI_0 \exp(-kx) \quad (1.15)$$

where $n = n(f)$ is the spectral efficiency of absorption of photons of energy hf .

These carriers give rise to photodiffusion, photoconductive, and photoelectromagnetic effects for no applied fields, applied electric fields, and applied magnetic fields, respectively. To describe photodiffusion and photoconduction, the continuity equation, the momentum equation, and Poisson's equation are used (1). These equations together with their associated initial and boundary conditions form the basis for photodetection analysis in semiconducting slabs, diodes, and transistors.

The continuity equation, in rearranged form, relates the change in current density to rate of carrier increase, recombination rate, and generation rates as

$$-\frac{\partial J_p}{\partial x} = \frac{p}{t_p} + \frac{\partial p}{\partial t} - (G_p + p_0/t_p) \quad (1.16)$$

$$-\frac{\partial J_n}{\partial x} = \frac{n}{t_n} + \frac{\partial n}{\partial t} - (G_n + n_0/t_n) \quad (1.17)$$

where

p = instantaneous hole density (holes/cm³) (or free hole concentration)

p_0 = equilibrium hole density (holes/cm³) (or free hole concentration)

J_p = hole current density (holes/sec-cm²)

t_p = hole lifetime (sec)

G_p = hole generation rate (holes/sec-cm³)

and the corresponding electron definitions.

The momentum equation relating inertial effects and effects of collision damping (viscous friction) to distributed forces arising from the electric field and diffusion pressure (or density gradient) is

$$\frac{\partial}{\partial t}(m_p J_p) + v_p m_p J_p = q p E - q \frac{D_p}{\mu_p} \frac{\partial p}{\partial x} \quad (1.18)$$

$$\frac{\partial}{\partial t}(m_n J_n) + v_n m_n J_n = q n E + q \frac{D_n}{\mu_n} \frac{\partial n}{\partial x} \quad (1.19)$$

where

q = charge of electron (coulomb)

m_p = mass of hole (gm/hole)

v_p = collision frequency of hole (1/sec) (i.e. reciprocal mean free time $1/t_p$ between collisions of a hole with the lattice)

D_p = hole diffusion constant (cm²/sec)

μ_p = hole mobility (cm²/volt-sec)

with analogous electron definitions. Since $\mu_p m_p = q t_p$ and $\mu_n m_n = q t_n$, eqs. 1.18 and 1.19 may be expressed as

$$- \frac{\partial p}{\partial x} = \frac{1}{D_p} J_p + \frac{1}{v_p D_p} \frac{\partial J_p}{\partial t} - \frac{\mu_p}{D_p} p E \quad (1.20)$$

$$+ \frac{\partial n}{\partial x} = \frac{1}{D_n} J_n + \frac{1}{v_n D_n} \frac{\partial J_n}{\partial t} - \frac{\mu_n}{D_n} n E \quad (1.21)$$

The current derivative terms are usually negligible in which case eqs. 1.20 and 1.21 are the familiar equations relating drift and diffusion current densities. Although eqs. 1.20 and 1.21 are nonlinear if E and p or E and n are both variable, this equation may be linearized for small signals.

The free carrier densities p and n are related by Poisson's equation to the electric field as

$$\frac{\partial E}{\partial x} = \frac{\rho}{\epsilon} = \frac{q}{\epsilon} (p - n + N_d - N_a) \quad (1.22)$$

where

ϵ = semiconductor permittivity (coulomb/volt-cm)

ρ = net charge density (coulomb/cm³)

N_d = donor doping density (electron/cm³) (or bound positive ion concentration)

N_a = acceptor doping density (holes/cm³) (or bound negative ion concentration)

Although any sample is macroscopically neutral, it is microscopically or locally non-neutral where ρ is nonzero. Generally local charge neutrality is assumed where the majority carrier density readjusts to accommodate minority density gradients. It is clear that eq. 1.22 requires bilateral active coupling between lines if this assumption is not made. The active transmission line analogs are drawn in Fig. 15. Since there is no shunt current (leakage current) in the E-line, its assigned current variable is arbitrary.

Depending on the problem to be analyzed, several assumptions allow the coupling to be unilateralized and the differential model simplified. Linvill and Gibbons have considered the difference equation form of eqs. 1.16, 1.17, 1.20, 1.21, and 1.22 and developed lumped, iterated structures analogous to those of Fig. 15 (21).

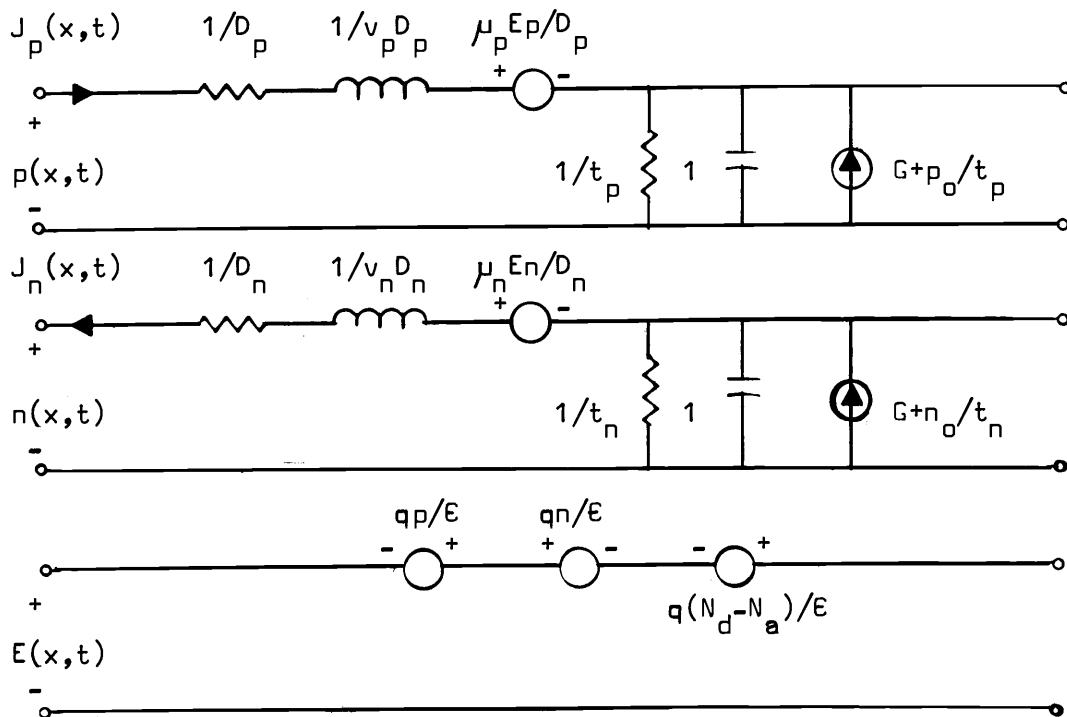


Fig. 15. Semiconductor photodetection analog.

Summary

In this discussion, the active transmission line has been placed in historical perspective and its current importance in realizing distributed amplifiers noted. In the following chapters it will become clear that active lines may be used to obtain other useful electrical characteristics. The importance of active lines in modeling many physical processes has also been discussed, and several representative examples presented.

The intent of this thesis is to fully develop the heretofore uninvestigated theory of active transmission lines, using a network theory approach. In so doing, the classical transmission line is generalized into the active line. Much of the classical line theory

may be extended directly. Following the active line analysis, a general synthesis scheme is presented allowing computerized design of active lines. Realizations of active lines are discussed in the concluding chapter.

II. TRANSMISSION LINES HAVING INDEPENDENT DISTRIBUTED SOURCES

Independent Distributed Sources

The differential section of the active transmission line drawn in Fig. 2 is described mathematically by eqs. 1.3 and 1.4. The distributed sources e and j may be independent, dependent, or both. In this chapter the sources are taken to be independent, that is they are independent of both voltage and current along the line.

Initial condition generators are this type of source. This is immediately clear when the Laplace transformations of the active transmission line equations are written. Eqs. 1.3 and 1.4 become

$$-\frac{\partial V(x,s)}{\partial x} = (r+sl)I(x,s) + E(x,s) - li(x,0) \quad (2.1)$$

$$-\frac{\partial I(x,s)}{\partial x} = (g+sc)V(x,s) + J(x,s) - cv(x,0) \quad (2.2)$$

where V and I are the transformed line voltage and current, E and J are the (explicitly) transformed distributed voltage and current source strengths, and $i(x,0)$ and $v(x,0)$ are the initial current and voltage specified along the line. Since the last two terms in the equations represent transformed distributed series voltage and shunt current sources respectively, it is clear that the terms $li(x,0)$ and $cv(x,0)$ represent initial condition impulse generators. In passing, we note that V and I are continuously differentiable in x and s when $Z = r + sl$ and $Y = g + sc$ are nonzero, and Z , Y , E , and J are continuously differentiable in x and s .

Passive and active coupling between lines introduces distributed sources which although dependent, are not dependent upon voltage and

current in that line. They are independent sources to the line in question and thus fall into this category. This is readily seen by considering the general coupled lines of Fig. 16 and their equivalent in Fig. 17. Unless coupling is unilateral, solutions become extremely involved (12, 17).

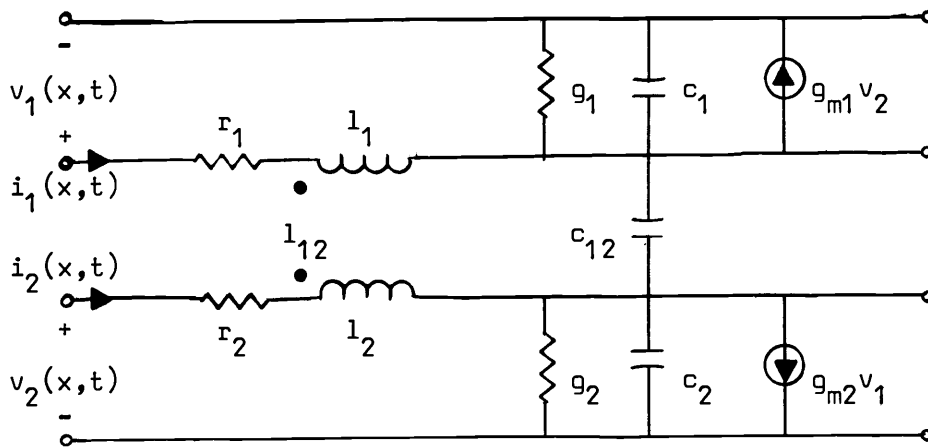


Fig. 16. Actively and passively coupled transmission line.

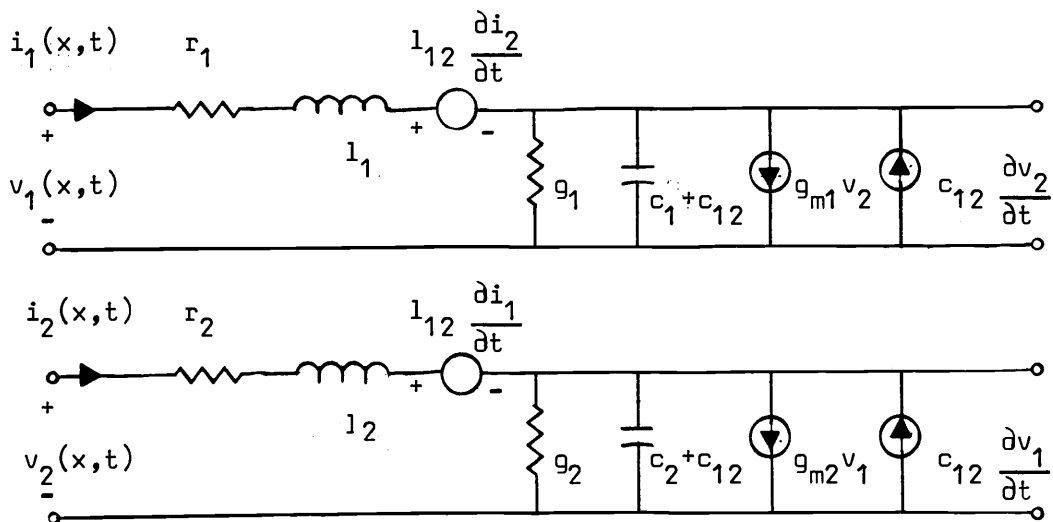


Fig. 17. Coupled line equivalent circuit using distributed dependent sources.

It is shown in the discussion that follows that independent distributed sources may be "extracted" from the line when accompanied by appropriate modifications of boundary conditions. To begin, we review two-port theory of linear networks having internal independent sources. The extension to n-ports is immediate.

Two-Port Theory of Linear Networks

Two-port theory has been employed for many years to characterize an often complicated electrical system by its port behavior. Various parameter sets including impedance, admittance, hybrid, and chain parameters relate port voltages and currents. These parameters are expressed in matrix form in Fig. 18. Although two-ports containing independent sources have not received extensive treatment in the past, they are readily accommodated by including a term corresponding to an independent source on the left hand side of the matrix equations in Fig. 18. Note that each two-port representation contains two independent sources. Thus the effect of independent sources is to change the boundary conditions of the two-port. The significance of these two independent sources may be interpreted in either of two ways.

Viewing the two-port equations as arising from the Taylor series expansion of port unknowns as functions of port knowns when retaining only zero and first order terms, it is clear that the independent sources correspond to the zero order terms.

Alternatively, a two-port network containing n independent sources may be viewed as an $(n+2)$ -port containing no independent sources. By linearity and thus superposition, the effects of n

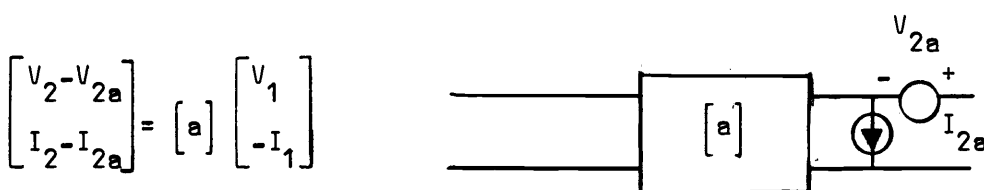
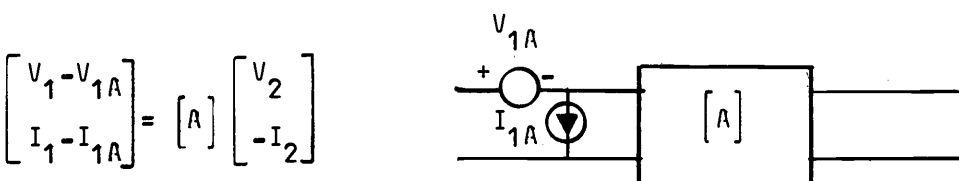
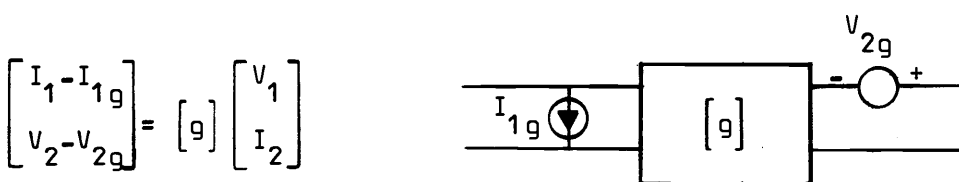
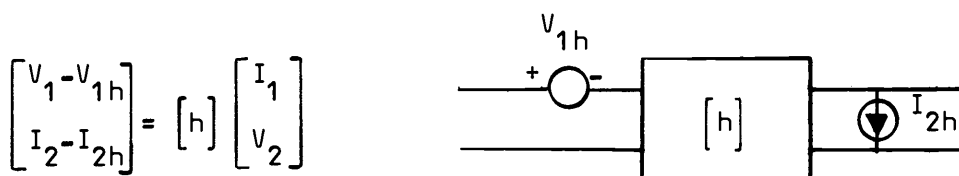
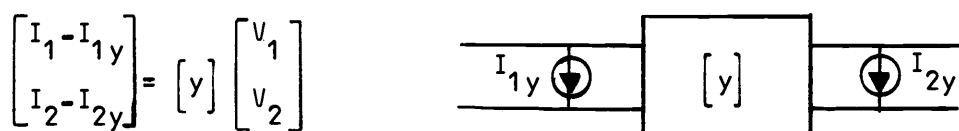
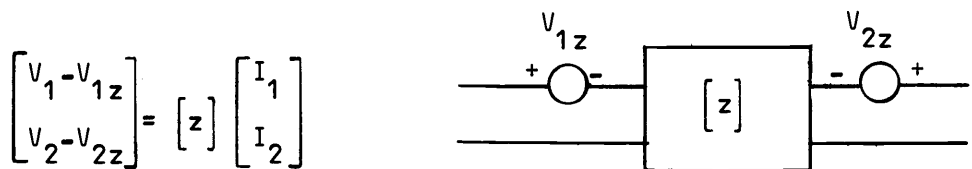
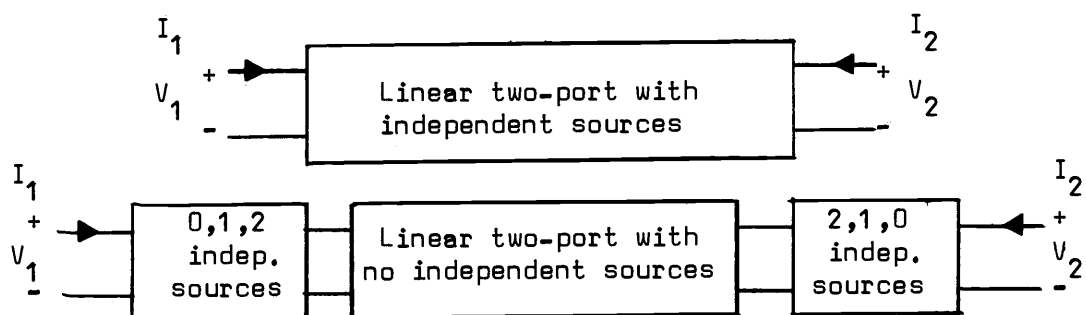


Fig. 18. Various characterizations of two-ports containing independent sources.

specified voltage and current sources at the n ports superimpose at ports 1 and 2. But by reciprocity, similar effects are produced by the two equivalent independent sources in Fig. 18 when the n independent voltage and current sources are set to zero. The type and placement of the two sources depend upon the parameter set chosen to characterize the two-port network. The matrix describing the two-port is found with the internal independent sources set to zero.

These independent port sources may be d.c. sources whose levels are those of the system in its quiescent state. For example, V_1 is the input voltage, and $V_1 - V_{1z}$ is the port voltage fluctuation about its d.c. level V_{1z} . The sources may be equivalent noise generators of the network and have a statistical nature, or they may correspond to other contaminating signals such as hum.

From the matrix relations of Fig. 18, V_{1z} and V_{2z} are equal to the open-circuit voltages at ports 1 and 2 respectively. In like manner, I_{1y} and I_{2y} are the short-circuit currents of ports 1 and 2 respectively, with similar interpretations for the hybrid parameters. The independent sources associated with the chain and inverse chain matrix characterizations do not equal terminal responses directly however. These responses must instead be multiplied by the appropriate two-port parameter. For the chain matrix characterization for example,

$$V_{1A} = -AV_2 \text{ for } I_2 = 0 \text{ (output opened), or} \quad (2.3)$$

$$= BI_2 \text{ for } V_2 = 0 \text{ (output shorted)} \quad (2.4)$$

with the input shorted ($V_1=0$) and

$$I_{1A} = -CV_2 \text{ for } I_2 = 0, \text{ or} \quad (2.5)$$

$$= DI_2 \text{ for } V_2 = 0 \quad (2.6)$$

with the input open ($I_1=0$).

Relationships between these equivalent independent sources may be derived.³ Consider the relation between (V_{1z}, V_{2z}) and (I_{1y}, I_{2y}) using the z matrix description of the network in Fig. 18, I_{1y} and I_{2y} are the applied port voltages, then from the admittance parameter definitions

$$\begin{bmatrix} I_{1y} \\ I_{2y} \end{bmatrix} = \begin{bmatrix} y_{11} & y_{12} \\ y_{21} & y_{22} \end{bmatrix} \begin{bmatrix} -V_{1z} \\ -V_{2z} \end{bmatrix} \quad (2.7)$$

These relations are tabulated in Table 1 where each box represents a matrix relation between row and column equivalent sources.

This two-port approach may be employed to describe the terminal behavior of an active transmission line having independent sources distributed continuously along its length.

Extraction Integrals for Active Transmission Lines

Since active transmission lines are described by linear partial differential equations, the port responses due to independent distributed sources may be superimposed. By linearity, the terminal behavior of the active line having independent distributed sources is identical to that of a line having no independent distributed sources which has two independent sources of proper type and value connected

³M.F. Moad developed several in: Two-port networks with independent sources. Proceedings of the IEEE 54(7):1008-1009. 1966; Addendum: Two-port networks with independent sources. Proceedings of the IEEE 54(12):1963-1964. 1966.

Table 1. Relationships between the various pairs of independent sources in Fig. 18.

	$-V_{1z}$	$-V_{2z}$	$-I_{1y}$	$-I_{2y}$	$-V_{1h}$	$-I_{2h}$	$-I_{1g}$	$-V_{2g}$	$-V_{1A}$	$-I_{1A}$	$-V_{2a}$	$-I_{2a}$
V_{1z}			z_{11}	z_{12}	-1	z_{12}	z_{11}	0	-1	z_{11}	0	z_{12}
V_{2z}			z_{21}	z_{22}	0	z_{22}	z_{21}	-1	0	z_{21}	-1	z_{22}
I_{1y}	y_{11}	y_{12}			y_{11}	0	-1	y_{12}	y_{11}	-1	y_{12}	0
I_{2y}	y_{21}	y_{22}			y_{21}	-1	0	y_{22}	y_{21}	0	y_{22}	-1
V_{1h}	-1	h_{12}	h_{11}	0			h_{11}	h_{12}	-1	h_{11}	h_{12}	0
I_{2h}	0	h_{22}	h_{21}	-1			h_{21}	h_{22}	0	h_{21}	h_{22}	-1
I_{1g}	g_{11}	0	-1	g_{12}	g_{11}	g_{12}			g_{11}	-1	0	g_{12}
V_{2g}	g_{21}	-1	0	g_{22}	g_{21}	g_{22}			g_{21}	0	-1	g_{22}
V_{1A}	-1	A	0	$-B$	-1	$-B$	0	A			A	$-B$
I_{1A}	0	C	-1	$-D$	0	$-D$	-1	C			C	$-D$
V_{2a}	a	-1	$-b$	0	a	0	$-b$	-1	a	$-b$		
I_{2a}	c	0	$-d$	-1	c	-1	$-d$	0	c	$-d$		

to its ports. The type and placement of these sources is determined by the matrix chosen to describe the line. For example, if a line is characterized by its z matrix, then independent voltage sources V_{1z} and V_{2z} are connected in series with its ports.

To find the strengths of these sources, the various parameters of the matrix are used. These are easily derived and are given in Table 2. The expression for V_{1z} is now derived in detail.

Since $V_1 = V_z$ and $V_2 = V_{2z}$ when $I_1 = I_2 = 0$, these independent source strengths correspond to the open-circuit terminal voltages of each port. To determine V_{1z} , we calculate the contribution $\Delta V_{1z}(x)$ to V_{1z} due to the sources $E(x,s)\Delta x$ and $J(x,s)\Delta x$ acting alone at x , determine the limiting expression when $\Delta x \rightarrow 0$, and integrate these contributions from $x = 0$ (the input) to $x = d$ (the output). From Fig. 19 and two-port theory,

$$\Delta V_{1z}(x) = \frac{z_{12}(x)}{z_{22}(x)} \frac{z_{22}(x)}{z_{11}(d-(x+\Delta x))+z_{22}(x)} \cdot [E(x,s)-z_{11}(d-(x+\Delta x))J(x,s)]\Delta x \quad (2.8)$$

for $\Delta x \rightarrow 0$. Here $z_{12}(x)/z_{22}(x)$ is the open-circuit voltage transfer ratio of the line- x -units long, $z_{22}(x)/[z_{11}(d-(x+\Delta x))+z_{22}(x)]$ is the voltage at the output port of the x -unit long line per unit distributed volt at x , and $[E(x,s)-z_{11}(d-(x+\Delta x))J(x,s)]$ is the distributed voltage at x . The Norton equivalent formed by the shunt current source and line $(d-x)$ -units long is converted to its Thevenin equivalent.

Therefore, the limiting expression becomes

$$dV_{1z}(x) = \frac{z_{12}(x)}{z_{11}(d-x)+z_{22}(x)} [E(x,s)-z_{11}(d-x)J(x,s)] dx \quad (2.9)$$

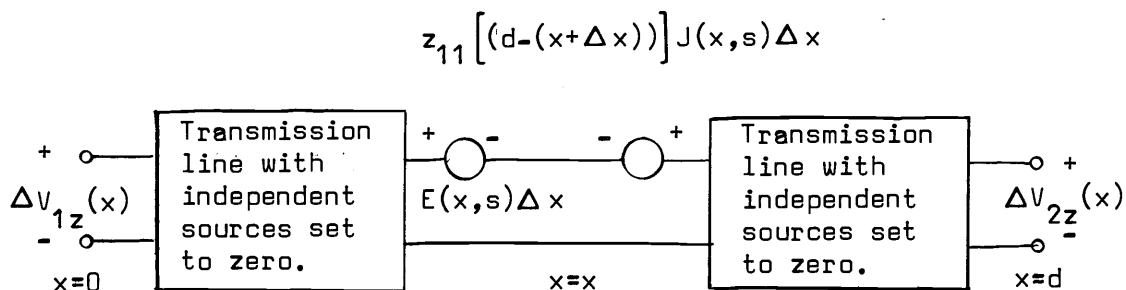


Fig. 19. Voltage contributions $\Delta V_{1z}(x)$ and $\Delta V_{2z}(x)$ due to independent sources $E(x)\Delta x$ and $J(x)\Delta x$ acting alone at x .

where $z_{11}(d-x)$ denotes the input impedance of the line to the right of position x ($(d-x)$ -units in length); and $z_{22}(x)$ and $z_{12}(x)$ denote the output and transfer impedances to the line to the left of position x (x -units in length), respectively. Thus, the open-circuit voltage at the input port due to independent distributed voltage and current sources is

$$V_{1z}(s) = \int_0^d \frac{z_{12}(x)}{z_{11}(d-x) + z_{22}(x)} [E(x,s) - z_{11}(d-x)J(x,s)] dx \quad (2.10)$$

Since the general active transmission line has been considered, the matrix parameters appearing in Table 2 are generally functions of s (although not written so explicitly) as well as x . The kernels of the integrals are the Green's functions or differential transfer functions for this problem.

Although the extraction integrals appear formidable, they are readily determined when the matrix parameters are expressible in closed form. Consider for example the uniform transmission line with independent distributed sources having characteristic impedance $Z_0(s) = \sqrt{(r+sl)/(g+sc)} = \sqrt{Z/Y}$ and propagation function $\gamma(s) = \sqrt{(r+sl)(g+sc)} = \sqrt{ZY}$. Since the impedance matrix $[Z(x,s)]$ for a uniform line x units

Table 2. Extraction integrals for an active transmission line (19).

$$V_{1z} = \int_0^d \frac{z_{12}(x)}{z_{11}(d-x)+z_{22}(x)} [E - z_{11}(d-x)J] dx$$

$$V_{2z} = - \int_0^d \frac{z_{21}(d-x)}{z_{11}(d-x)+z_{22}(x)} [E + z_{22}(x)J] dx$$

$$I_{1y} = \int_0^d \frac{y_{12}(x)}{y_{11}(d-x)+y_{22}(x)} [-J + y_{11}(d-x)E] dx$$

$$I_{2y} = - \int_0^d \frac{y_{21}(d-x)}{y_{11}(d-x)+y_{22}(x)} [J + y_{22}(x)E] dx$$

$$V_{1h} = \int_0^d \frac{h_{11}(d)h_{12}(x)}{h_{11}(x)+h_{11}(d-x)\Delta_h(x)} [E - h_{11}(d-x)J] dx$$

$$I_{2h} = - \int_0^d \frac{h_{22}(d)h_{21}(d-x)}{h_{22}(d-x)+h_{22}(x)\Delta_h(d-x)} [J + h_{22}(x)E] dx$$

$$V_{2g} = - \int_0^d \frac{g_{22}(d)g_{21}(d-x)}{g_{22}(d-x)+g_{22}(x)\Delta_g(d-x)} [E + g_{22}(x)J] dx$$

$$I_{1g} = \int_0^d \frac{g_{11}(d)g_{12}(x)}{g_{11}(x)+g_{11}(d-x)\Delta_g(x)} [J - g_{11}(d-x)E] dx$$

$$V_{1A} = \int_0^d \frac{A(d)A(x)}{A(x)A(d-x)+B(x)C(d-x)} \left[E + \frac{B(x)}{A(x)} J \right] dx$$

$$I_{1A} = \int_0^d \frac{D(d)C(x)}{D(x)D(d-x)+B(d-x)C(x)} \left[E + \frac{D(x)}{C(x)} J \right] dx$$

$$V_{2a} = \int_0^d \frac{a(d)a(d-x)}{a(x)a(d-x)+b(d-x)c(x)} \left[-J + \frac{b(d-x)}{a(d-x)} E \right] dx$$

$$I_{2a} = \int_0^d \frac{d(d)d(d-x)}{d(x)d(d-x)+b(x)c(d-x)} \left[J - \frac{c(d-x)}{d(d-x)} E \right] dx$$

Note: $\Delta_h(x)$ denotes determinant of h matrix of line to left of position x, etc.

long is (see the development leading to eq. 3.46)

$$\begin{bmatrix} Z(x,s) \\ 1 \end{bmatrix} = Z_0 \begin{bmatrix} \coth \gamma x & \operatorname{csch} \gamma x \\ \operatorname{csch} \gamma x & \coth \gamma x \end{bmatrix} \quad (2.11)$$

then $V_{1z}(s)$ becomes

$$\begin{aligned} V_{1z}(s) &= \int_0^d \frac{\operatorname{csch} \gamma x}{\coth \gamma x + \coth \gamma (d-x)} \left[E(x,s) - Z_0 \coth \gamma (d-x) J(x,s) \right] dx \\ &= \frac{1}{\sinh \gamma d} \int_0^d \left[E(x,s) \sinh \gamma (d-x) - Z_0 J(x,s) \cosh \gamma (d-x) \right] dx \quad (2.12) \end{aligned}$$

The remaining five basic two-port matrices may be found from eq. 2.11 using standard matrix conversions. Subsequent parameter substitution and simplification yield the extraction integrals for the uniform line in Table 3. To indicate the usefulness and importance of these results, several examples are now given.

Applications of the Extraction Integral

Problems involving port response to arbitrary initial conditions with specified terminations are readily analyzed using the extraction integrals. Suppose a line with characteristic impedance $Z_0 = \sqrt{Z/Y}$ and propagation constant $\gamma = \sqrt{ZY}$, is to have initial voltage V_0 and zero initial current. Further suppose the input port voltage V_1 is desired under open-circuit conditions at input and output. Since $E(x,s) = -li(x,0)$ and $J(x,s) = -cv(x,0) = -cV_0$, the input port voltage from Table 3 is,

$$V_{1z}(s) = \frac{cZ_0 V_0}{\sinh \gamma d} \int_0^d \cosh \gamma (d-x) dx = \frac{cZ_0 V_0}{\gamma} = \frac{cV_0}{Y} \quad (2.13)$$

The response depends on the form of Y . If $Y = sc$, then $V_1(s) = V_0/s$

Table 3. Extraction integrals for a uniform active transmission line (20).

$$V_{1z} = \frac{1}{\sinh \gamma d} \int_0^d \left[E \sinh \gamma(d-x) - Z_0 J \cosh \gamma(d-x) \right] dx$$

$$V_{2z} = \frac{-1}{\sinh \gamma d} \int_0^d \left[E \sinh \gamma x + Z_0 J \cosh \gamma x \right] dx$$

$$I_{1y} = \frac{1}{\sinh \gamma d} \int_0^d \left[J \sinh \gamma(d-x) - Y_0 E \cosh \gamma(d-x) \right] dx$$

$$I_{2y} = \frac{1}{\sinh \gamma d} \int_0^d \left[J \sinh \gamma x + Y_0 E \cosh \gamma x \right] dx$$

$$V_{1h} = \frac{1}{\cosh \gamma d} \int_0^d \left[E \cosh \gamma(d-x) - Z_0 J \sinh \gamma(d-x) \right] dx$$

$$I_{2h} = \frac{1}{\cosh \gamma d} \int_0^d \left[J \cosh \gamma x + Y_0 E \sinh \gamma x \right] dx$$

$$V_{2g} = \frac{-1}{\cosh \gamma d} \int_0^d \left[E \cosh \gamma x + Z_0 J \sinh \gamma x \right] dx$$

$$I_{1g} = \frac{1}{\cosh \gamma d} \int_0^d \left[J \cosh \gamma(d-x) - Y_0 E \sinh \gamma(d-x) \right] dx$$

$$V_{1A} = \int_0^d \left[E \cosh \gamma x + Z_0 J \sinh \gamma x \right] dx$$

$$I_{1A} = \int_0^d \left[J \cosh \gamma x + Y_0 E \sinh \gamma x \right] dx$$

$$V_{2a} = \int_0^d \left[-E \cosh \gamma(d-x) + Z_0 J \sinh \gamma(d-x) \right] dx$$

$$I_{2a} = \int_0^d \left[J \cosh \gamma(d-x) - Y_0 E \sinh \gamma(d-x) \right] dx$$

so $v_1(t) = V_0 u(t)$. If there is also differential shunt conductance so $Y = g + sc$, then $V_1(s) = V_0/(s+g/c)$ and $v_1(t) = V_0 \exp(-gt/c)u(t)$. In the first case the port voltage remains constant, while in the second it decays exponentially to zero.

Suppose instead that input and output ports are terminated in matched impedances Z_0 . Using a chain matrix characterization,

$$V_1(s) = \frac{1}{2}(V_{1A} - Z_0 I_{1A}) = \frac{cV_0}{2Y}(1 - e^{-d\sqrt{ZY}}) \quad (2.14)$$

since from Table 3, V_{1A} and $Z_0 I_{1A}$ are

$$V_{1A}(s) = \frac{cV_0}{Y}(1 - \cosh d\sqrt{ZY}) \quad (2.15)$$

$$Z_0 I_{1A}(s) = -\frac{cV_0}{Y} \sinh d\sqrt{ZY} \quad (2.16)$$

If a delay line is considered, then $Z = sl$ and $Y = sc$. Then $V_1(s) = \frac{V_0}{2s}(1 - e^{-d\sqrt{ZY}})$ and $v_1(t) = V_0 [u(t) - u(t - d\sqrt{lc})]$, so a pulse of $V_0/2$ volts of time duration $d\sqrt{lc}$ seconds appears at the input port beginning at $t = 0$.

Problems involving response to general independent distributed sources are likewise readily analyzed. Reconsider the traveling-wave transistor of Fig. 9 in which the input delay line is unilaterally actively coupled via transconductance/unit length g_m to the output delay line. If each line is terminated in its characteristic impedance, reflections from the ports of each line are eliminated. Thus the voltage along the input line is $V_1(x,s) = V_1(0,s)e^{-sYx}$ where $V_1(0,s) = V_1$ is the voltage applied to the input line. Therefore, the independent distributed current source of Fig. 10 becomes $J(x,s) =$

$g_m V_1(s) e^{-sYd}$. As before, given the excitation voltage of the input line port voltages are readily found. These are

$$V_{o1}(s) = \frac{g_m}{4sc} [1 - e^{-2Yd}] V_1 \quad (2.17)$$

$$V_{o2}(s) = \frac{g_m d}{2} \sqrt{\frac{1}{c}} e^{-Yd} V_1 \quad (2.18)$$

where the propagation constants of input and output lines are assumed equal. Thus for a unit step input voltage $v_1(t) = u(t)$, the output voltages are

$$v_{o1}(t) = \frac{g_m}{4c} [tu(t) - (t - 2d\sqrt{lc})u(t - 2d\sqrt{lc})] \quad (2.19)$$

$$v_{o2}(t) = \frac{g_m d}{2} \sqrt{\frac{1}{c}} u(t - d\sqrt{lc}) \quad (2.20)$$

The v_{o1} response begins at $t = 0$ and rises linearly from 0 to $\frac{g_m d}{2} \sqrt{\frac{1}{c}}$ volts in $2d\sqrt{lc}$ seconds. The v_{o2} response is delayed by $2d\sqrt{lc}$ seconds and rises abruptly from zero to $\frac{g_m d}{2} \sqrt{\frac{1}{c}}$ volts. In sinusoidal steady-state, the port 2 voltage gain from eq. 2.18 has magnitude $\frac{g_m d}{2} \sqrt{\frac{1}{c}}$ with phase shift $\omega d\sqrt{lc}$ radians.

Thus, the usefulness of the extraction integrals in analyzing active transmission lines having independent distributed sources should be clear. To recapitulate, the effects of these sources is to modify the boundary or port conditions of the line rather than its two-port parameters.⁴ Response and gain calculations are readily made utilizing the extraction integrals.

It should be pointed out that the presence of independent distri-

⁴In the next two chapters parameter modification occurs when dependent distributed sources are considered.

buted sources does not necessarily make the line active. In fact, considering the total line response to initial conditions from $t = -\infty$ to $+\infty$, there is no net energy delivered by the line and thus the line is passive. In current terminology however, the term active is used generically to indicate the presence of distributed sources along the line.

III. UNIFORM TRANSMISSION LINES HAVING DEPENDENT DISTRIBUTED SOURCES

Dependent Distributed Sources

Active transmission lines having dependent or controlled voltage and/or current sources distributed continuously along its length are now analyzed. Four types of dependent sources are considered:

1. $e = K_i i$, a current-controlled voltage source,
2. $e = K_v v$, a voltage-controlled voltage source,
3. $j = L_v v$, a voltage-controlled current source,
4. $j = L_i i$, a current-controlled current source.

Parameters K and L generally have spacial dependence. In this chapter they are considered constant. In the following chapter concerned with nonuniform active lines, they are variable.

It is convenient to analyze lines having either type 1 and type 3 sources or type 2 and type 4 sources simultaneously. These lines will be referred to as type 1-3 and type 2-4 lines, respectively. Since the classification will be clear, for brevity without loss of clarity, the subscript notation is eliminated which denotes source type. To clearly establish the difference between the two types of lines, consider the differential section for each case.

The type 1-3 line is drawn in Fig. 20 with its equivalent in Fig. 21. This type of active line may be analyzed as a line with no distributed sources but having its resistance/unit length, r , and conductance/unit length, g , values adjusted from r and g to r^* and g^* , respectively. r^* and g^* can be adjusted to have any value. Type 1-3 active lines are therefore readily analyzed using many of the classical

results for passive lines.

However the type 2-4 line shown in Fig. 22 has no such equivalent section.

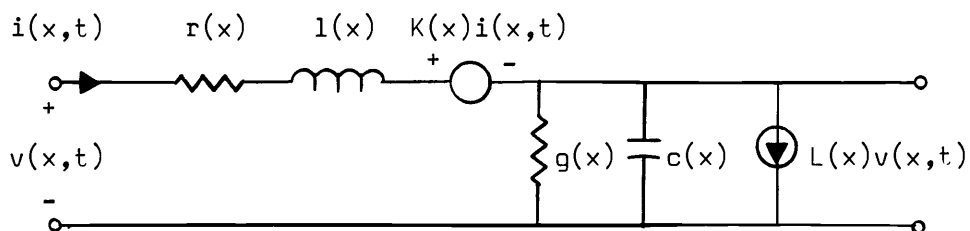


Fig. 20. Type 1-3 active line differential section.

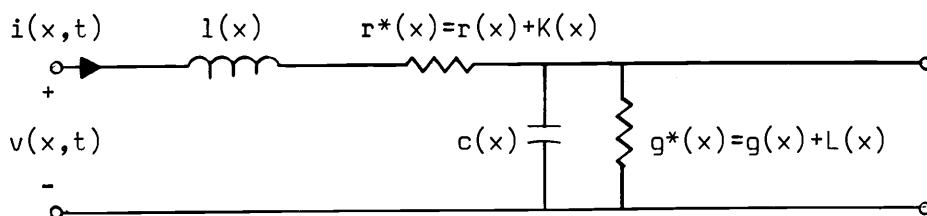


Fig. 21. Equivalent differential section of a type 1-3 active line.

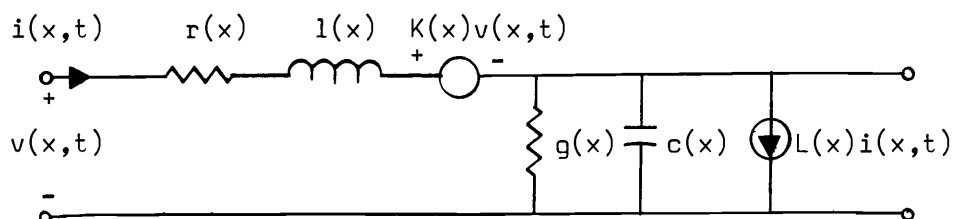


Fig. 22. Type 2-4 active line differential section.

Active Transmission Line Equations

To begin the discussion, eqs. 1.3 and 1.4 are manipulated into various forms convenient for subsequent analysis. The Telegrapher's equations or active transmission line equations describe either voltage v or current i along the active line, and result by eliminating appropriate terms from eqs. 1.3 and 1.4. These are

$$v_{xx} = rgv + (rc+lg)v_t + lcv_{tt} + (lj_t+rj-e_x) \quad (3.1)$$

$$i_{xx} = rgi + (rc+lg)i_t + lci_{tt} + (ce_t+ge-j_x) \quad (3.2)$$

for the uniform line. For the nonuniform line, the terms

$$(v_x+e)r_x/r + (r_x/r - l_x/l)li_t \quad (3.3)$$

$$(i_x+j)g_x/g + (g_x/g - c_x/c)cv_t \quad (3.4)$$

are added to the right hand sides of eqs. 3.1 and 3.2 respectively.

For notational convenience, x and t subscripts are employed to indicate spacial and time partial differentiations.⁵ Previous parameter conditions, noted for eqs. 1.1 and 1.2, insure that voltage and current is twice continuously differentiable so the order of x and t differentiations may be interchanged. Unless l and c are constant multiples of r and g , respectively, the second terms of eqs. 3.3 and 3.4 cannot be eliminated.

The Laplace transformation of these equations for the constant parameter line is

$$V_{xx} = ZYV + (ZJ-E_x) - [(lg+rc+slc)v(x,0) + lcv_t(x,0) + lj(x,0)] \quad (3.5)$$

$$I_{xx} = ZYI + (YE-J_x) - [(lg+rc+slc)i(x,0) + lci_t(x,0) + ce(x,0)] \quad (3.6)$$

⁵E.g. $v_t = \partial v / \partial t$, $v_{xx} = \partial^2 v / \partial x^2$, and $v_{xt} = \partial^2 v / \partial x \partial t$.

where $Z = r + sl$ and $Y = g + sc$. Nonuniform lines are described by eqs. 3.5 and 3.6 with additional right hand terms of

$$(V_x + E)Z_x/Z - i(x,0)(r_x/r - l_x/l)r1/Z \quad (3.7)$$

$$(I_x + J)Y_x/Y - v(x,0)(g_x/g - c_x/c)gc/Y \quad (3.8)$$

respectively. The parameter conditions for eqs. 2.1 and 2.2 insure that these derivatives exist.

Eqs. 3.1 and 3.2 are readily utilized for traveling-wave and sinusoidal steady-state analysis, while eqs. 3.5 and 3.6 are convenient for Laplace transform analysis. For nonzero initial conditions, the analysis technique of Chapter 2 is used. Thus, only zero initial condition lines need be considered here.

Traveling-Wave Analysis

Traveling-wave voltage solutions are obtained using the separation of variables technique by assuming a solution $v(x,t) = v_1(x)v_2(t)$. For the type 1-3 line, eq. 3.1 then becomes

$$v_{xx} = r*g*v + (r*c+g*l)v_t + lcv_{tt} \quad (3.9)$$

or

$$v_2 v_1'' = r*g*v_1 v_2 + (r*c+g*l)v_1 v_2' + lcv_1 v_2'' \quad (3.10)$$

where primes represent differentiation with respect to the function's argument. Dividing each side of eq. 3.10 by $v_1 v_2$,

$$\frac{v_1''}{v_1} = \frac{r*g*v_2 + (r*c+g*l)v_2' + lcv_2''}{v_2} = k^2 \quad (3.11)$$

where k^2 is an arbitrary complex constant. Rewriting eq. 3.11 yields the two ordinary differential equations,

$$v_1'' - k^2 v_1 = 0 \quad (3.12)$$

$$lcv_2'' + (r^*c + g^*l)v_2' + (r^*g^* - k^2)v_2 = 0 \quad (3.13)$$

The spacially dependent solution $v_1(x)$ of eq. 3.12 is

$$v_1(x) = A\exp(kx) + B\exp(-kx) \quad (3.14)$$

To conveniently express the time dependent solution, define constants a and b where

$$a = \frac{1}{2}(r^*/l + g^*/c) \quad (3.15)$$

$$b = \frac{1}{2}(r^*/l - g^*/c) \quad (3.16)$$

Eq. 3.13 can then be rewritten as

$$v_2'' + 2av_2' + [(a+b)(a-b) - k^2/lc]v_2 = 0 \quad (3.17)$$

The auxiliary equation of eq. 3.17, formed by assuming a time solution $v_2(t) = \exp(pt)$ and substituting into eq. 3.17 is

$$p^2 + 2ap + a^2 - b^2 - k^2/lc = 0 \quad (3.18)$$

Thus, parameter p is found to be

$$p = -a \pm \sqrt{b^2 + k^2/lc} \quad (3.19)$$

Therefore, the time dependent solution $v_2(t)$ is

$$v_2(t) = C\exp(-a + \sqrt{b^2 + k^2/lc})t + D\exp(-a - \sqrt{b^2 + k^2/lc})t \quad (3.20)$$

The general voltage solution of eq. 3.9 is the product of eqs. 3.14 and 3.20.

The steady-state sinusoidal voltage response along the line results by adjusting k to have the appropriate value. Since this corresponds $p = j\omega$ in the v_2 solution, k must equal

$$k = \sqrt{r^*g^* + j\omega(r^*c + g^*l) + (j\omega)^2lc} = \sqrt{(r^* + j\omega l)(g^* + j\omega c)} = \alpha + j\beta \quad (3.21)$$

from eq. 3.18. Alternatively, $p = -j\omega$ yields the conjugate value $k^* = \alpha - j\beta$. Thus from eqs. 3.14 and 3.20, the general voltage solution $v(x,t)$ is

$$v(x,t) = E e^{\alpha x} e^{+j(\omega t + \beta x)} + F e^{\alpha x} e^{-j(\omega t - \beta x)} \quad (3.22)$$

where the complex constants E and F are determined by the port conditions of the line. The solution has a traveling-wave characteristic. The term involving $\exp\left[-j(\omega t + \beta x)\right]$ represents waves which are attenuated by the factor $\exp(-\alpha)$ per unit length and travel to the left along the line with phase velocity $v_p = \omega/\beta$. The remaining term involving $\exp\left[-j(\omega t - \beta x)\right]$ represents waves traveling to the right with the same velocity and attenuation per unit length.

Using the same analysis procedure for the type (2-4) line yields somewhat different results. In this case the line voltage satisfies

$$v_{xx} + (L+K)v_x = (rg-LK)v + (rc+lg)v_t + lcv_{tt} \quad (3.23)$$

from eq. 3.1. Separation of variables results in the two ordinary differential equations,

$$v_1'' + (L+K)v_1' - k^2 v_1 = 0 \quad (3.24)$$

$$lcv_2'' + (rc+lg)v_2' + (rg-LK-k^2)v_2 = 0 \quad (3.25)$$

The general spacial solution $v_1(x)$ is

$$v_1(x) = A \exp \left[-\frac{1}{2}(L+K) \pm \sqrt{\frac{1}{4}(L+K)^2 + k^2} \right] x \quad (3.26)$$

The general time solution $v_2(t)$ is

$$v_2(t) = C \exp \left[-a \pm \sqrt{b^2 + (k^2 + LK)/lc} \right] t \quad (3.27)$$

Since eqs. 3.25 and 3.13 are similar, this results by replacing k^2 by $k^2 + LK$ in eq. 3.20.

In the sinusoidal steady-state, k must equal

$$k = \sqrt{(j\omega)^2 lc + j\omega(rc+lg) + rg - LK} = \alpha + j\beta \quad (3.28)$$

for type 2-4 lines. Denoting the radical factor $\sqrt{\frac{1}{4}(L+K)^2 + k^2} =$

$\sqrt{ZY + \frac{1}{4}(L-K)^2}$ in eq. 3.26 as $\Gamma_\alpha + j\Gamma_\beta$, the general voltage solution becomes

$$v(x,t) = E \exp\left[\left(-\frac{1}{2}(L+K) + \Gamma_\alpha\right)x\right] \exp\left[-j(\omega t + \Gamma_\beta x)\right] \\ + F \exp\left[\left(-\frac{1}{2}(L+K) - \Gamma_\alpha\right)x\right] \exp\left[-j(\omega t - \Gamma_\beta x)\right] \quad (3.29)$$

Waves traveling to the left with phase velocity $v_p = \omega/\Gamma_\beta$ are attenuated by $\exp\left[-\Gamma_\alpha + \frac{1}{2}(L+K)\right]$ per unit length while those traveling to the right have the same velocity but are attenuated by $\exp\left[-\Gamma_\alpha - \frac{1}{2}(L+K)\right]$. For $L+K > 0$, these latter waves suffer greater attenuation.

Characteristic Impedance

It has been shown that voltages and currents on active transmission lines in sinusoidal steady-state have traveling-wave characteristics. Corresponding voltage and current phasors are related by the characteristic impedance, Z_0 , of the line. These are readily determined.

First consider the type 1-3 active line where we relate the phasors v_1 and $-i_1$ of voltage and current waves, respectively, traveling to the left. The minus sign occurs because the wave travels opposite to the assumed current direction in Fig. 2. Substituting the first voltage term of eq. 3.22 into eq. 1.4 and solving for its associated current, we find that the characteristic impedance Z_{01} is

$$Z_{o1} = \frac{v_1}{-i_1} = \sqrt{\frac{r^{**} + j\omega l}{g^{**} + j\omega c}} = \sqrt{\frac{K+Z}{L+Y}} = Z_o \sqrt{\frac{1+K/Z}{1+L/Y}} \quad (3.30)$$

where $Z_o = \sqrt{Z/Y}$ is the characteristic impedance of the passive line.

The phasors v_2 and i_2 of voltage and current waves, respectively, traveling to the right have the same characteristic impedance, i.e. $v_2/i_2 = Z_{o2} = Z_{o1}$. The characteristic impedance of the active line is that of the passive line when $K = Z_o^2 L$ (i.e. $Z_{o1} = Z_{o2} = Z_o = \sqrt{K/L}$). Since K and L are real, r_g , l_c , and distortionless active lines can have their parameters adjusted to satisfy this condition.

Type 2-4 active lines have characteristic impedance which depend on the direction of wave travel as may be anticipated from the results of eq. 3.29. Repeating the previous operations using eqs. 3.29 and 1.4 yields the characteristic impedance for voltage and current waves traveling to the left,

$$Z_{o1} = \frac{v_1}{-i_1} = Z \left[\sqrt{\frac{1}{4}(K-L)^2 + ZY} - \frac{1}{2}(L-K) \right]^{-1} = \frac{1}{Y} \left[\sqrt{\frac{1}{4}(K-L)^2 + ZY} + \frac{1}{2}(L-K) \right] \quad (3.31)$$

and the characteristic impedance for waves traveling to the right,

$$Z_{o2} = \frac{v_2}{i_2} = Z \left[\sqrt{\frac{1}{4}(K-L)^2 + ZY} + \frac{1}{2}(L-K) \right]^{-1} = \frac{1}{Y} \left[\sqrt{\frac{1}{4}(K-L)^2 + ZY} - \frac{1}{2}(L-K) \right] \quad (3.32)$$

Using the propagation constant $\gamma = \sqrt{ZY}$ and characteristic impedance

$Z_o = \sqrt{Z/Y}$ for the passive line,

$$Z_{o1} = Z_o \left[\sqrt{\left| \frac{K-L}{2Y} \right|^2 + 1} + \frac{L-K}{2Y} \right] \quad (3.33)$$

$$Z_{o2} = Z_o \left[\sqrt{\left| \frac{K-L}{2Y} \right|^2 + 1} - \frac{L-K}{2Y} \right] \quad (3.34)$$

Clearly the two impedances differ by the factor $\pm Z_o(L-K)/2Y$. When

$K = L$, the characteristic impedance of the active line is equal to that

of the passive line ($Z_{o1} = Z_{o2} = Z_o$) and is independent of K and L. Another simplified situation exists in the active delay line at a frequency ω satisfying $\omega \sqrt{lc} = |K-L|/2$ which makes the radical in eqs. 3.33 and 3.34 vanish. At this frequency, $Z_{o1} = -Z_{o2} = Z_o$ for $L > K$ while $Z_{o1} = -Z_{o2} = -Z_o$ for $L < K$. Thus, at the frequency ω , average power flows only in one direction along the line.

Propagation Constant

The propagation constant, whose real part is the attenuation function, α (nepers/m), and whose imaginary part is the phase function, β (radians/m), was determined in the traveling-wave analysis discussion. Recapitulating, these quantities are independent of wave direction in the type 1-3 lines. From eqs. 3.21 and 3.22,

$$\alpha = \text{Re} \sqrt{(K+Z)(L+Y)} \quad (3.35)$$

$$\beta = \text{Im} \sqrt{(K+Z)(L+Y)} \quad (3.36)$$

Type 2-4 lines have functions which depend on wave direction. From eq. 3.29, denoting left-traveling and right-traveling wave quantities by subscripts 1 and 2, respectively,

$$\alpha_1 = \text{Re} \sqrt{\frac{1}{4}(L-K)^2 + ZY} - \frac{1}{2}(L+K) \quad (3.37)$$

$$\alpha_2 = \text{Re} \sqrt{\frac{1}{4}(L-K)^2 + ZY} + \frac{1}{2}(L+K) \quad (3.38)$$

and

$$\beta_1 = \beta_2 = \text{Im} \sqrt{\frac{1}{4}(L-K)^2 + ZY} \quad (3.39)$$

As previously noted, the waves have equal phase velocities since $\beta_1 = \beta_2$ but attenuation characteristics which differ by $\pm (L+K)/2$.

These results have graphical interpretations. For type 1-3 lines, the propagation constant ($\alpha + j\beta$) may lie in three distinct domains

depending on the values of r^* and g^* as shown in Figs. 23, 24, and 25. These figures are readily drawn from eq. 3.21 where domains of $(\alpha + j\beta)^2$ points are first considered, and then domains of $(\alpha + j\beta)$ points.

Since only single propagating modes may exist in type 1-3 lines, the line is active when $\alpha\beta > 0$.⁶ Thus, from this viewpoint, active

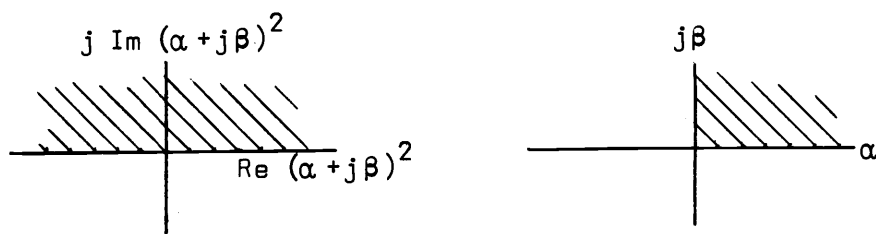


Fig. 23. Domain of propagation constant values when $r^*, g^* > 0$.

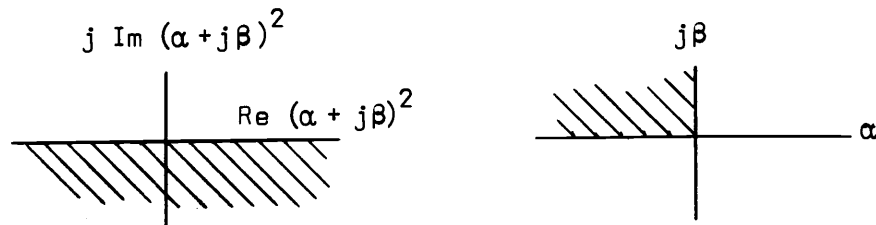


Fig. 24. Domain of propagation constant values when $r^*, g^* < 0$.

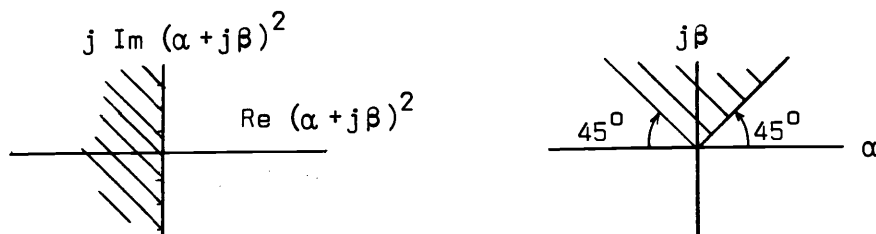


Fig. 25. Domain of propagation constant values when $r^* < 0, g^* > 0$ or $g^* < 0, r^* > 0$.

⁶Activity in single mode systems implies spacial wave growth in the direction of travel. In multimode systems, activity may be present although no waves are spacially growing (34).

lines result from their operation in the open domains of the second and fourth quadrants of the $(\alpha + j\beta)$ - plane. Since r^* and g^* can be adjusted to be negative values, active lines can be realized. This can cause stability problems as will be shown later in the chapter.

Type 2-4 active lines have more complicated propagation constant expressions given by eqs. 3.37 - 3.39. Following Wohlers' development (34), this type of line can be shown to be active. The domain in which propagation constants $(\alpha_1 + j\beta_1)$ and $(\alpha_2 + j\beta_2)$ values lie is drawn in Fig. 26.

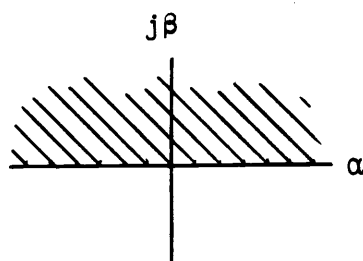


Fig. 26. Domain of propagation constant values.

Laplace Transform Analysis and Two-Port Parameters

Two-port parameters are readily determined for active transmission lines. The port conventions for an active line of length d is shown in Fig. 27. For type 1-3 active lines, the transformed voltage from eq. 3.5 satisfies

$$V_{xx}(x,s) = (Z+K)(Y+L)V(x,s) = k^2(s)V(x,s) \quad (3.40)$$

where $k^2(s) = (Z+K)(L+Y)$, $Z = r + sl$, and $Y = g + sc$. The transformed voltage solution of eq. 3.40 is

$$V(x,s) = V_a(s)e^{-kx} + V_b(s)e^{kx} \quad (3.41)$$

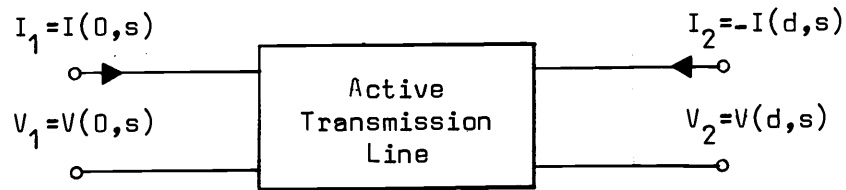


Fig. 27. Port conventions of an active line.

where $V_a(s)$ and $V_b(s)$ are arbitrary functions of s determined by port conditions. Therefore from eq. 3.41, the port voltages of Fig. 27 are

$$\begin{bmatrix} V_1 \\ V_2 \end{bmatrix} = \begin{bmatrix} 1 & 1 \\ e^{-kd} & e^{kd} \end{bmatrix} \begin{bmatrix} V_a \\ V_b \end{bmatrix} \quad (3.42)$$

Thus, the constants V_a and V_b may be expressed as

$$\begin{bmatrix} V_a \\ V_b \end{bmatrix} = \frac{1}{e^{kd} - e^{-kd}} \begin{bmatrix} e^{kd} & -1 \\ -e^{-kd} & 1 \end{bmatrix} \begin{bmatrix} V_1 \\ V_2 \end{bmatrix} \quad (3.43)$$

The transformed current solution from eqs. 2.1 and 3.41 is

$$I(x, s) = -\frac{1}{Z + K} V_x(x, s) = \frac{k}{Z + K} V_a e^{-kx} - \frac{k}{Z + K} V_b e^{kx} \quad (3.44)$$

The port currents of Fig. 27 are

$$\begin{bmatrix} I_1 \\ I_2 \end{bmatrix} = \frac{1}{Z + K} \begin{bmatrix} 1 & 1 \\ -e^{-kd} & e^{kd} \end{bmatrix} \begin{bmatrix} V_a \\ V_b \end{bmatrix} \quad (3.45)$$

Since the admittance matrix for the two-port is defined to be $\begin{bmatrix} I \\ y \end{bmatrix} = \begin{bmatrix} I \\ y \end{bmatrix} \begin{bmatrix} V \\ V \end{bmatrix}$, the admittance matrix results from substituting eq. 3.43 and simplifying

$$\begin{aligned} \begin{bmatrix} y_{11} & y_{12} \\ y_{21} & y_{22} \end{bmatrix} &= \sqrt{\frac{Y+L}{Z+K}} \frac{1}{e^{kd} - e^{-kd}} \begin{bmatrix} e^{kd} + e^{-kd} & -2 \\ -2 & e^{kd} + e^{-kd} \end{bmatrix} \\ &= \sqrt{\frac{Y+L}{Z+K}} \begin{bmatrix} \coth kd & -\operatorname{csch} kd \\ -\operatorname{csch} kd & \coth kd \end{bmatrix} \end{aligned} \quad (3.46)$$

where $k = \sqrt{(Z+K)(Y+L)}$. The radical factor is the reciprocal characteristic impedance of the line from eq. 3.30. The line is reciprocal since $y_{12} = y_{21}$ and has identical driving-point admittances. The other five basic two-port matrices may be easily determined using the standard conversions.

The admittance matrix of the type 2-4 active line is also readily found. The transformed voltage from eq. 3.5 satisfies

$$V_{xx} + (L+K)V_x - (ZY-LK)V = 0 \quad (3.47)$$

Letting $k_1, k_2 = -\frac{1}{2}(L+K) \pm \sqrt{\frac{1}{4}(L-K)^2 + ZY}$, eq. 3.47 has the solution

$$V(x,s) = V_a e^{k_1 x} + V_b e^{k_2 x} \quad (3.48)$$

Then the transformed current from eqs. 2.1 and 3.46 is

$$I(x,s) = -(V_x + KV)/Z = -[(k_1 + K)V_a e^{k_1 x} + (k_2 + K)V_b e^{k_2 x}]/Z \quad (3.49)$$

Repeating the previous manipulations and simplifying,

$$[y] = \frac{1}{Z} \begin{bmatrix} \frac{(k_2 + K)e^{k_1 d} - (k_1 + K)e^{k_2 d}}{e^{k_2 d} - e^{k_1 d}} & \frac{k_1 - k_2}{e^{k_2 d} - e^{k_1 d}} \\ \frac{(k_1 - k_2)e^{(k_1 + k_2)d}}{e^{k_2 d} - e^{k_1 d}} & \frac{(k_2 + K)e^{k_2 d} - (k_1 + K)e^{k_1 d}}{e^{k_2 d} - e^{k_1 d}} \end{bmatrix} \quad (3.50)$$

Because of the symmetrical form of k_1 and k_2 , the matrix elements are readily simplified to

$$y_{11} = \left[\frac{1}{2}(L-K) + \sqrt{\frac{1}{4}(L-K)^2 + ZY} \coth d \sqrt{\frac{1}{4}(L-K)^2 + ZY} \right] / Z \quad (3.51)$$

$$y_{12} = \left[e^{(K+L)d/2} \sqrt{\frac{1}{4}(L-K)^2 + ZY} \operatorname{csch} d \sqrt{\frac{1}{4}(L-K)^2 + ZY} \right] / Z \quad (3.52)$$

$$y_{21} = \left[e^{-(K+L)d/2} \sqrt{\frac{1}{4}(L-K)^2 + ZY} \operatorname{csch} d \sqrt{\frac{1}{4}(L-K)^2 + ZY} \right] / Z \quad (3.53)$$

$$y_{22} = \left[\frac{1}{2}(K-L) + \sqrt{\frac{1}{4}(L-K)^2 + ZY} \coth d \sqrt{\frac{1}{4}(L-K)^2 + ZY} \right] / Z \quad (3.54)$$

The network is nonreciprocal since $y_{21} = e^{-(K+L)d} y_{12}$ except when $K = -L$. The driving-point admittances are unequal unless $K = L$. Standard matrix conversions may again be used to find other parameter sets.

The y parameters for the uniform active line have been derived. In general, these involve hyperbolic functions having irrational arguments. Insight into the voltage gain, bandwidth, stability, and sensitivity of these networks may be gained using infinite product expansions, pole-zero patterns, and Bode plots. For this analysis, rgc active lines are examined. The results are immediately extendable to other line types.

Driving-Point Admittance—Type 1-3 RCG Active Lines

Consider the driving point admittances y_{11} and y_{22} found in eq. 3.46 as

$$y_{11} = y_{22} = \sqrt{\frac{g^* + sc}{r^*}} \coth d \sqrt{r^*(g^* + sc)} \quad (3.55)$$

where again $r^* = r + K$ and $g^* = g + L$. Expressing the coth function as the ratio of cosh and sinh functions and making use of the product expansions (3),

$$\cosh f(s) = \prod_{n=1}^{\infty} \left[1 + \frac{4f^2}{(2n-1)^2 \pi^2} \right] \quad (3.56)$$

$$\frac{\sinh f(s)}{f(s)} = \prod_{n=1}^{\infty} \left[1 + \frac{4f^2}{(2n)^2 \pi^2} \right] \quad (3.57)$$

then

$$y_{11} = \frac{1}{r^*d} \frac{\prod_{n=1}^{\infty} \left[1 + \frac{4d^2 r^* (g^* + sc)}{(2n-1)^2 \pi^2} \right]}{\prod_{n=1}^{\infty} \left[1 + \frac{4d^2 r^* (g^* + sc)}{(2n)^2 \pi^2} \right]} \quad (3.58)$$

Therefore, the zeros of y_{11} are

$$s_z = -g^*/c - (2n-1)^2 \pi^2 / 4d^2 r^* c, \quad n = 1, 2, \dots \quad (3.59)$$

while the poles are

$$s_p = -g^*/c - (2n)^2 \pi^2 / 4d^2 r^* c, \quad n = 1, 2, \dots \quad (3.60)$$

The poles and zeros alternate along the negative real axis of the s -plane beginning with a zero closest the origin and have no finite accumulation point. y_{11} and y_{22} are therefore meromorphic functions.

In the following chapter it is shown that the poles and zeros of any type 1-3 rcg active line have this same character, their exact spacing being set by the parameter distribution. It is clear from eqs. 3.59 and 3.60 that L acts as a translation factor while K is a modified scaling factor. Representing normalized s as s_N where $s =$

$-g^*/c + s_N \pi^2 / 4d^2 r^* c$, the normalized zeros and poles are

$$s_{Nz} = -(2n-1)^2, \quad n = 1, 2, \dots \quad (3.61)$$

$$s_{Np} = -(2n)^2, \quad n = 1, 2, \dots \quad (3.62)$$

respectively. The normalized pole-zero pattern is readily drawn in Fig. 28. Since r and g are nonnegative in classical transmission

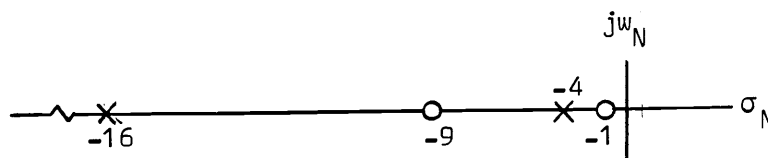


Fig. 28. Normalized pole-zero pattern of y_{11} and y_{22} .

lines, their pole-zero distributions are required to remain in the left-half plane. However, with type 1-3 active lines, r^* and/or g^* can be made negative. Thus, the pattern can be translated along the negative real axis and/or inverted.

The sinusoidal steady-state behavior of y_{11} and y_{22} is clearly shown by constructing the Bode plot of $y_{11}(j\omega)$. For convenience we use frequency ω_N and normalize $y_{11}(j\omega_N)$ against its d.c. value of $1/dr^*$. Under the frequency transformation,

$$y_{11}(s_N) = \frac{1}{r^*d} \frac{\pi}{2} \sqrt{s_N} \coth \frac{\pi}{2} \sqrt{s_N} \quad (3.63)$$

Approximating $|1 + j\omega_N|$ as 1 until frequency $1/a$ is reached and as $a\omega_N$ from that frequency onward, the magnitude plot of Fig. 29 is obtained. The phase plot can be obtained from numerical calculation.

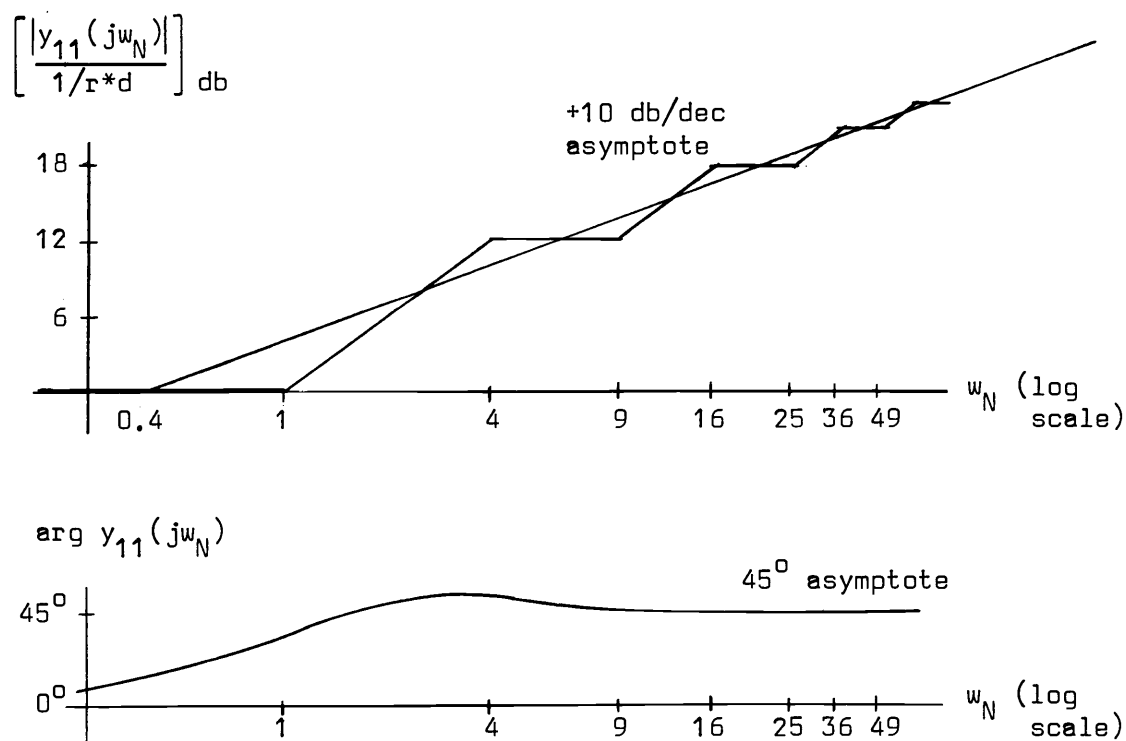


Fig. 29. Bode plots of driving-point admittance y_{11} and y_{22} .

The +10 db/dec high frequency asymptote follows from eq. 3.63. Since $|\coth \pi\sqrt{w_N}/2| \rightarrow 1$ as $w_N \rightarrow \infty$, then $\text{dr}^* |y_{11}(jw_N)| \sim \pi\sqrt{w_N}/2 = \pi\sqrt{w_N}/2$. The corner frequency of the asymptote is $(w_N)_c = (\pi/2)^2 = 0.405$. Since $\arg y_{11}(jw_N) \sim \sqrt{j}$, $\arg y_{11}(jw_N) \rightarrow 45^\circ$ as $w_N \rightarrow \infty$.

From these results it is seen that the (unnormalized) driving-point functions $y_{11}(jw)$ and $y_{22}(jw)$ have d.c. values of $\sqrt{g^*/r^*} \coth d\sqrt{r^*g^*}$, and a 10 db/dec magnitude asymptote with corner frequency $w_c = g^*/c + 0.405\pi^2/4d^2r^*c$. Also the phase of y_{11} and y_{22} approach 45° as $w \rightarrow \infty$.

If the entire pole-zero pattern is reflected into the right-half plane, the magnitude plot is unchanged but the phase becomes $(180^\circ - \arg y_{11}(jw_N))$. If only a portion of the pattern is shifted from one plane to the other, the same high frequency characteristic having a +10 db/dec magnitude asymptote and 45° or 135° phase asymptote is obtained. Thus, it is possible to significantly alter the low frequency characteristic of rcg active lines from that obtainable with rcg passive lines.

Transfer Admittance, Gain, and Bandwidth—Type 1-3 RCG Active Lines

The transfer admittance and gain functions are also readily investigated using Bode plots. From eqs. 3.46 and 3.57,

$$\begin{aligned}
 y_{12} = y_{21} &= -\sqrt{\frac{sc+q^*}{r^*}} \operatorname{csch} d\sqrt{r^*(g^*+sc)} \\
 &= -\frac{1}{\operatorname{dr}^*} \prod_{n=1}^{\infty} \left[1 + \frac{4d^2r^*(q^*+sc)}{(2n)^2\pi^2} \right]^{-1} \quad (3.64)
 \end{aligned}$$

The open-circuit voltage gain and short-circuit current gain T from eq. 3.46 is

$$T(s) = -\frac{y_{21}}{y_{22}} = -\frac{y_{21}}{y_{11}} = \frac{1}{\cosh d \sqrt{r^*(g^*+sc)}}$$

$$= \prod_{n=1}^{\infty} \left[1 + \frac{4d^2 r^*(g^*+sc)}{(2n-1)^2 \pi^2} \right]^{-1} \quad (3.65)$$

These functions have only poles distributed along the negative real axis which are given by eqs. 3.62 and 3.61, respectively. Thus, they have monotonically decreasing magnitude and phase functions. Consider for example the gain function $T(s)$. The normalized gain function

$$T(s_N) = 1/\cosh \pi \sqrt{s_N} / 2 \quad (3.66)$$

has poles given by eq. 3.61. From the corresponding pole-zero pattern of Fig. 30, the Bode plots of the normalized gain function are readily drawn in Fig. 31. Except for normalization factors, the y_{12} and y_{21} plots are identical to Fig. 31.

If the active line is terminated in some load admittance Y_L , then the voltage gain from eq. 3.46 becomes

$$T_V(s) = \frac{-y_{21}}{y_{22} + Y_L} = \left[\cosh d \sqrt{r^*(g^*+sc)} + Y_L dr^* \frac{\sinh d \sqrt{r^*(g^*+sc)}}{d \sqrt{r^*(g^*+sc)}} \right]^{-1} \quad (3.67)$$

The gain function has no zeros. Its poles are given by the values of s satisfying

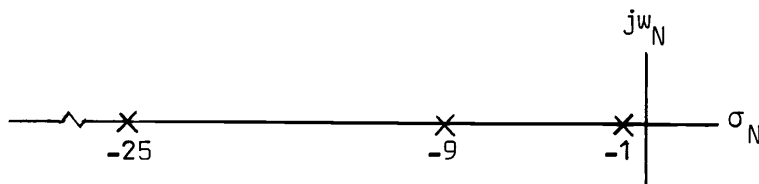


Fig. 30. Normalized pole-zero pattern of gain T .

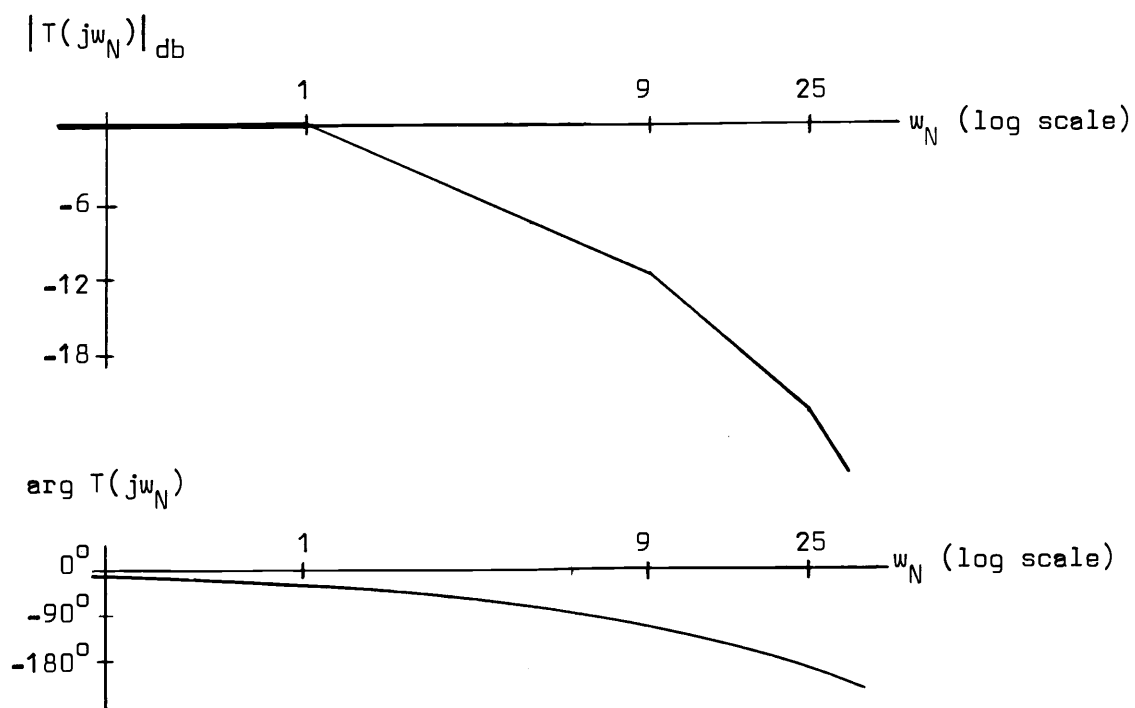


Fig. 31. Bode plots of gain T .

$$\cosh d \sqrt{r^*(g^*+sc)} + Y_L d r^* \frac{\sinh d \sqrt{r^*(g^*+sc)}}{d \sqrt{r^*(g^*+sc)}} = 0 \quad (3.68)$$

which is an equation of the form $F_1(s) + Y_L F_2(s) = 0$ to which root locus analysis techniques may be applied. The root locus of this expression may be determined for Y_L varying between 0 and ∞ . This assumes a resistive load but other type loads can equally well be used (16). Referring to Fig. 32, the normalized root locus begins at the zeros and travels along the negative real axis to the poles as the

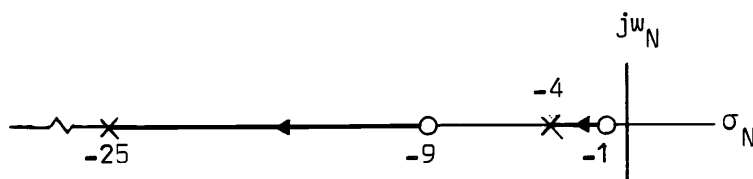


Fig. 32. Normalized root locus for poles of T_V as Y_L varies from 0 to ∞ .

load admittance is increased from zero to infinity. Thus, as the load resistance goes from infinity towards zero, the bandwidth increases and the gain decreases.

For the unterminated system, the bandwidth is determined by setting $|T(j\omega_N)| = 0.707$ in eq. 3.66 which yields

$$|T(j\omega_N)|^{-2} = |\cosh (1+j1)\theta/2|^2 = \frac{1}{2}(\cosh \theta + \cos \theta) = 2 \quad (3.69)$$

where $\theta = \pi \sqrt{\omega_N}/2$. Since the response is monotonic, the solution for θ is unique. Solving by iteration using $\theta_{n+1} = \cosh^{-1} (4 - \cos \theta_n)$ yields $\theta = 2.2$. Thus, the normalized 3 db radian frequency $(\omega_N)_{3db} = 0.98$. The corresponding 3 db Hertzian frequency is $(f_N)_{3db} = 0.156$. Therefore, the unnormalized 3 db radian frequency is

$$\omega_{3db} = g^*/c + 0.98\pi^2/4d^2r^*c = g^*/c + 2.2/d^2r^*c \quad (3.70)$$

or

$$f_{3db} = 0.159g^*/c + 0.35/d^2r^*c \quad (3.71)$$

for active transmission lines having pole patterns lying entirely in either half plane. When the pattern lies in both half planes, more involved calculations are required.

Step Response, Stability, Rise and Delay Time—Type 1-3 RCG Active Lines

Rise time and delay time of the unit step response are important quantities but quantitatively difficult to find. The unit step response of the network is found from eq. 3.65 to be

$$V_2(s) = \left[s \cosh d \sqrt{r^*(g^*+sc)} \right]^{-1} \quad (3.72)$$

which may readily be evaluated by the method of residues. Since

$$\begin{aligned}
\mathcal{L}^{-1}(s \cosh \sqrt{bs+a})^{-1} &= \mathcal{L}^{-1} \left[s \prod_{n=1}^{\infty} \left[1 + \frac{4(bs+a)}{(2n-1)^2 \pi^2} \right] \right]^{-1} \\
&= \left\{ \frac{1}{\cosh \sqrt{a}} + \sum_{n=1}^{\infty} \left[\frac{2e^{st}}{sb \frac{\sinh \sqrt{bs+a}}{\sqrt{bs+a}}} \right]_{s = -\frac{a}{b} - \frac{(2n-1)^2}{b} \left(\frac{\pi}{2}\right)^2} \right\} u(t) \\
&= \left[\frac{1}{\cosh \sqrt{a}} + 2e^{-\frac{a}{b}t} \sum_{n=1}^{\infty} \frac{(-1)^n e^{-\frac{(2n-1)^2}{b} \left(\frac{\pi}{2}\right)^2 t}}{\frac{2}{\pi} \frac{a}{2n-1} + (2n-1) \frac{\pi}{2}} \right] u(t) \quad (3.73)
\end{aligned}$$

for all a and b except $-a = (2n-1)^2 (\pi/2)^2$ for $n = 1, 2, \dots$ (this insures a single pole at the origin), the solution is written immediately as

$$v_2(t) = \left[\frac{1}{\cosh d \sqrt{r^*g^*}} + 2e^{-\frac{g^*}{c}t} \sum_{n=1}^{\infty} \frac{(-1)^n e^{-\frac{(2n-1)^2 \left(\frac{\pi}{2}\right)^2 \frac{t}{r^*cd^2}}}{\frac{2}{\pi} \frac{d^2 r^*g^*}{2n-1} + (2n-1) \frac{\pi}{2}} \right] u(t) \quad (3.74)$$

Another expression may be found by expressing the cosh function in an exponential series where

$$\left[s \cosh \sqrt{bs+a} \right]^{-1} = \frac{2}{s} \sum_{n=0}^{\infty} (-1)^n e^{-(2n+1)\sqrt{bs+a}}, \quad \text{Re } \sqrt{bs+a} > 0 \quad (3.75)$$

Since (26, p. 255)

$$\begin{aligned}
\mathcal{L}^{-1} \left[\frac{e^{-c\sqrt{bs+a}}}{s} \right] &= \left[\frac{e^{-c\sqrt{a}}}{2} \text{erfc} \left(\frac{c}{2\sqrt{t}} \sqrt{\frac{b}{t}} - \sqrt{\frac{at}{b}} \right) \right. \\
&\quad \left. + \frac{e^{c\sqrt{a}}}{2} \text{erfc} \left(\frac{c}{2\sqrt{t}} \sqrt{\frac{b}{t}} + \sqrt{\frac{at}{b}} \right) \right] u(t) \quad (3.76)
\end{aligned}$$

for $\text{Re } s > 0$ and $a, b > 0$, the voltage solution can also be written in terms of complementary error functions as

$$v_2(t) = \left[\sum_{n=0}^{\infty} (-1)^n \left[e^{-(2n+1)d\sqrt{r^*g^*}} \operatorname{erfc} \left(\frac{2n+1}{2} \sqrt{\frac{r^*cd^2}{t}} - \sqrt{\frac{g^*}{c}} t \right) \right. \right. \quad (3.77)$$

$$\left. \left. + e^{(2n+1)d\sqrt{r^*g^*}} \operatorname{erfc} \left(\frac{2n+1}{2} \sqrt{\frac{r^*cd^2}{t}} + \sqrt{\frac{g^*}{c}} t \right) \right] \right] u(t)$$

for r^* and $g^* > 0$. Although the involved expressions of eqs. 3.74 and 3.77 represent a function monotonically increasing from 0 to $1/\cosh d\sqrt{r^*g^*}$, they are tedious to evaluate.

The dominant root and excess phase functions can be used to advantage in approximating network functions such as the unit step response (9). With this method, the function $F(s)$,

$$F(s) = F(0) \frac{N(s)}{D(s)} = F(0) \frac{1+a_1s+a_2s^2+\dots}{1+b_1s+b_2s^2+\dots} = F(0) \frac{\prod_{n=1}^{\infty} (1+s/z_n)}{\prod_{n=1}^{\infty} (1+s/p_n)} \quad (3.78)$$

with an infinite (or finite) number of poles p_n and zeros z_n is approximated by

$$F_a(s) = F(0) \frac{(1+s/z_e) \exp(sm_z/z_e)}{(1+s/p_e) \exp(sm_p/p_e)} \quad (3.79)$$

z_e and p_e are the effective dominant zero and pole, and are numerically equal to the 3 db radian frequencies, ω_{3db} , of numerator and denominator magnitudes, respectively. The excess phase factors, m_z and m_p , are chosen so the phases of numerator and denominator of $F_a(j\omega)$ equal the phases of the numerator and denominator of $F(j\omega)$ at ω_{3db} , respectively. Kelly and Ghauri have shown that (15)

$$z_e = \left[\frac{c_1^2 - c_2}{c_1^3} \right]^{\frac{1}{2}} \quad (3.80)$$

$$m_z = \frac{-c_2/c_1^2}{2+c_2/c_1^2} + z_e \left[a_1 - \frac{1}{1+c_2 z_e/c_1^2} \right] \quad (3.81)$$

$$p_e = \left[\frac{d_1^2 - d_2}{d_1^3} \right]^{1/2} \quad (3.82)$$

$$m_p = \frac{-d_2/d_1^2}{2+d_2/d_1^2} + p_e \left[b_1 - \frac{1}{1+d_2 p_e/d_1^2} \right] \quad (3.83)$$

where $c_1 = a_1^2 - 2a_2$, $d_1 = b_1^2 - 2b_2$, $c_2 = a_2^2 - 2a_1 a_3 + a_4^2$, and $d_2 = b_2^2 - 2b_1 b_3 + b_4^2$. Applying eq. 3.79 to eq. 3.72, the output voltage $V_2(s)$ is approximated as

$$V_2(s) = \frac{1}{\cosh d \sqrt{r^* g^*}} \frac{1}{s(1+s/p_e) \exp(s m_p/p_e)} \quad (3.84)$$

so that

$$v_2(t) = \frac{1}{\cosh d \sqrt{r^* g^*}} (1 - e^{-p_e t}) u(t - m_p/p_e) \quad (3.85)$$

Thus, the approximate response rises exponentially from 0 to $1/\cosh d \sqrt{r^* g^*}$ volts with a time constant of $1/p_e$ seconds after a time delay of m_p/p_e seconds. The general expressions for p_e and m_p are prohibitively complicated but can be readily evaluated when numerical values of r^* , g^* and c are specified.

Since the response function of a causal linear network can have no poles in the right-half s -plane if the network is to be stable, several pertinent points can be made. The type 1-3 active line is stable if and only if all the poles of $T(s)$ (eq. 3.65) given by eq. 3.59 are in the left-half plane. Therefore, it is necessary that $r^* > 0$ and $g^* > -\pi^2/4d^2 r^*$ for the system to be stable. Returning

to the step response in eq. 3.74, this condition limits the exponents of the exponential terms of the sum to be negative so that the response is bounded.

An empirical result (30) often used for networks having monotonic frequency response relates the (10-90%) rise time t_r to f_{3db} as $f_{3db} t_r = 0.35$.⁷ Thus, from eq. 3.71, the reciprocal rise time for the active line is

$$t_r^{-1} = 0.455g^*/c + 1/d^2 r^* c \quad (3.86)$$

From eqs. 3.71, 3.86, and 3.65, increasing g^* or decreasing r^* increases the bandwidth, decreases rise time, and decreases or increases low frequency gain, respectively.

Elmore's method for finding both (0-50%) delay time, t_d , and rise time, t_r , for networks having monotonic frequency response can also be used (6). Denoting the normalized gain of the network as

$$\frac{T(s)}{T(0)} = \frac{1 + a_1 s + \dots}{1 + b_1 s + \dots} = 1 - (b_1 - a_1)s + (b_1^2 - a_1 b_1 + a_2 - b_2)s^2 + \dots \quad (3.87)$$

it can be shown that (9)

$$\frac{T(s)}{T(0)} = 1 - t_d s + (t_d^2 + t_r^2 / 2\pi)^2 s^2 / 2 + \dots \quad (3.88)$$

From these results,

$$t_d = b_1 - a_1 \quad (3.89)$$

$$t_r = \sqrt{2\pi [b_1^2 - a_1^2 + 2(a_2 - b_2)]}^{\frac{1}{2}} \quad (3.90)$$

It is an interesting and useful result that the coefficients of s and

⁷This follows immediately from the product of $f_{3db} = p_e / 2\pi$ in eq. 3.84 and $t_r = 2.2/p_e$ in eq. 3.105.

s^2 in the numerator and denominator polynomials of the normalized gain function can be used to approximate rise and delay times.

Consider the gain function of eq. 3.65 when $g^* = 0$. The cosh function of the denominator can be expanded in the series

$$\cosh d\sqrt{r^*c} = 1 + \frac{d^2 r^* c}{2!} s + \frac{(d^2 r^* c)^2}{4!} s^2 + \dots, \quad |s| < \infty \quad (3.91)$$

Comparing eq. 3.91 with eqs. 3.89 and 3.90, the delay and rise times are

$$t_d = 0.5d^2 r^* c \quad (3.92)$$

$$t_r = \sqrt{2\pi} \left[\frac{1}{4} - \frac{1}{12} \right]^{\frac{1}{2}} d^2 r^* c = \sqrt{\frac{\pi}{3}} d^2 r^* c = 1.02d^2 r^* c \quad (3.93)$$

Note that t_r is in good agreement with eq. 3.86 for $g^* = 0$. If g^* is nonzero, these expressions become more involved.

Express the denominator of the gain function eq. 3.65 as

$$\cosh \sqrt{a+bs} = \sum_{n=0}^{\infty} \frac{(a+bs)^n}{(2n)!}, \quad |s| < \infty \quad (3.94)$$

where $a = d^2 r^* g^*$ and $b = d^2 r^* c$. Using the binomial theorem

$$(a+bs)^n = \sum_{k=0}^n \binom{n}{k} a^{n-k} (bs)^k, \quad |s| < \left| \frac{a}{b} \right| \quad (3.95)$$

eq. 3.94 can be written as

$$\begin{aligned} \cosh \sqrt{a+bs} &= \sum_{n=0}^{\infty} \sum_{k=0}^n \frac{1}{(2n)!} \binom{n}{k} a^{n-k} (bs)^k \\ &= \sum_{k=0}^{\infty} \left[\sum_{n=k}^{\infty} \frac{1}{(2n)!} \binom{n}{k} b^k a^{n-k} \right] s^k = \sum_{k=0}^{\infty} B_k s^k, \quad |s| < \left| \frac{a}{b} \right| \end{aligned} \quad (3.96)$$

where B_k is

$$B_k = \frac{b^k}{k!} \sum_{n=0}^{\infty} \frac{(n+k)!}{(2(n+k))!n!} a^n = \frac{b^k}{k!} \frac{d^k}{da^k} \sum_{n=0}^{\infty} \frac{a^{n+k}}{(2(n+k))!} = \frac{b^k}{k!} \frac{d^k \cosh \sqrt{a}}{da^k} \quad (3.97)$$

The B_k coefficients when normalized against B_0 are the b_k of the general gain expression eq. 3.87 (the $a_k=0$). Evaluating the first three B 's,

$$B_0 = \cosh \sqrt{a} \quad (3.98)$$

$$B_1 = \frac{b}{2} \frac{\sinh \sqrt{a}}{\sqrt{a}} \quad (3.99)$$

$$B_2 = \left(\frac{b}{2}\right)^2 \frac{1}{2} \left[\frac{\cosh \sqrt{a}}{a} - \frac{\sinh \sqrt{a}}{a\sqrt{a}} \right] \quad (3.100)$$

Normalizing B_1 and B_2 and substituting into eqs. 3.89 and 3.90 gives the delay and rise time as

$$t_d = \frac{b}{2\sqrt{a}} \tanh \sqrt{a} \quad (3.101)$$

$$t_r = \sqrt{\frac{\pi}{2}} \frac{b}{\sqrt{a}} \left[\frac{\tanh \sqrt{a}}{\sqrt{a}} - \operatorname{sech}^2 \sqrt{a} \right]^{\frac{1}{2}} \quad (3.102)$$

Since $a = d^2 r^* g^*$ and $b = d^2 r^* c$,

$$t_d = \frac{dc}{2} \sqrt{\frac{r^*}{g^*}} \tanh d \sqrt{r^* g^*} \quad (3.103)$$

$$t_r = dc \sqrt{\frac{r^*}{g^*}} \sqrt{\frac{\pi}{2}} \left[\frac{\tanh d \sqrt{r^* g^*}}{d \sqrt{r^* g^*}} - \operatorname{sech}^2 d \sqrt{r^* g^*} \right]^{\frac{1}{2}} \quad (3.104)$$

Eqs. 3.103 and 3.104 reduce to eqs. 3.92 and 3.93, respectively, as $g^* \rightarrow 0$.

If the dominant pole and excess phase approximation method is used, it is readily shown that

$$t_r = \frac{2.2}{p_e} \quad (3.105)$$

$$t_d = \frac{0.69 + m_p}{p_e} \quad (3.106)$$

by solving the approximate unit step response (eq. 3.85) for rise and delay times. Here, the dead time m_p/p_e of the system is added to the calculated delay time.

Sensitivity—Type 1-3 RCG Active Lines

A question of considerable importance is the sensitivity of two-port gain to variations in distributed source strengths. The sensitivity of dependent variable y with respect to independent variable x is defined to be

$$S_x^y = \frac{\partial y}{\partial x} \frac{y}{x} = \frac{\partial(\ln y)}{\partial(\ln x)} \quad (3.107)$$

and measures the variability of y for variations in x . It is approximately equal to the logarithmic change in y per unit logarithmic change in x where all other independent variables are held fixed. A zero sensitivity of y at x_0 indicates the magnitude plot of $\ln y$ versus $\ln x$ has zero slope at x_0 . Minimizing sensitivity magnitude often forms a valuable design guide.

The sensitivity of the gain function $T(s)$ given by eq. 3.65 with respect to K and L from eq. 3.107 is

$$S_K^T = -\frac{K}{2} d^2 (g^* + sc) \frac{\tanh d \sqrt{(r+K)(g^* + sc)}}{d \sqrt{(r+K)(g^* + sc)}} \quad (3.108)$$

$$S_L^T = -\frac{L}{2} d^2 r^* \frac{\tanh d \sqrt{r^*(L+g+sc)}}{d \sqrt{r^*(L+g+sc)}} \quad (3.109)$$

respectively. These expressions are readily interpreted using pole-zero patterns and Bode plots. Their zeros are given by eq. 3.60 while their poles are given by eq. 3.59. They have normalized values given by eqs. 3.62 and 3.61. S_K^T has an additional zero at $s = -g^*/c$ or $s_N = 0$. Thus the normalized pole-zero patterns of S_K^T and S_L^T are given in Fig. 33 and 34, respectively. The normalized Bode plots of the sensitivity magnitudes are readily drawn Figs. 35 and 36.

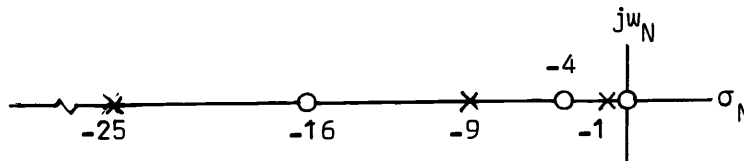


Fig. 33. Normalized pole-zero pattern of S_K^T .

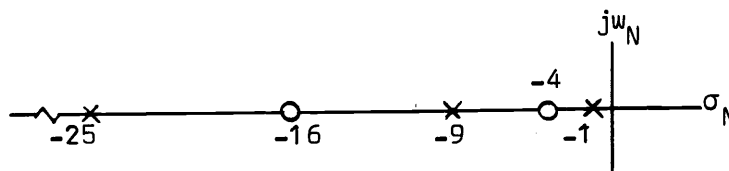


Fig. 34. Normalized pole-zero pattern of S_L^T .

$$\left[\frac{|S_K^T(jw_N)|}{\frac{\pi^2}{8(1+r/K)}} \right] \text{ db}$$

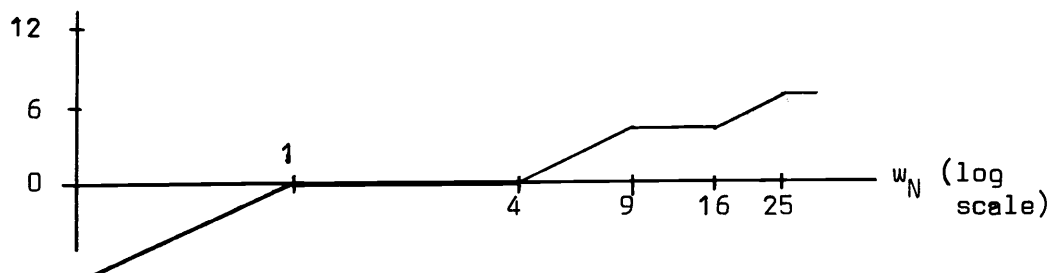


Fig. 35. Bode magnitude plot of sensitivity S_K^T .

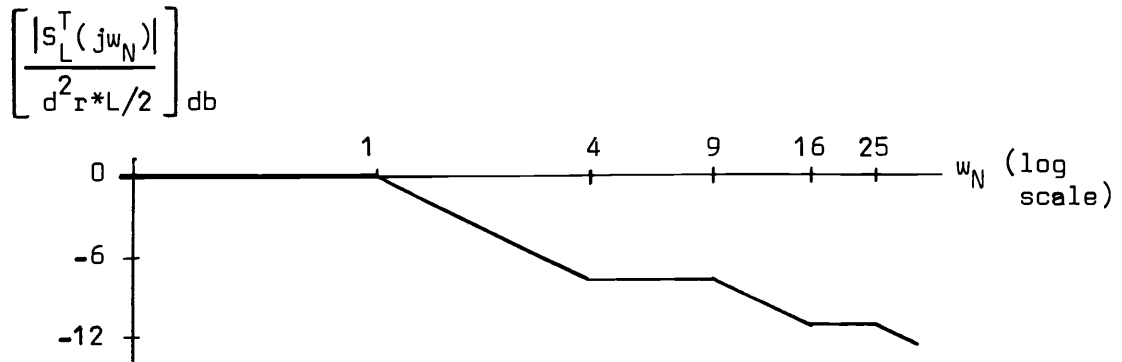


Fig. 36. Bode magnitude plot of sensitivity S_L^T .

$|S_K^T(jw)|$ has a d.c. value of

$$|S_K^T(0)| = \frac{Kd^2g^* \tanh d\sqrt{g^*(r+K)}}{2d\sqrt{g^*(r+K)}} \quad (3.110)$$

and increases monotonically with asymptotic slope +10 db/dec as $w \rightarrow \infty$. We noted for a stable system that $r^* > 0$ which implies $K > -r$ and that $g^* > -\pi^2/4d^2r^*$. Under these conditions, reducing K towards zero decreases the sensitivity at any frequency towards zero. This confirms the intuitive result that reducing the equivalent series resistance K reduces the gain sensitivity with respect to K of the two-port.

$|S_L^T(jw)|$ has a d.c. value of

$$|S_L^T(0)| = \frac{Ld^2r^* \tanh d\sqrt{r^*(g+L)}}{2d\sqrt{r^*(r+L)}} \quad (3.111)$$

and decreases monotonically with asymptotic slope -10 db/dec as $w \rightarrow \infty$. Again for a stable system, $r^* > 0$ and $L > -g-\pi^2/4d^2r^*$. Here, reducing the equivalent shunt conductance L towards zero decreases the sensitivity at any frequency towards zero.

This completes consideration of type 1-3 rcg active lines. Type 2-4 rcg active lines are now investigated.

Driving-Point Admittance—Type 2-4 RCG Active Lines

The driving-point admittances of type 2-4 active lines were given in eqs. 3.51 and 3.54. For rcg active lines, the admittances equal

$$y_{11} = \frac{1}{rd} \left[\frac{1}{2}(L-K) + \sqrt{\frac{1}{4}(L-K)^2 + r(g+sc)} \coth d \sqrt{\frac{1}{4}(L-K)^2 + r(g+sc)} \right] \quad (3.112)$$

$$y_{22} = \frac{1}{rd} \left[\frac{1}{2}(L-K) - \sqrt{\frac{1}{4}(L-K)^2 + r(g+sc)} \coth d \sqrt{\frac{1}{4}(L-K)^2 + r(g+sc)} \right] \quad (3.113)$$

If $K = L$, then y_{11} equals y_{22} and has the characteristics of eq. 3.55 discussed previously. The more general case where $K \neq L$ can be expressed as

$$y_{11} = \frac{1}{rd} \frac{\cosh f + \frac{1}{2}d(L-K) \frac{\sinh f}{f}}{\frac{\sinh f}{f}} \quad (3.114)$$

$$y_{22} = \frac{1}{rd} \frac{\cosh f - \frac{1}{2}d(L-K) \frac{\sinh f}{f}}{\frac{\sinh f}{f}} \quad (3.115)$$

where $f = d \sqrt{\frac{1}{4}(L-K)^2 + r(g+sc)}$. The poles of the driving-point functions eqs. 3.112 and 3.113 are given by eq. 3.57 as

$$s_p = -\frac{1}{c} \left[g + \frac{(L-K)^2}{4r} \right] - (2n)^2 \frac{\pi^2}{4d^2 rc}, \quad n = 1, 2, \dots \quad (3.116)$$

The poles of y_{11} and y_{22} are translated further from the origin along the negative real axis by making $K \neq L$. This is in contrast with the reflection and bidirectional translation properties of type 1-3 active lines. Introducing normalized complex frequency s_N where $s =$

$$-\frac{1}{c} \left[g + \frac{(L-K)^2}{4r} \right] + \frac{\pi^2}{4d^2 rc} s_N, \text{ the normalized poles of the driving-}$$

point functions are given by eq. 3.62.

The zeros of y_{11} and y_{22} are determined from the zeros of

$$\cosh f + \frac{1}{2}d(L-K) \frac{\sinh f}{f} = 0 \quad (3.117)$$

$$\cosh f - \frac{1}{2}d(L-K) \frac{\sinh f}{f} = 0 \quad (3.118)$$

respectively. Under the frequency normalization, the normalized zeros satisfy eqs. 3.117 and 3.118 when $f = \pi \sqrt{s_N}/2$. A general solution to the transcendental equations is not expressible in closed form. However a root locus technique, generalized to account for negative values of $\frac{1}{2}d(L-K)$ as well as positive values, can be employed to draw the normalized root locus of eqs. 3.117 and 3.118. It is instructive to form the root locus indirectly from graphical considerations.

Letting

$$N(f) = \cosh f + k \frac{\sinh f}{f} = 0 \quad (3.119)$$

where $k = \frac{1}{2}d(L-K)$ is real, the zeros of $N(f)$ are determined by letting $f = u + jv$, and then separating and equating real and imaginary parts to zero. Examining the resulting equations, it is found that the zeros must lie on the jv -axis of the complex f -plane. Additionally, there is a double zero at the origin for $k = -1$ and two real zeros $\pm u_1$ for $k < -1$.

The imaginary roots satisfy

$$\tan v = -\frac{v}{k} \quad (3.120)$$

excluding the first pair for $k < -1$. For $k \leq -1$, the real root pair satisfy

$$\tanh u = -\frac{u}{k} \quad (3.121)$$

Plotting the periodic function $\tan v$ and the line $(-v/k)$ having slope $(-1/k)$ in Fig. 37, the v values at intersection points $\pm v_1$,

${}^+v_2, \dots$ are the zeros of eq. 3.120. Note that as $k \rightarrow -1$, ${}^+v_1 \rightarrow 0$, so that the first pair of imaginary zeros approach the origin. For $k < -1$ these zeros move onto the real axis of the f -plane.

Plotting the function $\tanh u$ and the line $(-u/k)$ in Fig. 38, the u values at intersection points ${}^+u_1$ are the two real zeros of eq. 3.119 for $k \leq -1$. Thus for $k < -1$, eq. 3.119 has these two real zeros ${}^+u_1$ and an infinite number of imaginary zeros ${}^+jv_2, {}^+jv_3, \dots$

The behavior of the zeros of $N(f)$ is summarized in the root locus for $N(f)$ drawn in Fig. 39 for k varying between $-\infty$ and $+\infty$. The zeros

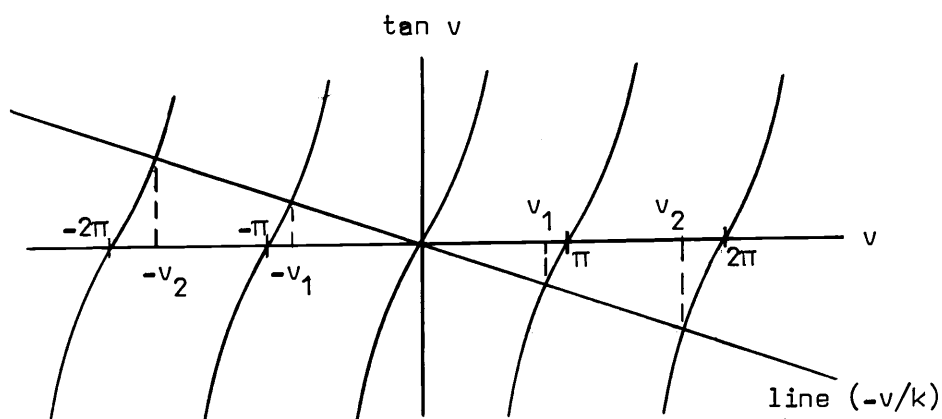


Fig. 37. Graphical construction yielding the imaginary zeros of eq. 3.119 (excluding the first pair for $k < -1$).

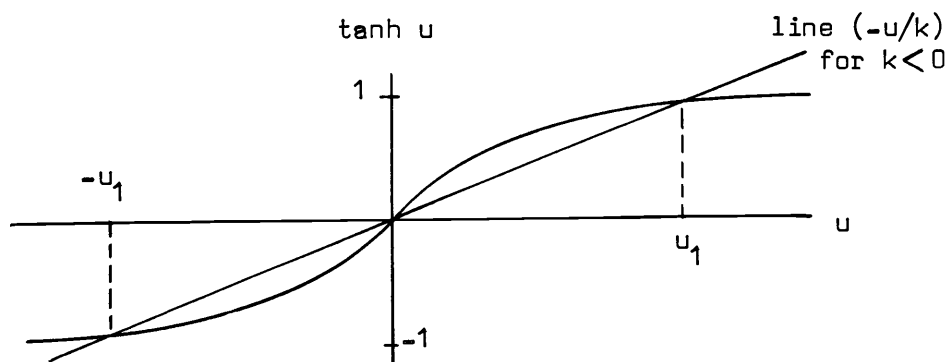


Fig. 38. Graphical construction yielding the real zero pair of eq. 3.119 for $k \leq -1$.

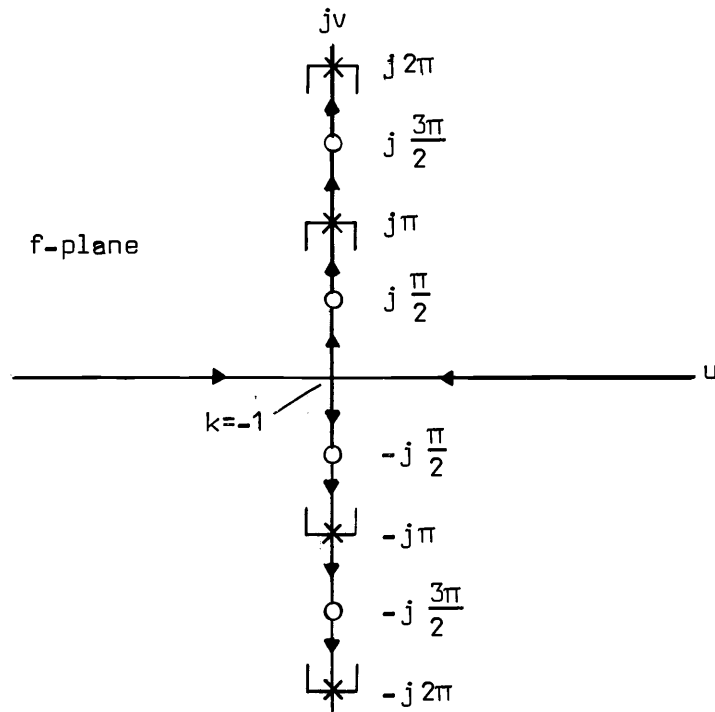


Fig. 39. Root locus for $N(f)$ as k varies from $-\infty$ to $+\infty$.

$^+ jv_n$ of $N(f)$ are bounded by

$$(2n-1) \frac{\pi}{2} < jv_n \leq (2n) \frac{\pi}{2}, \quad n = 1, 2, \dots \quad (3.122)$$

for $k > 0$, and by

$$(2n-2) \frac{\pi}{2} \leq jv_n < (2n-1) \frac{\pi}{2}, \quad n = 2, 3, \dots \quad (3.123)$$

for $k < 0$. The first zeros $^+ jv_1$ are imaginary for $-1 < k < 0$ where

$$0 < jv_1 \leq \frac{\pi}{2} \quad (3.124)$$

but have real values $^+ u_1$ for $k \leq -1$ where

$$0 \leq u_1 < \infty \quad (3.125)$$

Since $N(f)$ given by eq. 3.119 does not have an essential singularity in the finite f -plane, it can be expressed as an infinite product

in terms of its zeros using the Weierstrass factor theorem (33).⁸

Therefore

$$N(f) = c \prod_{n=1}^{\infty} (f + jv_n)(f - jv_n) = c \prod_{n=1}^{\infty} (f^2 + v_n^2) \quad (3.126)$$

for $k > -1$ and

$$N(f) = c(f + u_1)(f - u_1) \prod_{n=2}^{\infty} (f^2 + v_n^2) \quad (3.127)$$

for $k \leq -1$, where c is a constant.

Recalling that normalized complex frequency $s_N = (2/\pi)^2 f^2$, the normalized zeros of y_{11} and y_{22} in the s_N -plane must equal

$$s_{Nn} = -(2/\pi)^2 v_n^2 = -(2v_n/\pi)^2, \quad n = 1, 2, \dots \quad (3.128)$$

where $s_{N1} = -(2u_1/\pi)^2$ if $k \leq -1$. Thus, the normalized zeros of the admittance functions y_{11} (eq. 3.117) and y_{22} (eq. 3.118) can be bounded as

$$-(2n)^2 \leq s_{Nn} < -(2n-1)^2, \quad n = 1, 2, \dots \quad (3.129)$$

for $k > 0$, and as

$$-(2n-1)^2 < s_{Nn} \leq -(2n-2)^2, \quad n = 2, 3, \dots \quad (3.130)$$

for $k < 0$. The first zero s_1 is bounded by

$$-1 \leq s_{N1} < 0 \quad (3.131)$$

for $-1 < k < 0$ and

$$-\infty < s_{N1} \leq 0 \quad (3.132)$$

for $k \leq -1$.

⁸ A function has an essential singularity at point p_0 if its Laurent series representation in the region surrounding p_0 possesses an infinite number of $(p-p_0)$ terms having negative exponents.

The normalized root locus for the zeros of the driving-point admittances is drawn in Fig. 40 from eq. 3.128 and Fig. 39. The locus depends on the $(L-K)$ value since $k = \frac{1}{2}d(L-K)$. The normalized poles of y_{11} and y_{22} , given by eq. 3.62, are located at $-(2n)^2$ for $n = 1, 2, \dots$. Thus in the root locus, every zero of y_{11} moves between its adjacent poles; i.e. z_{N2} begins at -4 and terminates at -16 , z_{N3} begins at -16 and terminates at -25 , etc. Note the z_{N1} begins at $-\infty$, travels through the origin (corresponding to unnormalized frequency $s = -g/c - 1/d^2rc$), and terminates at -4 . y_{22} has the same characteristics with a change in arrow direction.

Since complex frequency s was normalized so $s = -\frac{1}{c} \left[g + \frac{(L-K)^2}{4r} \right] + \frac{\pi^2}{4d^2rc} s_N$, increasing $(L-K)$ from zero has two effects on the (unnormalized) pole-zero pattern of y_{11} and y_{22} . First, the entire pattern is translated further from the origin along the negative real axis. Second, the zeros of y_{11} approach the poles of y_{11} while the zeros of y_{22} move away from the poles (with the exception of the first zero of y_{22}).

The sinusoidal steady-state character of y_{11} and y_{22} can also be assessed from the root locus diagram. Since the poles and zeros of y_{11} in Fig. 40 interlace with a zero closest the origin for $L-K \geq -4.14/d$,

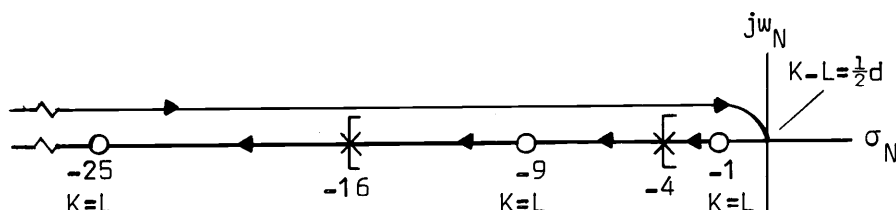


Fig. 40. Normalized root locus of zeros of y_{11} as $(L-K)$ varies from $-\infty$ to $+\infty$ (or y_{22} reversing the arrow direction).

the Bode plots have the same monotonic increasing character as Fig. 29. The poles and zeros of y_{22} also interlace with a zero closest the origin for $L-K \leq 4.14/d$. When $L-K < -4.14/d$, y_{11} has a pole closest the origin; when $L-K > 4.14/d$, y_{22} has a pole closest the origin. Their Bode plots must have +10 db/dec magnitude asymptotes and 45° phase asymptotes. Increasing $(L-K)$ from zero increases the bandwidth of y_{11} while the bandwidth of y_{22} decreases slightly and then increases.

From eqs. 3.112 and 3.113, y_{11} and y_{22} must have d.c. values of

$$y_{11}(0) = \frac{1}{rd} \left[\frac{1}{2}d(L-K) + d \sqrt{\frac{1}{4}(L-K)^2 + rg} \coth d \sqrt{\frac{1}{4}(L-K)^2 + rg} \right] \quad (3.133)$$

$$y_{22}(0) = \frac{1}{rd} \left[\frac{1}{2}d(K-L) + d \sqrt{\frac{1}{4}(L-K)^2 + rg} \coth d \sqrt{\frac{1}{4}(L-K)^2 + rg} \right] \quad (3.134)$$

Clearly, increasing $(L-K)$ from zero to infinity increases the magnitude of $y_{11}(0)$ indefinitely but decreases $y_{22}(0)$ towards zero. For $L-K = 0$,

$$y_{11}(0) = y_{22}(0) = d \sqrt{rg} \coth d \sqrt{rg} \quad (3.135)$$

In passing it should be noted that the series solutions to eq. 3.119 have been investigated (15). Following Kelly and Ghausi, express the n^{th} positive imaginary zero of eq. 3.119 as

$$v_n = (2n-1)\pi/2 + c_n \quad (3.136)$$

where c_n is the correction factor due to nonzero $k = \frac{1}{2}d(L-K)$. Since

v_n satisfies eq. 3.120

$$(2n-1)\pi/2 + c_n = -k \tan \left[(2n-1)\pi/2 + c_n \right] = k \cot c_n \quad (3.137)$$

the n^{th} correction satisfies

$$c_n = \cot^{-1} \frac{1}{k} \left[(2n-1)\pi/2 + c_n \right] \quad (3.138)$$

Using the series expansion for $\cot^{-1} x$ and solving for c_n by iteration,

its approximation for $|k| < 8$, accurate to at least 3%, is

$$c_n = (2n-1) \frac{\pi}{2} \left[\frac{k}{(2n-1)^2 (\pi/2)^2 + k} \right] \quad (3.139)$$

so that

$$v_n = (2n-1) \frac{\pi}{2} \left[1 + \frac{4k}{(2n-1)^2 \pi + 4k} \right] \quad (3.140)$$

Thus, the normalized zeros of y_{11} , eq. 3.114, for $|d(L-K)| < 16$ are

$$s_{Nz} = -(2n-1)^2 \left[1 + \frac{4d(L-K)}{(2n-1)^2 \pi + 2d(L-K)} \right], \quad n = 1, 2, \dots \quad (3.141)$$

The normalized zeros of y_{22} are given by eq. 3.141 by replacing $(L-K)$ by $(K-L)$. Returning to Fig. 40, these are the zeros when $L \approx K$.

Transfer Admittance, Gain, and Bandwidth—Type 2-4 RCG Active Lines

The transfer admittances from eqs. 3.52 and 3.53 are

$$y_{12} = \frac{1}{rd} e^{\frac{1}{2}d(k+L)} d \sqrt{\frac{1}{4}(L-K)^2 + r(g+sc)} \operatorname{csch} d \sqrt{\frac{1}{4}(L-K)^2 + r(g+sc)} \quad (3.142)$$

$$y_{21} = \frac{1}{rd} e^{-\frac{1}{2}d(k+L)} d \sqrt{\frac{1}{4}(L-K)^2 + r(g+sc)} \operatorname{csch} d \sqrt{\frac{1}{4}(L-K)^2 + r(g+sc)} \quad (3.143)$$

Using the product expansions of eq. 3.57

$$y_{12} = \frac{1}{rd} e^{\frac{1}{2}d(k+L)} \left[\prod_{n=1}^{\infty} \left[1 + \frac{4d^2 \left[\frac{1}{4}(L-K)^2 + r(g+sc) \right]}{(2n)^2 \pi^2} \right] \right]^{-1} \quad (3.144)$$

$$y_{21} = e^{-d(k+L)} y_{12} \quad (3.145)$$

They have d.c. values of

$$y_{12}(0) = \frac{1}{rd} e^{\frac{1}{2}d(k+L)} \sqrt{\frac{1}{4}(L-K)^2 + rg} \operatorname{csch} d \sqrt{\frac{1}{4}(L-K)^2 + rg} \quad (3.146)$$

$$y_{21}(0) = e^{-d(L+K)} y_{12}(0) \quad (3.147)$$

It is clear that the transfer admittances have the same poles and y_{22} (given by eq. 3.116) and are all-pole functions.

The open-circuit voltage gain $T_V(s)$ from eqs. 3.53 and 3.54 is

$$T_V(s) = -\frac{y_{21}}{y_{22}} = e^{-\frac{1}{2}d(K+L)} \left[\cosh f + \frac{1}{2}d(K-L) \frac{\sinh f}{f} \right]^{-1} \quad (3.148)$$

while the short-circuit gain $T_I(s)$ from eqs. 3.51 and 3.53 is

$$T_I(s) = -\frac{y_{21}}{y_{22}} = e^{-\frac{1}{2}d(K+L)} \left[\cosh f - \frac{1}{2}d(K-L) \frac{\sinh f}{f} \right]^{-1} \quad (3.149)$$

where again $f = d \sqrt{\frac{1}{4}(L-K)^2 + rg + sc}$. Thus, the poles of T_V and T_I are the zeros of y_{22} and y_{11} , respectively. Their normalized values are bounded in Fig. 40 and are given explicitly by eq. 3.141 for $K \approx L$.

The d.c. gains from eqs. 3.148 and 3.149 are

$$T_V(0) = e^{-\frac{1}{2}d(K+L)} \left[\cosh d \sqrt{\frac{1}{4}(L-K)^2 + rg} + \frac{1}{2}d(K-L) \frac{\sinh d \sqrt{\frac{1}{4}(L-K)^2 + rg}}{d \sqrt{\frac{1}{4}(L-K)^2 + rg}} \right]^{-1} \quad (3.150)$$

$$T_I(0) = e^{-\frac{1}{2}d(K+L)} \left[\cosh d \sqrt{\frac{1}{4}(L-K)^2 + rg} - \frac{1}{2}d(K-L) \frac{\sinh d \sqrt{\frac{1}{4}(L-K)^2 + rg}}{d \sqrt{\frac{1}{4}(L-K)^2 + rg}} \right]^{-1} \quad (3.151)$$

Since the gains are all-pole functions, their Bode magnitude and phase plots have monotonically decreasing characters similar to Fig. 31. By adjusting $-(K+L)$ to sufficiently large values, low frequency gain exceeding unity is achieved. Gain under arbitrary loading is carried out using root locus techniques as before in eq. 3.67.

Unless other approximations are employed, system bandwidth must be calculated using iterative techniques. Setting $f = \pi\sqrt{s_N}/2$ in eqs. 3.148 and 3.149 to form the frequency normalized gain functions, and

setting their magnitudes equal to 0.707 for $s_N = j\omega_N$ yields

$$\begin{aligned} (\cosh \theta + \cos \theta) + \left[\frac{d(K-L)}{\theta} \right]^2 (\cosh \theta - \cos \theta) \pm \frac{d(K-L)}{\sqrt{2}\theta} (\sinh \theta + \sin \theta) \\ = 4 \left[1 \pm \frac{1}{4} d(K-L)^2 \right]^2 \end{aligned} \quad (3.152)$$

when $\theta = \pi \sqrt{\omega_N}/2$. The plus sign is used when T_V is considered, and the minus sign for T_I . Solving this equation for θ , the normalized 3 db radian frequency is $\omega_N \text{ 3db} = \theta \sqrt{2}/\pi$. Since complex radian frequency

$s = -\frac{1}{c} \left[g + \frac{(L-K)^2}{4r} \right] + \frac{j\pi^2}{4d^2rc} s_N$, the 3 db radian frequency is

$$\omega_{3\text{db}} = \frac{1}{c} \left[g + \frac{(L-K)^2}{4r} \right] + \frac{0.95}{d^2rc} \theta \quad (3.153)$$

with the corresponding Hertzian frequency $f_{3\text{db}}/2\pi$.

Elmore's results may again be used to advantage for approximating $f_{3\text{db}}$. For networks having normalized gains given by eq. 3.87 and monotonic frequency response, $f_{3\text{db}} t_r = 0.35$. Thus from eq. 3.90, these networks have a 3 db frequency of

$$f_{3\text{db}} = 0.14 \left[b_1^2 - a_1^2 + 2(a_2 - b_2) \right]^{-\frac{1}{2}} \quad (3.154)$$

To utilize this result, the denominator of the gain functions, eqs. 3.148 and 3.149, is expressed in an infinite series of s . The cosh term was expanded in eq. 3.96. Its first three terms are given by eqs. 3.98, 3.99, and 3.100. In like manner, the $\sinh \sqrt{a+bs} / \sqrt{a+bs}$ function can be expanded as

$$\frac{\sinh \sqrt{a+bs}}{\sqrt{a+bs}} = \sum_{k=0}^{\infty} B_k s^k, \quad |s| < \left| \frac{a}{b} \right| \quad (3.155)$$

where

$$\begin{aligned}
 B_k &= \frac{b^k}{k!} \sum_{n=0}^{\infty} \frac{(n+k)!}{(2(n+k)+1)!n!} a^n = \frac{b^k}{k!} \frac{d^k}{da^k} \sum_{n=0}^{\infty} \frac{a^{n+k}}{(2(n+k)+1)!} \\
 &= \frac{b^k}{k!} \frac{d^k}{da^k} \frac{\sinh \sqrt{a}}{\sqrt{a}}
 \end{aligned} \tag{3.156}$$

Evaluating the first three B_k 's gives

$$B_0 = \frac{\sinh \sqrt{a}}{\sqrt{a}} \tag{3.157}$$

$$B_1 = \frac{b}{2} \left[\frac{\cosh \sqrt{a}}{a} - \frac{\sinh \sqrt{a}}{a \sqrt{a}} \right] \tag{3.158}$$

$$B_2 = \left(\frac{b}{2}\right)^2 \left[\frac{\sinh \sqrt{a}}{2a \sqrt{a}} + \frac{3}{2} \frac{\sinh \sqrt{a}}{a^2 \sqrt{a}} - \frac{3}{2} \frac{\cosh \sqrt{a}}{a^2} \right] \tag{3.159}$$

Thus, the denominator $D(s)$ of the gain functions, eqs. 3.148 and 3.149, becomes

$$\begin{aligned}
 D(s) &= \left[\cosh \sqrt{a} + \frac{1}{2}d(K-L) \frac{\sinh \sqrt{a}}{\sqrt{a}} \right] + s \frac{b}{2} \left[\frac{\sinh \sqrt{a}}{\sqrt{a}} \right. \\
 &\quad \left. + \frac{1}{2}d(K-L) \left(\frac{\cosh \sqrt{a}}{a} - \frac{\sinh \sqrt{a}}{a \sqrt{a}} \right) \right] + s^2 \left(\frac{b}{2}\right)^2 \left[\frac{\cosh \sqrt{a}}{2a} - \frac{\sinh \sqrt{a}}{2a \sqrt{a}} \right. \\
 &\quad \left. + \frac{1}{2}d(K-L) \left(\frac{\sinh \sqrt{a}}{2a^2 \sqrt{a}} (a+3) - \frac{3}{2} \frac{\cosh \sqrt{a}}{a^2} \right) \right] + \dots \\
 &= B_0' + B_1' s + B_2' s^2 + \dots
 \end{aligned} \tag{3.160}$$

where the plus is used for T_V and the minus for T_I . Normalization of the B_1' and B_2' against B_0' and substitution into eq. 3.154 immediately yields f_{3db} for numerical values of $a = d^2 \sqrt{rg + \frac{1}{4}(L-K)^2}$, $b = d^2 rc$, and $(K-L)$.

Step Response, Stability, Rise and Delay Time—Type 2-4 RCG Active Lines

The unit step voltage response of the active line from eq. 3.148 is

$$V_2(s) = e^{\frac{1}{2}d(K+L)} \frac{1}{s} \left[\cosh d \sqrt{\frac{1}{4}(L-K)^2 + r(g+sc)} + \frac{1}{2}d(K-L) \frac{\sinh d \sqrt{\frac{1}{4}(L-K)^2 + r(g+sc)}}{d \sqrt{\frac{1}{4}(L-K)^2 + r(g+sc)}} \right] \quad (3.161)$$

If $K = L$, this equation reduces to eqs. 3.73 or 3.77 when multiplied by e^{-Kd} . Otherwise the poles of eq. 3.161 must be identified either through graphical techniques or eq. 3.141 when $L \approx K$, as

$$s_p = -\frac{1}{c} \left[g + \frac{(L-K)^2}{4r} \right] - (2n-1)^2 \frac{\pi^2}{4d^2rc} [1+c_n] \quad (3.162)$$

c_n is the correction factor required when $k = \frac{1}{2}d(L-K)$ is nonzero which was introduced in eq. 3.136. Then, by the residue method

$$v_2(t) = e^{-\frac{1}{2}d(K+L)} \left(\frac{1}{\cosh \sqrt{a} + \frac{1}{2}d(K-L) \frac{\sinh \sqrt{a}}{\sqrt{a}}} + 2e^{-\frac{a}{b}t} \sum_{n=1}^{\infty} \frac{(-1)^n e^{-(2n-1)^2 \left(\frac{\pi}{2}\right)^2 (1+c_n)^2 \frac{t}{b}}}{D_n [a + (2n-1)^2 \left(\frac{\pi}{2}\right)^2 (1+c_n)^2]} \right) u(t) \quad (3.163)$$

where

$$D_n = \frac{\cos (2n-1) \frac{\pi c_n}{2}}{(2n-1) \frac{\pi}{2} (1+c_n)} \left[1 - \frac{\frac{1}{2}d(K-L)}{(2n-1)^2 \left(\frac{\pi}{2}\right)^2 (1+c_n)^2} \right] - \frac{1}{2}d(K-L) \frac{\sin (2n-1) \frac{\pi c_n}{2}}{(2n-1)^2 \left(\frac{\pi}{2}\right)^2 (1+c_n)^2} \quad (3.164)$$

with $a = d^2 \sqrt{rg + \frac{1}{4}(L-K)^2}$ and $b = d^2rc$. The step response rises mono-

tonically from 0 to $e^{-\frac{1}{2}d(K+L)} \left[\cosh \sqrt{a} + \frac{1}{2}d(K-L) \frac{\sinh \sqrt{a}}{\sqrt{a}} \right]^{-1}$ volts.

Simplification results from the dominant-pole, excess-phase approximation of the step response. Comparing eq. 3.146 with eq. 3.78 and 3.79, the approximate response is

$$V_2(s) = \frac{e^{-\frac{1}{2}d(K+L)}}{\cosh \sqrt{a} + \frac{1}{2}d(K-L) \frac{\sinh \sqrt{a}}{\sqrt{a}}} \frac{1}{s(1+s/p_e) \exp(sm_p/p_e)} \quad (3.165)$$

so that

$$v_2(t) = \frac{e^{-\frac{1}{2}d(K+L)}}{\cosh \sqrt{a} + \frac{1}{2}d(K-L) \frac{\sinh \sqrt{a}}{\sqrt{a}}} (1 - e^{-p_e t}) u(t - m_p/p_e) \quad (3.166)$$

This exponential response has a time constant $1/p_e$ and a dead time of m_p/p_e . p_e and m_p (given by eqs. 3.82 and 3.83) are determined from the expansion of eq. 3.160.

The system is absolutely stable since all the poles of eqs. 3.148 and 3.149 are in the left-half s-plane.

The rise and delay time follow immediately from the denominator expansion of eq. 3.148 using Elmore's results. Reiterating, the coefficients of s and s^2 are

$$b_1 = \frac{b}{2} \left[\frac{\sinh \sqrt{a}}{\sqrt{a}} + \frac{1}{2}d(K-L) \left(\frac{\cosh \sqrt{a}}{a} - \frac{\sinh \sqrt{a}}{a \sqrt{a}} \right) \right] / B_0 \quad (3.167)$$

$$b_2 = \left(\frac{b}{2} \right)^2 \left[\frac{\cosh \sqrt{a}}{2a} - \frac{\sinh \sqrt{a}}{2a \sqrt{a}} + \frac{1}{2}d(K-L) \left(\frac{\sinh \sqrt{a}}{2a^2 \sqrt{a}} (a+3) - \frac{3}{2} \frac{\cosh \sqrt{a}}{a^2} \right) \right] / B_0 \quad (3.168)$$

respectively, where

$$B_o = \cosh \sqrt{a} + \frac{1}{2}d(K-L) \frac{\sinh \sqrt{a}}{\sqrt{a}} \quad (3.169)$$

Rise and delay time follow from substitution into eq. 3.89 for t_d and eq. 3.90 for t_r . If the dominant pole, excess phase approach is used, eqs. 3.105 and 3.106 yield t_r and t_d , respectively.

Sensitivity—Type 2-4 RCG Active Lines

The general sensitivity expression for T_V or T_I is prohibitively complicated. Considerable simplification results when the source strengths are equal, i.e. $K = L$. Here, the open-circuit voltage gain and short-circuit current gain from eqs. 3.148 and 3.149 both equal

$$T(s) = e^{-Kd} / \cosh d \sqrt{r(g+sc)} \quad (3.170)$$

The sensitivity of gain T with respect to K is

$$S_K^T = -Kd \quad (3.171)$$

which is frequency independent. Thus, to minimize the network's gain sensitivity with respect to parameter K , set $K = 0$. But this is in conflict with the requirement of large $-K$ for large low-frequency gain, and hence a compromise must be made.

Mixed-Type Lines

It should now be clear that simply changing r to r^* and g to g^* in any of the type 2-4 line expressions yields the expressions for lines having mixed-type sources distributed along its length. These conversions are thus easily made.

Pertinent system parameters of uniform active lines have been

examined in this chapter. The admittance parameters were chosen to characterize rcg active lines. The results are readily extended to other parameter sets (such as z or h), and different types of lines (e.g. lc active lines).

Both time domain and frequency domain behavior and s-plane characteristics have been investigated. Various approximations were introduced to make analysis tractable, and to aid in forming useful design criteria and results.

The question now arises if nonuniform structures have significantly different characteristics from a pole-zero viewpoint and if they can be employed to add flexibility in meeting design requirements. This question is investigated in the following chapter. It is seen that the very general nature of their parameters does not change significantly.

IV. NONUNIFORM TRANSMISSION LINES HAVING DEPENDENT DISTRIBUTED SOURCES

Two-Port Parameters

In this chapter, nonuniform active transmission lines are examined from a general point of view. The nature of their two-port parameters is surveyed. Various results from linear, second-order, homogeneous, partial differential equation theory can advantageously be used for this purpose. The voltage and current along active lines are described by this class of differential equation. A summary of the important conclusions and results will give direction to this development.

The two-port parameters are expressed in terms of the voltage solution of the partial differential equation describing the active line. They are simplified using the basic set solution and the self-adjoint properties of the active line equations. Lack of pole-zero cancellation is shown by utilizing the Wronskian of the basic set solutions. Sturm-Liouville theory establishes the general pole-zero locations. Many of the powerful theorems concerning lumped, passive networks are seen to parallel those of active lines.

To begin, the partial differential equations describing voltage and current along the active line are written. From eqs. 2.1 and 2.2, the transformed voltage $V(x,s)$ and current $I(x,s)$ on initially relaxed type 1-3 active lines satisfy

$$\left(\frac{1}{Z^*} V_x\right)_x - Y^*V = 0 \quad (4.1)$$

$$\left(\frac{1}{Y^*} I_x\right)_x - Z^*I = 0 \quad (4.2)$$

where $Z^*(x,s) = K(x)+r(x)+sl(x)$ and $Y^*(x,s) = L(x)+g(x)+sc(x)$.

Alternatively, voltage and current on initially relaxed type 2-4 active lines satisfy

$$\left(\frac{1}{Z}V_x + \frac{K}{Z}V\right)_x + \frac{L}{Z}V_x + \left(\frac{KL}{Z} - Y\right)V = 0 \quad (4.3)$$

$$\left(\frac{1}{Y}I_x + \frac{L}{Y}I\right)_x + \frac{K}{Y}I_x + \left(\frac{KL}{Y} - Z\right)I = 0 \quad (4.4)$$

where $Z(x,s) = r(x)+sl(x)$ and $Y(x,s) = g(x)+sc(x)$. Both sets of equations describe voltage and current at every point, x , on the interior of the line for any complex frequency s . This is succinctly expressed by first defining the domain \underline{D}^s to be the three-dimensional space formed by the s -plane and the x -axis, where the open domain $D^s = \{(x,s): 0 < x < d, |s| < \infty\}$ and the closed domain $\underline{D}^s = \{(x,s): 0 \leq x \leq d, |s| < \infty\}$. Then, the active line equations hold for all (x,s) in D^s .

The two-port parameters of an active line are easily expressed if either its voltage or current solution is known. For example, consider the admittance parameters in terms of the voltage solutions. Denote the port voltages $V_1(s) = V(0,s)$ and $V_2(s) = V(d,s)$ of the active line as $V(0)$ and $V(d)$, respectively.

For type 1-3 active lines, the corresponding port currents from eqs. 2.1 and 2.2 are

$$I_1(s) = I(0) = -V_x(0)/Z^*(0) \quad (4.5)$$

$$I_2(s) = -I(d) = V_x(d)/Z^*(d) \quad (4.6)$$

Since the admittance parameters are defined in terms of these port voltages and currents, the admittance matrix can be immediately written as

$$[y] = \begin{bmatrix} -\frac{1}{Z^*(0)} \frac{V_x(0)}{V(0)} \Big|_{V(d)=0} & -\frac{1}{Z^*(0)} \frac{V_x(0)}{V(d)} \Big|_{V(0)=0} \\ \frac{1}{Z^*(d)} \frac{V_x(d)}{V(0)} \Big|_{V(d)=0} & \frac{1}{Z^*(d)} \frac{V_x(d)}{V(d)} \Big|_{V(0)=0} \end{bmatrix} \quad (4.7)$$

Type 2-4 active lines have port currents, from eqs. 2.1 and 2.2, given by

$$I_1(s) = I(0) = -V_x(0)/Z(0) - K(0)V(0)/Z(0) \quad (4.8)$$

$$I_2(s) = -I(d) = V_x(d)/Z(d) + K(d)V(d)/Z(d) \quad (4.9)$$

Thus, the admittance matrix for the type 2-4 active line is

$$[y] = \begin{bmatrix} -\frac{K(0)}{Z(0)} - \frac{1}{Z(0)} \frac{V_x(0)}{V(0)} \Big|_{V(d)=0} & -\frac{K(0)}{Z(0)} \frac{V(0)}{V(d)} - \frac{1}{Z(0)} \frac{V_x(0)}{V(d)} \Big|_{V(0)=0} \\ \frac{K(d)}{Z(d)} \frac{V(d)}{V(0)} + \frac{1}{Z(d)} \frac{V_x(d)}{V(0)} \Big|_{V(d)=0} & \frac{K(d)}{Z(d)} + \frac{1}{Z(d)} \frac{V_x(d)}{V(d)} \Big|_{V(0)=0} \end{bmatrix} \quad (4.10)$$

Since active transmission lines are described by partial differential equations of second order, the general voltage solution V can be expressed as the sum of two linearly independent solutions v_a and v_b ,

$$V(x,s) = a_1(s)v_a(x,s) + a_2(s)v_b(x,s) \quad (4.11)$$

where a_1 and a_2 are arbitrary functions of s determined by port conditions. Unless v_a and v_b are properly chosen, complicated two-port parameter expressions result using this general solution. This is readily demonstrated by writing the driving-point admittance for type 1-3 active lines. Substituting the general voltage solution of eq. 4.11 into the y_{11} expression in eq. 4.7 yields

$$y_{11} = -\frac{1}{Z^*(0)} \frac{v_{ax}(0)v_b(d) - v_a(d)v_{bx}(0)}{v_a(0)v_b(d) - v_a(d)v_b(0)} \quad (4.12)$$

As usual, the x subscripts denote partial differentiation with respect to x ; for example, $v_{ax} = \partial v_a / \partial x$. Since in general, y_{11} contains eight transcendental functions in s , its pole-zero distribution is prohibitively complicated to determine.⁹ Considerable simplification results when the independent solutions v_a and v_b are chosen to have particular characters at $x = 0$ or $x = d$.

The Basic Set

The basic set solution of the active transmission line equations greatly simplifies the two-port parameter expressions. Express the voltage V in terms of the two independent basic set solutions v_1 and v_2 ,

$$V(x,s) = a_1(s)v_1(x,s) + a_2(s)v_2(x,s) \quad (4.13)$$

where a_1 and a_2 are determined by port conditions. The basic set has the following properties (24): $v_1(0,s) = 1$, $v_{1x}(0,s) = 0$, $v_2(0,s) = 0$, and $v_{2x}(0,s) = 1$. That is, v_1 has unit value and zero slope at $x = 0$, while v_2 has zero value and unit slope at $x = 0$. It is precisely these properties which simplifies y_{11} in eq. 4.12 and the two-port parameters of the active lines.

Using the basic set results in the admittance parameters of eq. 4.7 yields the type 1-3 active line admittance matrix,

⁹S.C. Dutta Roy has compiled these expressions for passive lines in: Matrix parameters of nonuniform transmission lines. IEEE Transactions on Circuit Theory 12(3):142-143. 1965.

$$\begin{aligned}
 [y] &= \begin{bmatrix} \frac{1}{Z^*(0)} \frac{v_1(d)}{v_2(d)} & -\frac{1}{Z^*(0)} \frac{1}{v_2(d)} \\ \frac{1}{Z^*(d)} \frac{v_1'(d)v_2(d) - v_1(d)v_2'(d)}{v_2(d)} & \frac{1}{Z^*(d)} \frac{v_2'(d)}{v_2(d)} \end{bmatrix} \\
 &= \begin{bmatrix} \frac{1}{Z^*(0)} \frac{v_1(d)}{v_2(d)} & -\frac{1}{Z^*(0)} \frac{1}{v_2(d)} \\ -\frac{1}{Z^*(0)} \frac{1}{v_2(d)} & \frac{1}{Z^*(d)} \frac{v_2'(d)}{v_2(d)} \end{bmatrix} \quad (4.14)
 \end{aligned}$$

where, for convenience, primes denote differentiation with respect to x . The admittance matrix for type 2-4 active lines is

$$\begin{aligned}
 [y] &= \begin{bmatrix} \frac{1}{Z(0)} \frac{v_1(d) - K(0)v_2(d)}{v_2(d)} & -\frac{1}{Z(0)} \frac{1}{v_2(d)} \\ -\frac{1}{Z(d)} \frac{v_1(d)v_2'(d) - v_2(d)v_1'(d)}{v_2(d)} & \frac{1}{Z(d)} \frac{v_2'(d) + K(d)v_2(d)}{v_2(d)} \end{bmatrix} \\
 &= \begin{bmatrix} \frac{1}{Z(0)} \frac{v_1(d) - K(0)v_2(d)}{v_2(d)} & -\frac{1}{Z(0)} \frac{1}{v_2(d)} \\ -\frac{e^{-\int_0^d (K+L)dx}}{Z(0)} \frac{1}{v_2(d)} & \frac{1}{Z(d)} \frac{v_2'(d) + K(d)v_2(d)}{v_2(d)} \end{bmatrix} \quad (4.15)
 \end{aligned}$$

The simplification of y_{21} in eqs. 4.14 and 4.15 results from Abel's identity. This will be shown in the next section.

The complete sets of two-port parameters for type 1-3 and type 2-4 active lines are tabulated in Tables 4 and 5, respectively. For notational convenience, the basic set current solutions are occasionally utilized in Table 5. From these tables, it is clear that when

the zeros of the two basic set solutions $v_1(d,s)$ and $v_2(d,s)$ and their spacial derivatives are identified, the pole-zero distributions of the two-port parameters can be found. Generally, the two-port parameters cannot be expressed in closed form, since closed form voltage and current solutions exist for only very special parameter distributions (11). This will not hinder these results being utilized later in the chapter. It should be noted that in lieu of closed form expressions, infinite series solutions and infinite product solutions can be used to find dominant time and frequency domain behavior (as was done in Chapter 3).

Table 4. Two-port parameters for the type 1-3 active transmission line expressed in terms of the basic set voltage solution at $x=d$ (15).

$$\begin{aligned}
 [z] &= \begin{bmatrix} Z^*(0) \frac{v_2'}{v_1'} & Z^*(d) \frac{1}{v_1'} \\ Z^*(d) \frac{1}{v_1'} & Z^*(d) \frac{v_1'}{v_1'} \end{bmatrix} & [y] &= \begin{bmatrix} \frac{1}{Z^*(0)} \frac{v_1'}{v_2} & -\frac{1}{Z^*(0)} \frac{1}{v_2} \\ -\frac{1}{Z^*(0)} \frac{1}{v_2} & \frac{1}{Z^*(d)} \frac{v_2'}{v_2} \end{bmatrix} \\
 [h] &= \begin{bmatrix} Z^*(0) \frac{v_2'}{v_1} & \frac{1}{v_1} \\ -\frac{1}{v_1} & \frac{1}{Z^*(d)} \frac{v_1'}{v_1} \end{bmatrix} & [g] &= \begin{bmatrix} \frac{1}{Z^*(0)} \frac{v_1'}{v_2'} & -\frac{Z^*(d)}{Z^*(0)} \frac{1}{v_2'} \\ \frac{Z^*(d)}{Z^*(0)} \frac{1}{v_2'} & Z^*(d) \frac{v_2'}{v_2'} \end{bmatrix} \\
 [A] &= \begin{bmatrix} \frac{Z^*(0)}{Z^*(d)} v_2' & Z^*(0) v_2 \\ \frac{1}{Z^*(d)} v_1' & v_1 \end{bmatrix} & [a] &= \begin{bmatrix} v_1 & Z^*(0) v_2 \\ \frac{1}{Z^*(d)} v_1' & \frac{Z^*(0)}{Z^*(d)} v_2' \end{bmatrix}
 \end{aligned}$$

Table 5. Two-port parameters for the type 2-4 active transmission line expressed in terms of the basic set solutions at $x = d$.

$$[z] = \begin{bmatrix} \frac{1}{Y(0)} \frac{i_1 - L(0)i_2}{i_2} & \frac{1}{Y(0)} \frac{1}{i_2} \\ \frac{e^{c(d)}}{Y(0)} \frac{1}{i_2} & \frac{1}{Y(d)} \frac{i_2' + L(d)i_2}{i_2} \end{bmatrix}$$

$$[y] = [\text{see eq. 4.15}]$$

$$[h] = \begin{bmatrix} Z(0) \frac{v_2}{v_1 - K(0)v_2} & \frac{1}{v_1 - K(0)v_2} \\ -\frac{e^{c(d)}}{v_1 - K(0)v_2} & Y(d) \frac{i_2}{i_2' + L(d)i_2} \end{bmatrix}$$

$$[g] = \begin{bmatrix} Y(0) \frac{i_2}{i_1 - L(0)i_2} & -\frac{Z(d)}{Z(0)} \frac{1}{v_2' + K(d)v_2} \\ \frac{Z(d)}{Z(0)} \frac{e^{c(d)}}{v_2' + K(d)v_2} & Z(d) \frac{v_2}{v_2' + K(d)v_2} \end{bmatrix}$$

$$[A] = \begin{bmatrix} \frac{Z(0)}{Z(d)} e^{-c(d)} (v_2' + K(d)v_2) & Z(0) e^{-c(d)} v_2 \\ Y(0) e^{-c(d)} i_2 & e^{-c(d)} v_2 \end{bmatrix}$$

$$[a] = \begin{bmatrix} v_1 - K(0)v_2 & Z(0)v_2 \\ Y(0)i_2 & \frac{Z(0)}{Z(d)} (v_2' + K(d)v_2) \end{bmatrix}$$

Note: $c(d) = - \int_0^d (K+L) dx$

It will prove helpful to review the basic set solution introduced by Morse and Feshbach (24). Consider the general linear, second-order, homogeneous, partial differential equation describing the function $F(x,s)$,

$$p(x,s)F_{xx}(x,s) + q(x,s)F_x(x,s) + r(x,s)F(x,s) = Q(f) = 0 \quad (4.16)$$

for (x,s) in D^S . The linear, second-order, partial differential operator, Q , is introduced for notational ease in later equations. The basic set solution of $Q(F) = 0$ is the Taylor series solution in x , with s as a parameter, which is partitioned into two sums of even and odd powers of x . This is shown in the following manner. $F(x,s)$ is analytic and has a Taylor series representation at all ordinary points in D^S of eq. 4.16 (this is, all (x,s) in \underline{D}^S where $q(x,s)/p(x,s)$ and $r(x,s)/p(x,s)$ are nonsingular).¹⁰ Thus, the functions

$$F(x,s) = a_0 + (x-a)a_1 + (x-a)^2 a_2 + \dots \quad (4.17)$$

$$p(x,s) = p(a) + (x-a)p'(a) + \dots \quad (4.18)$$

$$q(x,s) = q(a) + (x-a)q'(a) + \dots \quad (4.19)$$

$$r(x,s) = r(a) + (x-a)r'(a) + \dots \quad (4.20)$$

can be expanded in Taylor series where primes denote differentiations with respect to x and the constants are functions of s , i.e. $a_n = a_n(s)$, $p^{(n)}(a) = p^{(n)}(a,s)$, $q^{(n)}(a) = q^{(n)}(a,s)$, and $r^{(n)}(a) = r^{(n)}(a,s)$. The a_n 's are determined by substituting eqs. 4.17-4.20

into eq. 4.16 and collecting like powers of x ,

¹⁰A function is analytic at a point if its partial derivatives exist at the point and in a neighborhood about the point. Analytic functions have Taylor series representations. Singular points are points in the (x,s) -space where the function fails to be analytic.

$$0 = [2a_2p(a) + a_1q(a) + a_0r(a)] + (x-a) [6a_3p(a) + 2a_2p'(a) + 2a_2q(a) + a_1q'(a) + a_1r(a) + a_0r'(a)] + \dots \quad (4.21)$$

A polynomial of infinite degree which is identically equal to zero for all x in D^s has zero coefficients for all powers of $(x-a)$. Therefore from eq. 4.21,

$$2a_2p(a) + a_1q(a) + a_0r(a) = 0 \quad (4.22)$$

$$6a_3p(a) + 2a_2p'(a) + 2a_2q(a) + a_1q'(a) + a_1r(a) + a_0r'(a) = 0 \quad (4.23)$$

and so on. The first equation gives a_2 in terms of a_0, a_1 ; the second gives a_3 in terms of a_0, a_1 and a_2 and thus in terms of a_0, a_1 ; etc.

The basic set results by expressing the Taylor series solution as the sum of two independent solutions,

$$F(x,s) = a_0F_1(x,s) + a_1F_2(x,s) \quad (4.24)$$

where

$$F_1(x,s) = 1 + (x-a)^2 \frac{a_2}{a_0} + (x-a)^4 \frac{a_4}{a_0} + \dots \quad (4.25)$$

and

$$F_2(x,s) = (x-a) \left[1 + (x-a)^2 \frac{a_3}{a_1} + (x-a)^4 \frac{a_5}{a_1} + \dots \right] \quad (4.26)$$

Clearly F_1 has unit value and zero slope at $x = a$ while F_2 has zero value and unit slope at $x = a$. Boundary conditions determine a_0 and a_1 . This series holds within the sphere of convergence having radius equal to the distance between (a,s) and the nearest singular point of the partial differential equation, (eq. 4.16). Various methods may be used to determine the basic set (15). This will not concern us here.

The Wronskian and Self-Adjoint Systems

The results of Tables 4 and 5 have interesting interpretations. In later sections, the general location of the poles and zeros of the two-port parameters are established. This section is concerned with investigating the possibility of pole-zero cancellation and two-port parameter simplification.

Several useful results arise from consideration of the Wronskian of any two linearly independent voltage solutions, v_a and v_b , of the voltage equation

$$Q(V) = p(x,s)V_{xx}(x,s) + q(x,s)V_x(x,s) + r(x,s)V(x,s) = 0 \quad (4.27)$$

The Wronskian of the two solutions v_a and v_b is defined as

$$W(v_a, v_b) = v_a \frac{\partial v_b}{\partial x} - v_b \frac{\partial v_a}{\partial x} = v_a v_{bx} - v_b v_{ax} \quad (4.28)$$

for all (x,s) in D^S . The Wronskian is therefore a function of both x and s . The partial differential equation describing the Wronskian is formed by operating on v_a and v_b in the following manner and manipulating the results,

$$v_a Q(v_b) - v_b Q(v_a) = p(x,s)W_x(x,s) + q(x,s)W(x,s) = 0 \quad (4.29)$$

The general Wronskian solution from eq. 4.29 is

$$W(x,s) = W(x_0,s) \exp \left[- \int_{x_0}^x \left[q(x,s)/p(x,s) \right] dx \right] \quad (4.30)$$

The Wronskian has the property of being nonzero at all points of D^S . This fact eliminates the possibility of pole-zero cancellation between basic set quantities involved in the two-port parameters, as described in the next paragraph. Proof by contradiction establishes

this Wronskian property. From eq. 4.30, W cannot vanish at any point except perhaps at a singular point. Thus, W is identically zero in domains where q/p is nonsingular if, and only if, W_0 is zero. But this would require $v_a = cv_b$ (c is a constant), so the solutions v_a and v_b would not be linearly independent. Therefore, since v_a and v_b are linearly independent, the Wronskian $W(v_a, v_b)$ is nonzero in domains where q/p is nonsingular. The parameter conditions noted for the active line equations (eqs. 1.1, 1.2, 2.1 and 2.2) insures that q/p is nonsingular in \underline{D}^S . Thus, W is nonzero in D^S , i.e. $W \neq 0$ in D^S . By continuity requirements, $W \neq 0$ in \underline{D}^S as well.

The Wronskian of the basic set solutions from eq. 4.28 is

$$W(v_1, v_2) = v_1 v_{2x} - v_2 v_{1x} \neq 0 \quad (4.31)$$

for all (x,s) in \underline{D}^S . Therefore, the zeros of $v_1(d)$ and $v_{2x}(d)$ do not coincide with the zeros of $v_{1x}(d)$ and $v_2(d)$. Applying this result to the entries in Tables 4 and 5, it is clear that there can be no cancellation between basic set zeros in numerator and denominator. Z^* and Y^* in Table 4 and Z and Y in Table 5 introduce an additional pole or zero which can cause a single pole-zero cancellation, at most. Thus, the zeros of a two-port parameter are the zeros of its numerator function. The poles of a two-port parameter are the zeros of its denominator function. Since the numerators of y_{21} in eqs. 4.14 and 4.15 both involve the Wronskian of the basic set solution at $x = d$, this motivates further examination of the Wronskian.

The Wronskian of eq. 4.30 assumes a particularly simple form when

$$q(x,s) = p_x(x,s) \quad (4.32)$$

Such systems are called self-adjoint, and have a Wronskian which

satisfies

$$W(x,s) = W(x_0,s) \exp(-\ln p(x,s)/p(x_0,s)) = W(x_0,s)p(x_0,s)/p(x,s) \quad (4.33)$$

for all (x,s) in \underline{D}^s . Rearranging eq. 4.33 results in the identity (referred to as Abel's identity),

$$W(x,s)p(x,s) = W(x_0,s)p(x_0,s) = k(s) \quad (4.34)$$

where $k(s)$ represents some function in s and is independent of x . This is an extremely useful result which allows simplification in y_{21} and other two-port parameters.

Since Abel's identity, eq. 4.34, holds for all x in \underline{D}^s , the function $k(s)$ can be evaluated by judiciously choosing x_0 . Choose $x_0 = 0$ where from eq. 4.28, the Wronskian of the basic set is equal to unity. Then eq. 4.34 becomes

$$W(x,s)p(x,s) = p(0,s) \quad (4.35)$$

The type 1-3 active line equations (eqs. 4.1 and 4.2) are in self-adjoint form. Their comparison with eq. 4.27 shows that $q = p_x$, where $p = 1/Z^*$ in the voltage equation and $p = 1/Y^*$ in the current equation. Thus, the Wronskian of their basic set voltage solutions must satisfy

$$W(v_1(x,s), v_2(x,s))/Z^*(x,s) = 1/Z^*(0,s) \quad (4.36)$$

from eq. 4.35. An analogous expression is readily written for basic set current solutions. The ratio of W and the series impedance anywhere along the line equals the reciprocal series impedance at $x = 0$. Therefore, $y_{21} = -W(d)/Z^*(d)v_2(d) = -1/Z^*(0)v_2(d)$ in eq. 4.14.

The type 2-4 active line equations (eqs. 4.3 and 4.4) are not in self-adjoint form. However, any linear, second-order, homogeneous,

partial differential equation denoted as

$$b_1(x,s)F_{xx}(x,s) + b_2(x,s)F_x(x,s) + b_3(x,s)F(x,s) = 0 \quad (4.37)$$

where $b_1 \neq 0$ for all (x,s) in \underline{D}^S , can be expressed in the following self-adjoint form

$$(p(x,s)F_x(x,s))_x + r(x,s)F(x,s) = 0 \quad (4.38)$$

by letting

$$p(x,s) = p(0,s) \exp \int_0^x \frac{b_2(x,s)}{b_1(x,s)} dx \quad (4.39)$$

and

$$r(x,s) = p(x,s) \frac{b_3(x,s)}{b_1(x,s)} \quad (4.40)$$

Such a linear, second-order, equation is called a Sturm-Liouville equation. Their properties are utilized in later sections.

The type 2-4 active line equations are readily expressed in self-adjoint form as

$$\left[\frac{\exp \int_0^x (K+L) dx}{Z} V_x \right]_x + \left[\left(\frac{K}{Z} \right)_x + \frac{KL}{Z} - Y \right] \left[\exp \int_0^x (K+L) dx \right] V = 0 \quad (4.41)$$

$$\left[\frac{\exp \int_0^x (K+L) dx}{Y} I_x \right]_x + \left[\left(\frac{L}{Y} \right)_x + \frac{KL}{Y} - Z \right] \left[\exp \int_0^x (K+L) dx \right] I = 0 \quad (4.42)$$

Here $p = \left[\exp \int_0^x (K+L) dx \right] / Z$ in the voltage equation and $p =$

$\left[\exp \int_0^x (K+L) dx \right] / Y$ in the current equation. Thus, from eq. 4.35, the

Wronskian of the basic set voltage solutions is

$$W(v_1(x,s), v_2(x,s)) e^{\int_0^x (K+L) dx} / Z(x,s) = 1/Z(0,s) \quad (4.43)$$

An analogous expression involving the basic set current solution is readily written. Eq. 4.43 is used to simplify y_{21} in the admittance matrix of eq. 4.15.

It is appropriate here to note reciprocity conditions. Clearly, from eq. 4.14, type 1-3 active lines are reciprocal since $y_{12} = y_{21}$. However from eq. 4.15, type 2-4 active lines are nonreciprocal unless

$$\exp \left[- \int_0^x (K+L) dx \right] = 1 \quad (4.44)$$

or

$$\int_0^x (K+L) dx = 0 \quad (4.45)$$

This is consistent with the result observed for uniform type 2-4 lines in Chapter 3 where $K = -L$ was required for reciprocity.

Sturm-Liouville Theory

The general location of the poles and zeros of the two-port parameters can be established from the classical Sturm-Liouville theory for fairly arbitrary active lines. In the remaining chapter, Sturm-Liouville theory is used to relate the voltage solutions (or current solutions) and the poles and zeros of the driving-point admittance functions. Although the theory cannot be used to find the critical frequencies of the transfer admittance functions, these can be obtained from previous basic set relations. These results can be directly

applied to any of the other two-port parameters in Tables 4 and 5.

To begin this development, note that any linear two-port (lumped or distributed, passive or active) has driving-point (and transfer) immittance parameters of the form

$$z(s) = c \frac{\prod_{n=1}^N (1+s/z_n)}{\prod_{m=1}^M (1+s/p_m)} \quad (4.46)$$

$$y(s) = c \frac{\prod_{n=1}^{N'} (1+s/z_{n'})}{\prod_{m'=1}^{M'} (1+s/p_{m'})} \quad (4.47)$$

where c is a constant, s is the complex frequency, and p and z are the network poles and zeros. For lumped networks, M , M' , N , and N' are finite integers, while for distributed networks they are infinite.¹¹ The product expansion holds for any function which does not have an essential singularity in the finite (x,s) -space by the Weierstrass factor theorem (33).

The poles of $z(s)$ and zeros of $y(s)$ are the open-circuit natural frequencies of the network (when driven by a current source), while the zeros of $z(s)$ and poles of $y(s)$ are the short-circuit natural frequencies (when driven by a voltage source). Thus, the type of ideal source (voltage or current) driving the system determines whether the poles or zeros of $z(s)$ or $y(s)$ are the natural frequencies of the

¹¹An exception was formed by K.W. Heizer. Distributed rc networks with rational transfer functions. IRE Transactions on Circuit Theory 9(12):356-362. 1962.

system. For nonideal sources whose Thevenin and Norton equivalents have the same nonzero, finite input impedance, the natural frequencies of the network are identical.

Consider the driving-point admittance y_{11} of an active line where

$$y_{11} = \left. \frac{I_1}{V_1} \right|_{V_2=0} \quad (4.48)$$

The zeros of y_{11} are the complex frequencies for which zero input port current flows for nonzero input port voltage with the output port shorted. The poles of y_{11} are the complex frequencies for which input port current flows for zero input port voltage with the output port shorted. These conditions under which the complex frequencies are determined are shown in Fig. 41. Analogous statements can be made for y_{22} . The problem of determining the critical frequencies of the network may alternatively be viewed as the problem of determining the eigenvalues of the partial differential equation describing the network under appropriate boundary conditions. The critical frequencies are directly related to the eigenvalues. To show this, the eigenvalue problem is now described and several pertinent theorems introduced.

Consider the Sturm-Liouville equation having the (self-adjoint) form

$$(p(x)v_x)_x - [q(x) + \lambda(s)r(s)]v = 0 \quad (4.49)$$

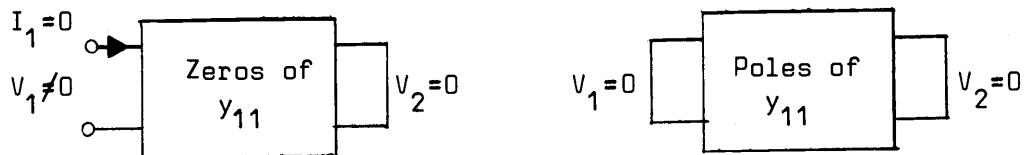


Fig. 41. Conditions under which the zeros and poles of y_{11} are determined.

for (x,s) in D^S with boundary conditions $V(x,s) = 0$, $V_x(x,s) = 0$, or $V_x(x,s) + aV(x,s) = 0$ at $x = 0$ and $x = d$. a is a positive constant at $x = d$, and a negative (not necessarily equal) constant at $x = 0$. Coefficients $q(x)$ and $r(x)$ are continuous, $p(x)$ is continuously differentiable, with $p(x)$, $r(x) > 0$ and $q(x) \geq 0$ for x in D^S . The values of λ for which a nonzero solution exists which satisfies both the partial differential equation and boundary conditions are the eigenvalues. The corresponding solutions are the eigenfunctions. The eigenvalue problem consists of determining these λ values. A number of theorems relate the properties of the eigenvalues and eigenfunctions (5, 13, 32). For our purposes, the following theorems are useful:

Theorem 1. Eigenvalues are negative real numbers.

Theorem 2. The eigenvalues are simple, isolated, and infinite in number having no accumulation point along the negative real axis of the complex λ -plane.

Theorem 3. Consider the problem having the boundary conditions at $x = 0$ and $x = d$ shown below:

First Set	
$-\lambda_n^1$	$V=0$
$-\lambda_n^2$	$V=0$ $V_x=0$
$-\lambda_n^3$	$V_x=0$

Second Set	
$-\lambda_n^4$	$V=0$
$-\lambda_n^5$	$V=0$ $V_x+aV=0$
$-\lambda_n^6$	$V_x+aV=0$

Denoting the n^{th} eigenvalue as $-\lambda_n^k$ where k represents the boundary condition set, the eigenvalues are separated as

$$-\lambda_{n+1}^3 \leq -\lambda_n^1 \leq -\lambda_n^2 \leq -\lambda_n^3 \leq -\lambda_{n-1}^1$$

and

$$-\lambda_{n+1}^6 \leq -\lambda_n^4 \leq -\lambda_n^5 \leq -\lambda_n^6 \leq -\lambda_{n-1}^4$$

Theorem 4. In some cases, $\lambda = 0$ is an eigenvalue. This is easily tested.

The type 1-3 active line equations (eqs. 4.1 and 4.2) and the type 2-4 active line equations (eqs. 4.41 and 4.42) have the form of the Sturm-Liouville equation (eq. 4.49). Different boundary conditions, consisting of open and short-circuit combinations, are imposed when determining critical frequencies. The possible boundary conditions of type 1-3 active lines are listed in the first set, while those of type 2-4 active lines are listed in the second set. The boundary conditions on voltage under open-circuit conditions result from eqs. 4.5 and 4.6 and eqs. 4.8 and 4.9, respectively. We now proceed to relate the parameter λ and the complex frequency s in the active line equations.

Driving-Point Admittance—Type 1-3 Active Lines

Consider first the type 1-3 active transmission line voltage equation

$$\left(\frac{V}{Z^*}\right)_x - Y^*V = 0 \quad (4.50)$$

where $Z^* = r^* + sl$ and $Y^* = g^* + sc$. To use the Sturm-Liouville theory results, the x and s dependencies in Z^* and Y^* must be separable.

Thus, for the r^*lg^*c active line whose local time constants, $a = l(x)/r^*(x)$ and $b = c(x)/g^*(x)$, are constant along the line, the voltage equation is

$$\left(\frac{V}{r^*(x)}\right)_x - g^*(x) \left[(1+as)(1+bs) \right] V = 0 \quad (4.51)$$

Since constant parameter passive lines having $a = b$ are called distor-

tionless lines, this more general active line shall be referred to as pseudo-distortionless. By comparison with eq. 4.50, this line has parameter $\lambda(s) = (1+as)(1+bs)$.

r^*cg^* and r^*lg^* active lines are described by the equations

$$\left[\frac{V_x}{r^*(x)} \right]_x - [g^*(x) + sc(x)] V = 0 \quad (4.52)$$

$$\left[\frac{I_x}{g^*(x)} \right]_x - [r^*(x) + sl(x)] I = 0 \quad (4.53)$$

respectively. These lines have parameter $\lambda(s) = s$. If the voltage equation rather than the current equation had been written in eq. 4.53, the more stringent condition requiring that $a = l(x)/r^*(x)$ be constant would have been necessary.

For lc active lines,

$$\left[\frac{V_x}{l(x)} \right]_x - s^2 c(x) V = 0 \quad (4.54)$$

where parameter $\lambda(s) = s^2$. Here $r^*(x) = 0$ and $g^*(x) = 0$ so that an lc active line is formed by setting $K(x) = -r(x)$ and $L(x) = -g(x)$. The results of eqs. 4.51-4.54 are important for they relate λ and s in the different types of lines.

The coefficients of the voltage (and current) equations must also satisfy the coefficient conditions noted for the Sturm-Liouville equation, eq. 4.49. For the pseudo-distortionless r^*lg^*c active line of eq. 4.51, $r^*(x) > 0$ and is C^1 (once continuously differentiable for all x in $\underline{D^S}$) and $g^*(x) > 0$ and is C^0 (continuous for all x in $\underline{D^S}$). For the r^*cg^* active line of eq. 4.52, $r^*(x) > 0$ and is C^1 , $g^*(x) \geq 0$ and is C^0 , and $c(x) > 0$ and is C^0 , with analogous conditions for the r^*lg^* active line of eq. 4.53. For the lc active line of eq. 4.74, $l(x) > 0$ and is C^1 and $c(x) > 0$ and is C^0 .

The distribution of the eigenvalues for the problem follow from Theorems 1 and 2. The eigenvalues are negative, real, simple, and may be arranged in order of decreasing magnitude as $-\lambda_1, -\lambda_2, \dots$ where $-\lambda_n \rightarrow -\infty$ as integer $n \rightarrow \infty$. From this infinite-dimensional set denoted as $\{-\lambda_n\}$, the critical frequency distributions are determined.

For the lc active line of eq. 4.54,

$$s_n = \pm j\sqrt{\lambda_n}, \quad n = 1, 2, \dots \quad (4.55)$$

so that the critical frequencies are simple, isolated, and lie along the $j\omega$ -axis of the s -plane in conjugate pairs.

For either the r^*g^*c or r^*g^*l active lines of eqs. 4.52 and 4.53, respectively,

$$s_n = -\lambda_n, \quad n = 1, 2, \dots \quad (4.56)$$

so these frequencies are simple, isolated, and lie along the negative real axis of the s -plane.

For the pseudo-distortionless r^*lg^*c active line of eq. 4.51,

$$(1+as_n)(1+bs_n) = -\lambda_n, \quad n = 1, 2, \dots \quad (4.57)$$

A root locus conveniently locates the values of s_n for any λ_n from 0 to ∞ . Expressing eq. 4.57 in the usual form for root locus analysis,

$$1 + \lambda \frac{1}{(1+as)(1+bs)} = 0 \quad (4.58)$$

Assume without lack of generality that $a \geq b$. Then the locus, having two branches, begins at $s = -1/a$ and $s = -1/b$, and terminates on $+90^\circ$ asymptotes at $|s| = \infty$ as shown in Fig. 42. The roots are equal when

$$\lambda = \lambda_c = (a-b)^2/4ab \quad (4.59)$$

and have values of

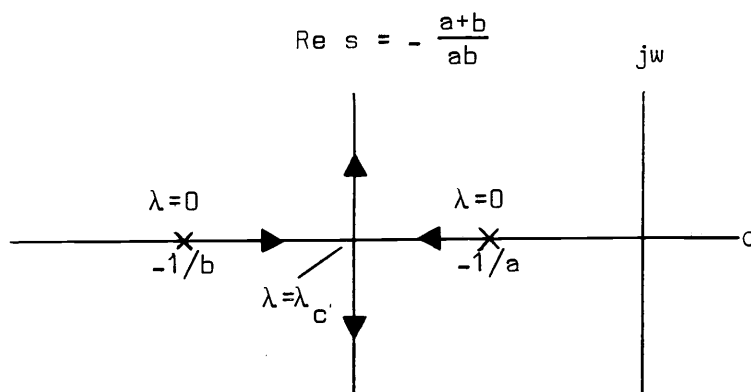


Fig. 42. The root locus of eq. 4.58 as λ varies from 0 to ∞ .

$$s = s_c = -(a+b)/2ab \quad (4.60)$$

where s_c also forms the branch asymptote. When $\lambda > \lambda_c$, the critical frequencies are complex conjugates having a real part given eq. 4.60 and imaginary parts of

$$\beta = - \left[\frac{\lambda}{ab} - \frac{1}{2} \left(\frac{a-b}{ab} \right)^2 \right]^{\frac{1}{2}} \quad (4.61)$$

Thus, the critical frequencies of the pseudo-distortionless r^*lg^*c active line are simple and isolated; a finite number may be negative real while an infinite number are complex conjugates having constant real parts.

Theorem 3 relates the distributions of eigenvalues to one another under different boundary conditions. These critical frequencies and the boundary conditions are directly related to the poles and zeros of the admittance functions. The zeros of y_{11} are the critical frequencies which correspond to the voltage equation with boundary conditions $V_{1x} = V_2 = 0$ or current equations where $I_1 = I_{2x} = 0$. The poles of y_{11} are then critical frequencies which correspond to the eigenvalues of the voltage equation with another set of boundary conditions, namely $V_1 =$

$V_2 = 0$, or the current equation with $I_{1x} = I_{2y} = 0$. Denote these infinite-dimensional sets of eigenvalues as $\{-\lambda_n^z\}$ and $\{-\lambda_n^p\}$, respectively. Under these conditions, Theorem 3 relates $-\lambda_n^z$ and $-\lambda_n^p$ as

$$-\lambda_{n+1}^z < -\lambda_n^p < -\lambda_n^z < -\lambda_{n-1}^p \quad (4.62)$$

for any positive integer n . That is, $-\lambda_n^p$ lies further from the λ -plane origin than does $-\lambda_n^z$. Inequalities may be used since there can be at most, a single pole and zero which are equal (corresponding to $\lambda_k^z = \lambda_k^p$) as previously noted. Applying these results to eqs. 4.55, 4.56, and 4.57, the driving-point admittance for the various lines can be expressed in infinite product form. As noted by Theorem 4, some problems have an eigenvalue $\lambda = 0$. To establish whether zero is an eigenvalue, the active line equations (eqs. 2.1 and 2.2) are examined for nonzero solutions when $\lambda = 0$.

The lc active line has a driving-point impedance

$$y(s) = c \frac{\prod_{n=1}^{\infty} (s^2 + \lambda_n^z)}{s \prod_{n=1}^{\infty} (s^2 + \lambda_n^p)} \quad (4.63)$$

from eq. 4.55 where c is a constant and $\lambda_{n-1}^p < \lambda_n^z < \lambda_n^p < \lambda_{n+1}^z$. The pole at the origin results since the lc active line can have nonzero current flow with zero voltage at the input port when the output port is shorted when $s = 0$. The pole $s = 0$ follows also from the driving-point admittance results of eq. 4.14. Equivalently stated, the lc active line current equations, given by eq. 4.54 when I replaces V and l and c are interchanged, has a nonzero solution for $\lambda=0$ for boundary conditions $I_x(0) = I_x(d) = 0$. Therefore, lc active lines have driving-

point admittance characterized by a pole at the origin and conjugate imaginary zeros and poles alternating into infinity of the s-plane (beginning with the zeros).

The r*cg* active line has a driving-point impedance

$$y(s) = c \frac{\prod_{n=1}^{\infty} (s + \lambda_n^z)}{\prod_{n=1}^{\infty} (s + \lambda_n^p)} \quad (4.64)$$

from eq. 4.56 where $\lambda_{n-1}^p < \lambda_n^z < \lambda_n^p < \lambda_{n+1}^z$. It is characterized by poles and zeros which alternate along the negative real axis of the s-plane with a zero closest the origin. The same equation results for the driving-point impedance of a r*lg* active line but with $\lambda_{n-1}^z < \lambda_n^p < \lambda_n^z < \lambda_{n+1}^p$. Thus, these lines have the same pole-zero characteristic where a pole is closest the origin of the s-plane. Recall that the current equation, eq. 4.43, was considered for this line type.

The pseudo-distortionless r*lg*c active line has a driving-point impedance

$$y(s) = \frac{c}{(1+as)} \frac{\prod_{n=1}^k (s + s_n^z) \prod_{n=k+1}^{\infty} [(s + s_c)^2 + (\beta_n^z)^2]}{\prod_{n=1}^j (s + s_n^p) \prod_{n=j+1}^{\infty} [(s + s_c)^2 + (\beta_n^p)^2]} \quad (4.65)$$

from eq. 4.57 when $k = \max n$ for which $\lambda_n^z < \lambda_c$ and $\lambda_n^p < \lambda_c$, respectively. The parameters are associated with the root locus of Fig. 42; $a = l(x)/r(x)$ was one local time constant of the line (eq. 4.51), s_c formed the real part of the critical frequencies and the root locus branch (eq. 4.60), β was the imaginary part of the critical

frequency, and λ_c was the demarcation eigenvalue which, if exceeded, yielded complex critical frequencies. Using the same reasoning as for the lc active line, $\lambda = 0$ is a current eigenvalue. Correspondingly, $s = -1/a$ (but not $s = -1/b$) is a pole of $y(s)$. The pole at $s = -1/a$ also follows from the driving-point admittance results of eq. 4.14. Poles and zeros alternate along the negative real axis (beginning with pole $s = 1/a$) on each side of the asymptote (assuming they exist there), and along the asymptote itself.

The particular distribution of the eigenvalues along the negative real axis of the complex λ -plane, and thus the poles and zeros of y_{11} and y_{22} in the s -plane, depends on the $p(x)$, $q(x)$, and $r(x)$ distributions of eq. 4.49 and the boundary conditions imposed.

For purposes of comparison, the general driving-point immittance properties of type 1-3 active lines are now summarized. Their admittance functions are given by eqs. 4.63, 4.64, and 4.65. Applying the eigenvalue results of eqs. 4.55, 4.56, and 4.57, analogous impedance expressions are readily written. The driving-point impedances are identical poles. Clearly these immittances are real functions when s is real. Under the parameter conditions noted for various lines, they have no poles or zeros in the right-half s -plane. Since their poles and zeros interlace, their Bode-plots must have zero or positive real parts for $0 \leq \omega < \infty$ for $s = j\omega$. Due to the maximum and minimum modulus theorem, the real part of the immittances must be nonnegative for $\text{Re } s > 0$. Thus, the driving-point immittances are positive-real functions. The degrees of numerator and denominator polynomials are infinite. Driving-point functions of $r*lg*$ and $r*cg*$ lines have poles and zeros

alternating along the negative real axis, while lc lines have poles and zeros alternating along the imaginary axis. Driving-point admittance functions of r*cg* and r*lg* lines have a zero and pole, respectively, closest the origin, while lc active lines have a zero at the origin.

It is interesting to note that these results parallel the following general theorems of lumped, linear, passive networks from network analysis. Driving-point immittance functions are positive-real functions. The degrees of numerator and denominator polynomials are finite and cannot differ by more than one. Driving-point functions of rcg and rlg networks have pole-zero patterns alternating along the negative real axis, and lc networks have them alternating along the imaginary axis of the s-plane. Driving-point admittance functions of rcg and rlg networks have a zero and a pole closest to the origin, respectively, perhaps at the origin itself. The lowest critical frequency of an lc network is either a pole or a zero at the origin. An lc ladder network having a topology analogous to the transmission line has a zero at the origin. Two-port driving-point functions have identical poles except for so-called private poles.

Transfer Admittance and Gain—Type 1-3 Active Lines

The results found for the driving-point admittance parameters can be used to determine the nature of the transfer admittance. Since

$$y_{12} = \frac{I_1}{V_2} \Big|_{V_1=0} \quad (4.66)$$

the poles of y_{12} are the values of s for which $I_1 \neq 0$ when $V_1 = 0$ for $V_2 = 0$. However, the zeros of y_{12} cannot be found by interpreting eq. 4.66 in a similar manner because of the ambiguity of requiring both $V_1 = 0$ (input shorted) and $I_1 = 0$ (zero input current). These conditions are shown in Fig. 43. The basic set solution expressed in eq. 4.14 resolves this difficulty. Since the transfer admittances are

$$y_{12} = y_{21} = -\frac{1}{Z^*(0)v_2} \quad (4.67)$$

it is clear that y_{12} has no zeros but has poles identical to those of y_{11} and y_{22} . The poles have the form found in eqs. 4.63, 4.64 and 4.65 for the various lines. Thus, type 1-3 active lines have transfer functions that are all-pole functions whose denominators are polynomials of infinite degree. The poles of y_{12} and y_{21} are identical with those of y_{11} and y_{22} .

Again, these results parallel the following theorems of lumped, linear, passive network analysis. The order of numerator and denominator polynomials is finite and may differ by more than one. The poles of the transfer function are the same as those of the driving-point function (unless private poles exist). Zeros may fall anywhere in the s -plane but must occur in conjugate pairs if complex.

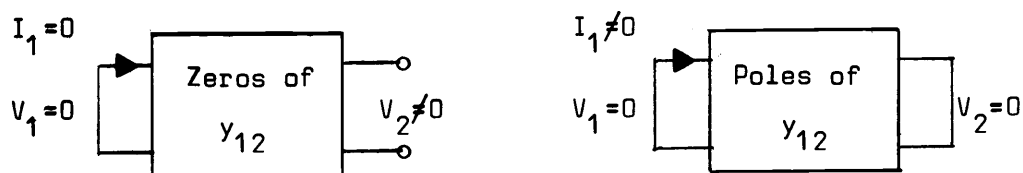


Fig. 43. Conditions under which the zeros and poles of y_{12} are determined.

The open-circuit voltage transfer function T_V is

$$T_V(s) = -\frac{y_{21}}{y_{22}} = \frac{Z^*(d)}{Z^*(d)} \frac{1}{v_2'} \quad (4.68)$$

T_V has a single zero $s = -r^*(d)/l(d)$, and poles which are the zeros of y_{22} and $s = -r^*(0)/l(0)$.

The short-circuit current transfer function T_I is

$$T_I(s) = -\frac{y_{21}}{y_{11}} = \frac{1}{v_1} \quad (4.69)$$

T_I is an all-pole function whose poles which are the zeros of y_{11} .

For summation purposes, the nonuniform r^*cg^* line is now compared with the uniform r^*cg^* line extensively considered in Chapter 3. The driving-point admittances have poles and zeros distributed along the negative real axis of the s -plane with a zero closest the origin. Thus, the Bode magnitude plot of y_{11} and y_{22} must be monotonically increasing with phase bounded between 0° and 90° . The transfer admittance y_{12} must equal y_{21} , can have no zeros, and must have poles identical to those of y_{11} . Thus, their Bode magnitude and phase plots are monotonically decreasing. The short-circuit current gain has the same response form. The open-circuit voltage gain also has a monotonically decreasing response for sufficiently large w . Therefore, the general pole-zero distribution and frequency response forms do not differ appreciably. But such quantities as gain, bandwidth, and rise and delay time may differ appreciably.

Driving-Point Admittance—Type 2-4 Active Lines

These considerations are now applied to type 2-4 active lines.

They are described by the voltage equation, eq. 4.41, as

$$\left[\frac{e^{\int_0^x (K+L) dx}}{Z} V_x \right]_x + \left[\left(\frac{K}{Z} \right)_x + \frac{KL}{Z} - Y \right] e^{\int_0^x (K+L) dx} V = 0 \quad (4.70)$$

where $Z = r + sl$ and $Y = g + sc$. Again x and s dependencies are separated in order to use the Sturm-Liouville theory.

For the rlgc active line with constant local time constants $a = l(x)/r(x)$ and $b = c(x)/g(x)$,

$$\left[\frac{e^{\int_0^x (K+L) dx}}{r} V_x \right]_x + \left[\left(\frac{K}{r} \right)_x + \frac{KL}{r} - g(1+as)(1+bs) \right] e^{\int_0^x (K+L) dx} V = 0 \quad (4.71)$$

The pseudo-distortionless line has parameter $\lambda(s) = (1+as)(1+bs)$.

rcg and rlg active lines are described by the equations

$$\left[\frac{e^{\int_0^x (K+L) dx}}{r} V_x \right]_x + \left[\left(\frac{K}{r} \right)_x + \frac{KL}{r} - g - sc \right] e^{\int_0^x (K+L) dx} V = 0 \quad (4.72)$$

$$\left[\frac{e^{\int_0^x (K+L) dx}}{g} I_x \right]_x + \left[\left(\frac{L}{g} \right)_x + \frac{KL}{g} - r - sl \right] e^{\int_0^x (K+L) dx} I = 0 \quad (4.73)$$

where parameter $\lambda(s) = s$.

For the lc active line,

$$\left[\frac{e^{\int_0^x (K+L) dx}}{1} V_x \right]_x + \left[\left(\frac{K}{1} \right)_x + \frac{KL}{1} - s^2 c \right] e^{\int_0^x (K+L) dx} V = 0 \quad (4.74)$$

so that parameter $\lambda(s) = s^2$.

Most of the conclusions follow those made previously. The rlgc active line has a driving-point admittance given by eq. 4.65. Again $\lambda = 0$ is a current eigenvalue when $I_x(0) + L(0)I(0) = I_x(d) + L(d)I(d) = 0$ with the result that $s = -1/a = -r(x)/l(x)$ is a pole. However, $s = -1/b = -g(x)/c(x)$ is not a pole. This is consistent with the driving-point admittance results of eq. 4.15. The poles and zeros alternate along the negative real axis on each side of the asymptote (assuming they exist there), and along the asymptote itself.

The rcg and rlg active lines have driving-point admittances given by eq. 4.64. They are characterized by poles and zeros alternating along the negative real axis. The patterns begin with a zero closest the origin for rcg active lines and a pole closest the origin for rlg active lines.

The lc active line has driving-point admittances given by eq. 4.63. They have conjugate imaginary poles and zeros alternating into infinity beginning with a pole at the origin. $s = 0$ is a pole since $\lambda = 0$ is a current eigenvalue when $I(0) + L(0)I(0) = I_x(d) + L(d)I(d) = 0$. Again, this result is consistent with the driving-point admittance results of eq. 4.15.

The coefficients of the voltage (and current) equations must satisfy the coefficient conditions of eq. 4.49. Thus, for the pseudo-distortionless rlgc active line, $r(x) > 0$ and $r(x)$ and $K(x)$ are C^1 , $g(x) > 0$ and $g(x)$ and $L(x)$ are C^0 , and $\ln(K(x)/r(x))_x \leq -L(x)$. For the rcg active line of eq. 4.72, $r(x) > 0$ and $r(x)$ and $K(x)$ are C^1 ; $c(x) > 0$ and $c(x)$, $g(x)$, and $L(x)$ are C^0 ; and $\ln(K(x)r(x))_x \leq \frac{g(x)r(x)}{K(x)} - L(x)$.

Analogous conditions follow for the rlg active line of eq. 4.73. For the lc active line of eq. 4.74, $l(x) > 0$ and $l(x)$ and $K(x)$ are C^1 , $c(x) > 0$ and $c(x)$ and $L(x)$ are C^0 , and $\ln(K(x)/l(x))_x \leq -L(x)$.

The comparisons of the driving-point immittance properties with those of lumped, linear, passive networks are the same as those made before. They are therefore not repeated here.

Transfer Admittances and Gain—Type 2-4 Active Lines

Since the transfer admittances for type 2-4 active lines from eq. 4.15 are

$$y_{12} = - \frac{1}{Z(0)} \frac{1}{v_2(d)} \quad (4.75)$$

$$y_{21} = - e^{-\int_0^x (K+L) dx} / Z(0) v_2(d) \quad (4.76)$$

they have no zeros and have the same poles as y_{11} . Therefore, their Bode magnitude and phase plots must have monotonic decreasing characteristics. The same transfer admittance comparisons may be made as before.

Since the open-circuit voltage gain is

$$T_v = - \frac{y_{21}}{y_{22}} = \frac{Z(d)}{Z(0)} \frac{e^{-\int_0^x (K+L) dx}}{v_2'(d) + K(d)v_2(d)} \quad (4.77)$$

the only zero of T_v is $s = -r(d)/l(d)$. The poles of T_v are the zeros of y_{22} and $s = -r(0)/l(0)$.

The short-circuit current gain is

$$T_I = -\frac{y_{21}}{y_{11}} = \frac{Z(d)}{Z(0)} \frac{e^{-\int_0^x (K+L)dx}}{v_1(d) - K(0)v_2(d)} \quad (4.78)$$

which has only one zero at $s = -r(d)/l(d)$. The poles of T_I are the zeros of y_{11} and $s = -r(0)/l(0)$.

Again for summation purposes, the results for the nonuniform type 2-4 rcg active line are compared to those of the uniform rcg line of Chapter 3. The general characters of their pole-zero distributions are similar. Their driving-point admittances have poles and zeros alternating along the negative real axis of the s -plane with a zero closest the origin. The Bode magnitude plots of y_{11} and y_{22} must be monotonically increasing with phase bounded between 0° and 90° . The transfer admittances are all-pole functions. The poles are distributed along the negative real axis in the s -plane. Their Bode magnitude and phase plots decrease monotonically. The gain functions exhibit similar characteristics at high frequencies. Low frequency gain can be achieved by adjusting $-\int_0^d (K+L)dx$ to be sufficiently large.

Active Transmission Line Analysis—Concluding Remarks

It has been the purpose of this chapter to examine the general nature of active transmission lines. Two-port parameters expressed in terms of general voltage and current solutions were formulated. To make these expressions amenable for analysis, the basic set was introduced which reduced the parameter equations to rather simple form. By considering the Wronskian and self-adjoint nature of the active line, parameter simplifications resulted and pole-zero cancellation was

examined. To gain some physical insight into pole-zero locations, the class of active lines which fulfilled the parameter conditions of the Sturm-Liouville equation were considered. This allowed the general root locus of the poles and zeros of the parameters to be drawn and interpreted. Finally, these results were compared with those of the uniform active lines of Chapter 3. Nonuniform lines can be employed to add flexibility in meeting design requirements as the next chapter will show.

Having now completed the analysis of active lines, the synthesis of active lines is reviewed. In the next chapter, a general synthesis scheme allowing computerized design is presented.

V. SYNTHESIS OF ACTIVE TRANSMISSION LINES

Synthesis Using Variational Calculus

Synthesis of active transmission lines requires appropriate parameter distributions be found to fulfill consistent design requirements. Initial design is often affected by consulting design tables to ascertain whether any of the "standard" distributions (i.e. distributions of lines with readily expressible two-port parameters and other properties of interest) can be employed to meet requirements. If some exist, then economic and technological considerations dictate whether these lines can actually be realized.

Generally however, the realization will not require one of these specific tapers. Thus, a synthesis scheme for lines with arbitrary parameter distribution is required. A synthesis method using variational calculus has been introduced by Rohrer (27). This method is particularly well-suited for synthesizing active lines. In this approach, economic and technological limitations of parameter distributions are established a priori. Then parameter distributions are generated consistent with these limitations which satisfy the design requirements in some "optimum" manner. The synthesis is performed directly in either the time domain or frequency domain.

Rohrer has developed this synthesis method for general passive transmission lines (28). With simple notational change, it applies to type 1-3 active lines. The method is readily extendable to type 2-4 active lines.

Time Domain Synthesis—Type 1-3 Active Lines

Consider the active transmission line embedded between voltage sources e_1 and e_2 and resistances R_1 and R_2 in Fig. 44. A design problem of common interest is to obtain specific port voltages by adjusting parameter distributions accordingly. There is, of course, no guarantee that this can be done exactly.

Thus, the following is chosen to be the optimization criterion:
Minimize the quadratic error integral

$$E^* = \int_0^{\infty} \frac{1}{2} \left[W_1(t) \left(k_1 v_1(t) - v(0,t) \right)^2 + W_2(t) \left(k_2 v_2(t) - v(d,t) \right)^2 \right] dt \quad (5.1)$$

consistent with various conditions by adjusting r^* , l , g^* , and c to their "optimum" values. $v_1(t)$ and $v_2(t)$ are the input and output voltages required by the design, and $v(0,t)$ and $v(d,t)$ are the actual input and output voltages of the active line. Thus, $(v_1 - v(0,t))$ and $(v_2 - v(d,t))$ are "error" voltages at the ports. Nonnegative functions $W_1(t)$ and $W_2(t)$ together with constants k_1 and k_2 allow specification compromises to be made and therefore introduce design flexibility.

The minimization must be consistent with the active transmission line equations, port conditions, and parameter limitations. The internal behavior of the line is described by eqs. 1.3 and 1.4 as

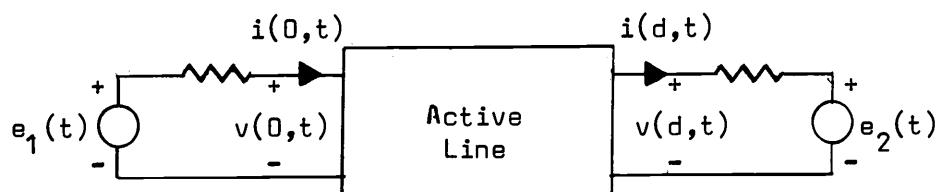


Fig. 44. General active line embedded between voltage sources and loads.

$$-v_x = r^*i + li_t \quad (5.2)$$

$$-i_x = g^*v + cv_t \quad (5.3)$$

for (x,t) in D^t where domain $D^t = \{(x,t): 0 < x < d, t \geq 0\}$. From Fig. 44, the port conditions are related to voltage sources e_1 and e_2 and resistances R_1 and R_2 as

$$e_1(t) = v(0,t) + R_1 i(0,t) \quad (5.4)$$

$$e_2(t) = v(d,t) - R_2 i(d,t) \quad (5.5)$$

Physical limitations, technological capabilities, and economic considerations dictate lower and upper parameter bounds. Therefore,

$$\begin{bmatrix} r^* \\ g^* \\ l \\ c \end{bmatrix}_{\min} \leq \begin{bmatrix} r^*(x) \\ g^*(x) \\ l(x) \\ c(x) \end{bmatrix} \leq \begin{bmatrix} r^* \\ g^* \\ l \\ c \end{bmatrix}_{\max} \quad (5.6)$$

or simply

$$\underline{p}_{\min} \leq \underline{p}(x) \leq \underline{p}_{\max} \quad (5.7)$$

where the parameter matrix \underline{p} is introduced for notational convenience.

The parameter distributions to be generated must lie within these bounds. A convenient but unnecessary requirement is initial line relaxation where

$$v(x,0) = i(x,0) = 0 \quad (5.8)$$

Subsequent mathematical operations require the time invariance of the network parameters to be explicitly constrained,

$$r^*_t = g^*_t = l_t = c_t = 0 \quad (5.9)$$

although this was assumed when the active transmission line equations

were written. These constraints are sufficient for our purposes although additional requirements can be imposed if deemed important.

The problem is now to minimize the error integral (eq. 5.1) under the conditions of eqs. 5.2-5.9. It is convenient to use Lagrange's method of multipliers in this minimization (5). Using this method, the error integral is appended with several of the constraints utilizing Lagrange multipliers. The problem of minimizing the error integral (eq. 5.1) under the constraints of eqs. 5.2-5.9 is equivalent to minimizing the augmented error integral

$$E = E^* + \int_0^d \int_0^{\infty} \left(\theta \left[v_x + r^* i + l i_t \right] + \phi \left[i_x + g^* v + c v_t \right] + \lambda^r r^*_t + \lambda^g g^*_t + \lambda^l l_t + \lambda^c c_t \right) dt dx \quad (5.10)$$

under the conditions of eqs. 5.4-5.8. Lagrange multipliers $\theta(x,t)$, $\phi(x,t)$, $\lambda^r(x,t)$, $\lambda^g(x,t)$, $\lambda^l(x,t)$, and $\lambda^c(x,t)$ of the constraints of eqs. 5.2, 5.3, and 5.9, respectively, are independent functions whose solutions arise from, and become part of, the synthesis process. It is convenient in writing later equations to remove partial derivatives of v , i , r^* , g^* , l , and c in the augmented error integral. After integration by parts, the integral becomes

$$E = \int_0^d \int_0^{\infty} \left(\left[-\theta_x v + \theta r^* i - \theta_t l i \right] + \left[-\phi_x i + \phi g^* v - \phi_t c v \right] - \lambda^r_t r^* - \lambda^g_t g^* - \lambda^l_t l - \lambda^c_t c \right) dt dx + \int_0^{\infty} \left(\frac{1}{2} W_1(t) \left[k_1 v_1(t) - v(0,t) \right]^2 + \frac{1}{2} W_2(t) \left[k_2 v_2(t) - v(d,t) \right]^2 + \left[\theta v + \phi i \right]_{x=0}^d \right) dt + \int_0^d \left(\left[\theta l i + \phi c v + \lambda^r r^* + \lambda^g g^* + \lambda^l l + \lambda^c c \right]_{t=0}^{\infty} \right) dx \quad (5.11)$$

For a (local) minimum in E , the fundamental theorem of the calculus of variations requires that the first variation in E , denoted as δE , satisfy $\delta E \geq 0$ (2,7). Suppose E is a functional involving n independent functions, i.e. $E = E(y_1, \dots, y_n)$. The first variation δE is then

$$\delta E = \sum_{i=1}^n \frac{\partial E}{\partial y_i} \delta y_i \quad (5.12)$$

Writing $y_i = y_i + \delta y_i$ where y_i are the functions minimizing E , then the first variation of y_i , denoted as δy_i , is the fluctuation of y_i about y_i . Since the n functions are independent, their first variations are independent. Thus, any of the δy_i can be set equal to zero. Setting the δy_i equal to zero except for $i = j$, the fundamental theorem requires $\partial E / \partial y_j \geq 0$. But since the sign of δy_j is arbitrary, $\partial E / \partial y_j = 0$. If however y_j is constrained between $y_{j \min}$ and $y_{j \max}$ and assumes a bounding value, then its first variation $\delta y_j \geq 0$ or $\delta y_j \leq 0$, respectively. This is reflected in that $\partial E / \partial y_j > 0$ when $y_j = y_{j \min}$ and $\partial E / \partial y_j < 0$ when $y_j = y_{j \max}$ (27). These form the basic concepts which are now utilized in forming the synthesis method.

δE may be written in terms of the first variations of v , i , r^* , g^* , l , and c , denoted as δv , δi , δr^* , δg^* , δl , and δc , respectively. When Lagrange multipliers are used, v , i , r^* , g^* , l , and c are treated as independent functions. Their first variations are therefore independent. Thus from eq. 5.11, δE is

$$\delta E = \int_0^d \int_0^{\infty} \left(\delta v(x,t) \left[-\theta_x + \theta g^* - \theta_t c \right] + \delta i(x,t) \left[-\theta_x + \theta r^* - \theta_t l \right] + \delta r^*(x) \left[\theta i - \lambda_t^r \right] \right. \\ \left. + \delta g^*(x) \left[\theta v - \lambda_t^g \right] + \delta l(x) \left[-\theta_t i - \lambda_t^l \right] + \delta c(x) \left[-\theta_t v - \lambda_t^c \right] \right) dt dx$$

$$\begin{aligned}
& + \int_0^{\omega} \left(\delta v(d,t) \left[-w_2(t)(k_2 v_2(t) - v(d,t)) + \theta(d,t) \right] + \delta i(d,t) \phi(d,t) \right) dt \\
& + \int_0^{\omega} \left(\delta v(0,t) \left[-w_1(t)(k_1 v_1(t) - v(0,t)) - \theta(0,t) \right] - \delta i(0,t) \phi(0,t) \right) dt \\
& + \int_0^d \left(\delta v(x, \omega) \phi(x, \omega) c(x) + \delta i(x, \omega) \theta(x, \omega) l(x) + \delta r^*(x) \lambda^r(x, \omega) \right. \\
& + \delta g^*(x) \lambda^g(x, \omega) + \delta l(x) \left[\theta(x, \omega) l(x) + \lambda^l(x, \omega) \right] + \delta c(x) \left[\phi(x, \omega) c(x) \right. \\
& \left. \left. + \lambda^c(x, \omega) \right] \right) dx \\
& - \int_0^d \left(\text{same as the above integral changing } \omega \text{ to } 0 \right) dx \tag{5.13}
\end{aligned}$$

Surveying eq. 5.13, there are six differential equations (called Euler's differential equations) which arise from coefficients of the first variations within the surface (double) integral. Boundary conditions for these differential equations arise from the corresponding first variations within boundary integrals. Interpretation of eq. 5.13 leads to a set of equations which describe an "adjoint" active transmission line (shown in Fig. 45) whose solution is used in the optimization process. This will now be made clear in the following discussion.

The coefficients of $\delta v(x,t)$ and $\delta i(x,t)$ equal zero,

$$- \phi_x + \theta r^* - \theta_t l = 0 \tag{5.14}$$

$$- \theta_x + \phi g^* - \phi_t c = 0 \tag{5.15}$$

for all (x,t) in D^t since $\delta v(x,t)$ and $\delta i(x,t)$ are arbitrary. These "adjoint line" equations are analogous to the active line equations,

eqs. 5.2 and 5.3, when x and t are negative.

The boundary conditions of the adjoint line follow from the coefficients of the variations $\delta v(0,t)$ and $\delta v(d,t)$ on the x -boundaries ($x=0$, and $x=d$). Since $\delta v(0,t)$ and $\delta v(d,t)$ are arbitrary, their coefficients must equal zero so

$$W_1(t) \left[k_1 v_1(t) - v(0,t) \right] + \theta(0,t) - \phi(0,t)/R_1 = 0 \quad (5.16)$$

$$W_2(t) \left[k_2 v_2(t) - v(d,t) \right] - \theta(d,t) - \phi(d,t)/R_2 = 0 \quad (5.17)$$

Here, it is recognized that the port voltage and current variations on the original line are constrained by eqs. 5.4 and 5.5 as

$$\delta v(0,t) + R_1 \delta i(0,t) = 0 \quad (5.18)$$

$$\delta v(d,t) - R_2 \delta i(d,t) = 0 \quad (5.19)$$

The voltage and current along the adjoint line at $t = \infty$ follow from the coefficients of variations $\delta v(x, \infty)$ and $\delta i(x, \infty)$ along the $t = \infty$ boundary integral. Since $\delta v(x, \infty)$ and $\delta i(x, \infty)$ are arbitrary, $\phi(x, \infty) = \theta(x, \infty) = 0$

$$(5.20)$$

Since the initial conditions along the original line are specified by eq. 5.8, the initial condition variations are constrained to be

$$\delta v(x,0) = \delta i(x,0) = 0 \quad (5.21)$$

Therefore, from the integral along the $t = 0$ boundary, the coefficients of $\delta v(x,0)$ and $\delta i(x,0)$ which are $\phi(x,0)$ and $\theta(x,0)$, respectively, are arbitrary.

The various adjoint line characteristics are summarized with the original line characteristics in Fig. 45. The internal behavior of the adjoint line is described by eqs. 5.14 and 5.15. The port behavior is given by eqs. 5.16 and 5.17. Here arises the interesting fact that the "error voltages" previously mentioned energize or drive the adjoint

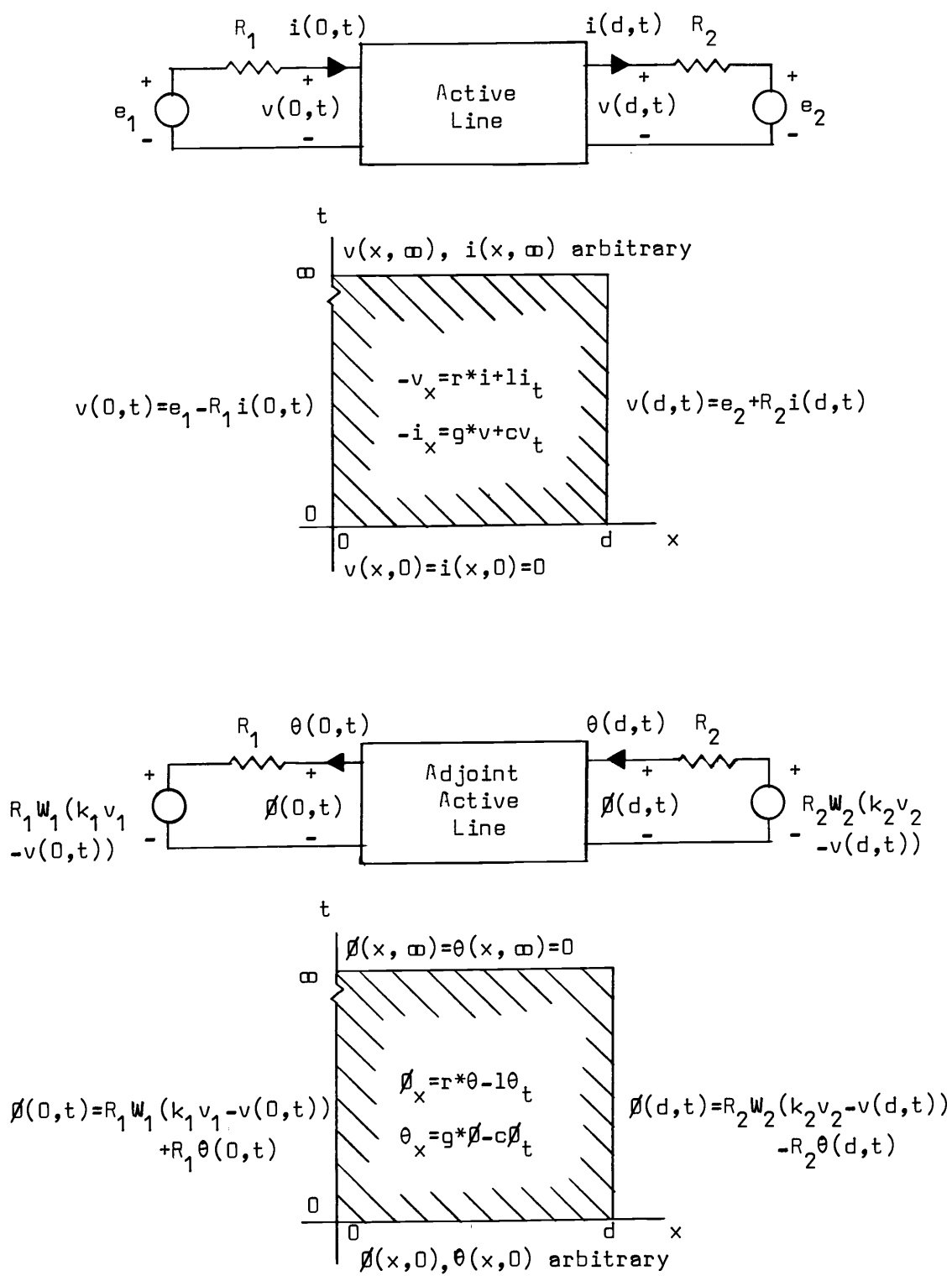


Fig. 45. Time domain variational synthesis requires time domain solution of the original active line and the adjoint line shown. Their constraints are labelled on the (x, t) -plane.

line. Physically, as the error voltages become smaller, the adjoint line responses become smaller. It will be seen that this is reflected mathematically in that the parameter distributions are approaching their optimum distributions. If we consider time as running backward from ∞ to 0, the adjoint line has zero initial conditions and arbitrary final conditions. Thus, there is a symmetry between the original active line and the adjoint line.

It remains to interpret the λ Lagrange multipliers and the parameter bounds given by eq. 5.7. The partial differential equations describing the Lagrange multipliers λ^r , λ^g , λ^l , and λ^c follow from the coefficients of δr^* , δg^* , δl , and δc in the surface integral. As was noted before, the variations are required to possess a certain sign when the parameters assume limiting values. Thus,

$$\begin{bmatrix} \theta_i - \lambda_t^r \\ \phi_v - \lambda_t^g \\ -\theta_{t,i} - \lambda_t^l \\ -\phi_{t,v} - \lambda_t^c \end{bmatrix} \begin{array}{l} < 0, \underline{p}(x) = p_{\max} \\ = 0, p_{\min} \leq \underline{p}(x) \leq p_{\max} \\ > 0, \underline{p}(x) = p_{\min} \end{array} \quad (5.22)$$

for (x,t) in D^t , where for notational convenience the \underline{p} matrix of eq. 5.7 is used.

The boundary values of these λ arise from the coefficients of the parameter variations δr^* , δg^* , δl , and δc on the $t = 0$ and $t = \infty$ boundaries. From eq. 5.13, these are

$$\begin{bmatrix} \lambda^r(x,0) \\ \lambda^g(x,0) \\ \lambda^l(x,0) \\ \lambda^c(x,0) \end{bmatrix} \begin{array}{l} < 0, \underline{p}(x) = p_{\max} \\ = 0, p_{\min} \leq \underline{p}(x) \leq p_{\max} \\ > 0, \underline{p}(x) = p_{\min} \end{array} \quad (5.23)$$

and

$$\begin{bmatrix} -\lambda^r(x, \omega) \\ -\lambda^g(x, \omega) \\ -\lambda^l(x, \omega) \\ -\lambda^c(x, \omega) \end{bmatrix} \begin{array}{l} < \underline{0}, \underline{p}(x) = \underline{p}_{\max} \\ = \underline{0}, \underline{p}_{\min} \leq \underline{p}(x) \leq \underline{p}_{\max} \\ > \underline{0}, \underline{p}(x) = \underline{p}_{\min} \end{array} \quad (5.24)$$

Combining these results yields

$$\begin{bmatrix} \lambda^r(x, \omega) - \lambda^r(x, 0) \\ \lambda^g(x, \omega) - \lambda^r(x, 0) \\ \lambda^l(x, \omega) - \lambda^l(x, 0) \\ \lambda^c(x, \omega) - \lambda^c(x, 0) \end{bmatrix} \begin{array}{l} < \underline{0}, \underline{p}(x) = \underline{p}_{\max} \\ = \underline{0}, \underline{p}_{\min} \leq \underline{p}(x) \leq \underline{p}_{\max} \\ > \underline{0}, \underline{p}(x) = \underline{p}_{\min} \end{array} \quad (5.25)$$

which is extremely useful. When eq. 5.22 is integrated with respect to t , eq. 5.25 can be utilized to yield

$$\int_0^{\omega} \begin{bmatrix} \theta_i \\ \beta_v \\ -\theta_{t i} \\ -\beta_{t v} \end{bmatrix} dt = \begin{array}{l} < \underline{0}, \underline{p}(x) = \underline{p}_{\max} \\ = \underline{0}, \underline{p}_{\min} \leq \underline{p}(x) \leq \underline{p}_{\max} \\ > \underline{0}, \underline{p}(x) = \underline{p}_{\min} \end{array} \quad (5.26)$$

This is the parameter optimization criteria from which the optimum distributions of r^* , g^* , l , and c can be found. Since for interior parameter solutions, the various integrals of eq. 5.26 are identically zero, they may be differentiated any number of times with respect to x . Differentiating once and simplifying yields the result that $r^*(x)/l(x) = g^*(x)/c(x)$ for the optimum line.¹² For the general synthesis however, optimality is not assumed.

The general synthesis method follows directly from these various

¹²From this result and the results related to eq. 4.65 in Chapter 4, it is interesting to note that the poles and zeros of the immittance parameters of an optimum active line have constant negative real parts.

results. If the adjoint transmission line equations (eqs. 5.14, 5.15) are satisfied along with their boundary conditions (eqs. 5.16, 5.17) and "initial" conditions (eq. 5.20), then the first variation of the augmented error integral eq. 5.13 is

$$\delta E = \int_0^d \int_0^{\infty} \begin{bmatrix} \theta_i \\ \rho_v \\ -\theta_{t,i} \\ -\rho_{t,v} \end{bmatrix} dt \begin{bmatrix} \delta r^*(x) \\ \delta g^*(x) \\ \delta l(x) \\ \delta c(x) \end{bmatrix}^T dx \quad (5.27)$$

where T denotes the transpose. The gradient of the augmented error integral, eq. 5.11, with respect to the parameters is

$$\underline{\nabla E} = \left[\frac{\partial E}{\partial r^*} \quad \frac{\partial E}{\partial g^*} \quad \frac{\partial E}{\partial l} \quad \frac{\partial E}{\partial c} \right]^T = \int_0^d \int_0^{\infty} \begin{bmatrix} \theta_i \\ \rho_v \\ -\theta_{t,i} \\ -\rho_{t,v} \end{bmatrix} dt dx \quad (5.28)$$

The first variation of eq. 5.13 may be expressed as

$$\delta E = \int_0^d (\underline{\nabla E})_x \delta P^T dx \quad (5.29)$$

so that

$$(\underline{\nabla E})_x = \int_0^{\infty} \begin{bmatrix} \theta_i \\ \rho_v \\ -\theta_{t,i} \\ -\rho_{t,v} \end{bmatrix} dt \quad (5.30)$$

is the local gradient matrix for

$$\underline{\delta P(x)} = \begin{bmatrix} \delta r^*(x) \\ \delta g^*(x) \\ \delta l(x) \\ \delta c(x) \end{bmatrix} \quad (5.31)$$

Employing the local gradient to alter parameter values in the direction of steepest descent to reduce the error, a practical iterative synthesis method results. Here then, we let

$$\begin{bmatrix} r_{n+1}^*(x) \\ g_{n+1}^*(x) \\ l_{n+1}(x) \\ c_{n+1}(x) \end{bmatrix} = \begin{bmatrix} r_n^*(x) \\ g_n^*(x) \\ l_n(x) \\ c_n(x) \end{bmatrix} - \begin{bmatrix} a_n^r \\ a_n^g \\ a_n^l \\ a_n^c \end{bmatrix} \int_0^\omega \begin{bmatrix} \theta_n(x,t) i_n(x,t) \\ \phi_n(x,t) v_n(x,t) \\ -\theta_{tn}(x,t) i_n(x,t) \\ -\phi_{tn}(x,t) v_n(x,t) \end{bmatrix} dt \quad (5.32)$$

for all x in D^t to generate the parameter distributions. The a 's are nonnegative numbers that control step size.

The flow chart of the synthesis procedure is shown in Fig. 46. The source voltages (e_1, e_2) and their internal resistances (R_1, R_2) are given and the constants (W_1, W_2, k_1, k_2) of the optimization integral chosen. The maximum acceptable value E_{\max} of the augmented error integral for program termination is set. The desired port responses $v_1(t)$ and $v_2(t)$ are specified. The parameters \underline{p} are bounded and constants \underline{a} of eq. 5.32 chosen.

Upon choosing the initial parameter distribution, the voltages $v(x,t)$ and currents $i(x,t)$ along the active line are determined. The error voltages $W_1(k_1 v_1 - v(0,t))$ and $W_2(k_2 v_2 - v(d,t))$ are calculated and the approximation criterion tested to determine whether the optimum solution has been attained. If E_n is less than E_{\max} , the optimum parameter distribution is $\underline{p}_n(x)$. Otherwise the program continues and the adjoint voltage $\phi(x,t)$ and current $\theta(x,t)$ are found.

Since the adjoint line is described by equations identical with those solved previously, the same analysis program may be used with only slight modification. Time and distance are made negative and

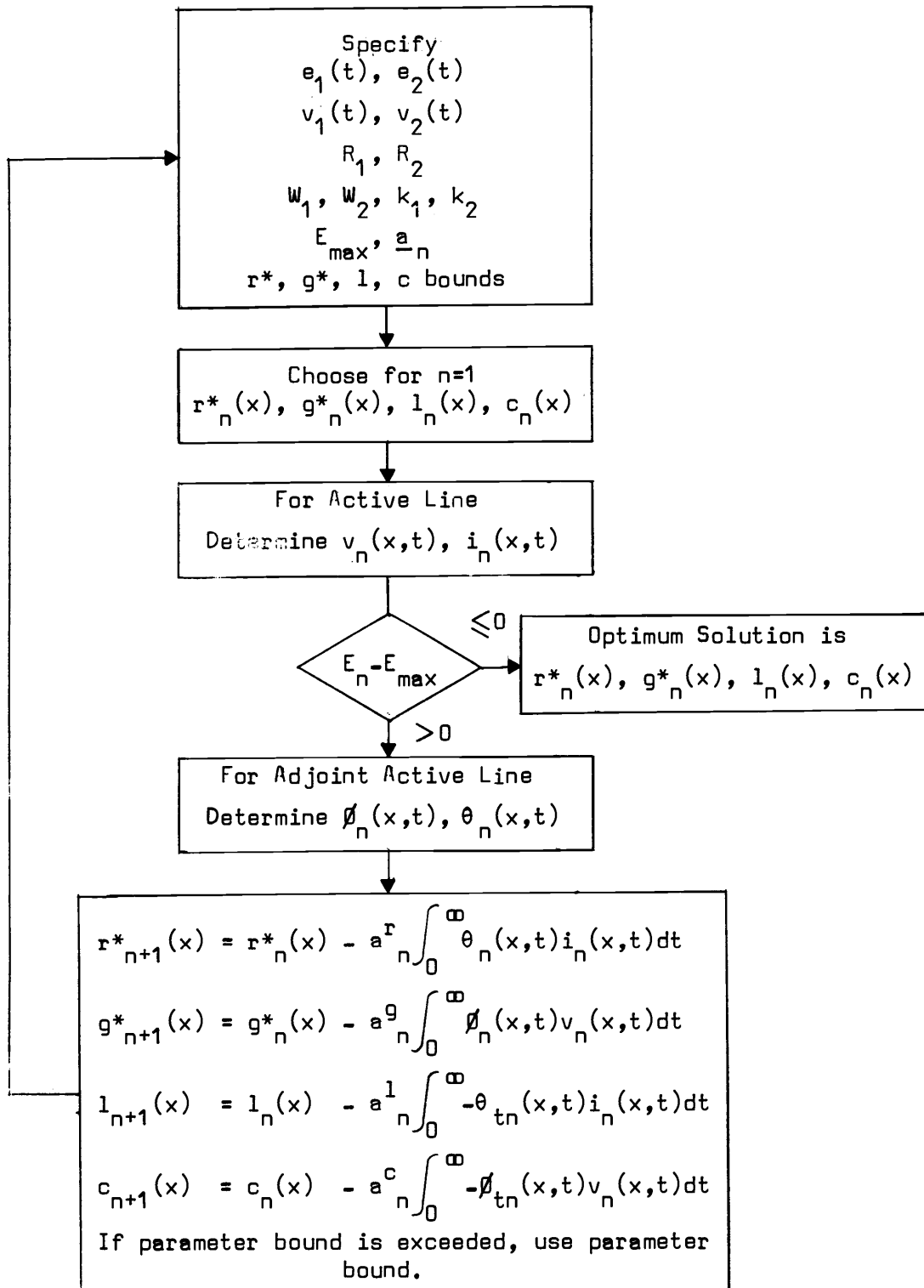


Fig. 46. Flow chart of time domain calculations to determine optimum parameter distributions for type 1-3 active lines.

voltage source e_1 is replaced by $R_1 W_1(k_1 v_1 - v(0, t))$ and source e_2 by $R_2 W_2(k_2 v_2 - v(d, t))$.

The r^* , g^* , l , and c parameter distributions are found from v , i , ϕ and θ in eq. 5.32. If the parameter bounds of eq. 5.6 are exceeded, the parameter assumes the value of the bound. This process reiterates until an acceptable distribution is determined.

Frequency Domain Synthesis—Type 1-3 Active Lines

Frequency domain synthesis can equally well be carried out. Its development using phasor notation is analogous to that of the time domain synthesis. Denoting the source voltages as $E_1(w)$ and $E_2(w)$ with port impedances $Z_1(w)$ and $Z_2(w)$, the quadratic error integral is

$$E^* = \int_{-\infty}^{\infty} \left(\frac{1}{2} W_1(w) |k_1 v_1(w) - v(0, w)|^2 + W_2(w) |k_2 v_2(w) - v(d, w)|^2 \right) dw \quad (5.33)$$

Again, real nonnegative functions W_1 and W_2 and constants k_1 and k_2 introduce design flexibility.

The transmission line equations (eqs. 2.1 and 2.2) in the frequency domain are

$$-V_x = (r^* + j\omega l) I \quad (5.34)$$

$$-I_x = (g^* + j\omega c) V \quad (5.35)$$

for (x, w) in D^W where $D^W = \{(x, w) : 0 < x < d, |w| < \infty\}$. The port conditions are

$$E_1(w) = V(0, w) + Z_1(w) I(0, w) \quad (5.36)$$

$$E_2(w) = V(d, w) - Z_2(w) I(d, w) \quad (5.37)$$

where port impedances Z_1 and Z_2 are real functions (this insures the

optimum network elements are realizable). The parameter values are bounded as before in eq. 5.7 and are explicitly constrained to be frequency independent

$$r_w^* = g_w^* = l_w = c_w = 0 \quad (5.38)$$

The error integral is augmented to include the constraints imposed by the active line equations and frequency independence of the parameters by introducing Lagrange multipliers $\phi(x,w)$, $\theta(x,w)$, $\lambda^r(x,w)$, $\lambda^g(x,w)$, $\lambda^l(x,w)$, and $\lambda^c(x,w)$ to obtain

$$\begin{aligned} E = E^* + \int_0^d \int_{-\infty}^{\infty} \theta [V_x + (r^* + jw l) I] + \phi [I_x + (g^* + jw c) V] \\ + \lambda^r r_w^* + \lambda^g g_w^* + \lambda^l l_w + \lambda^c c_w \Big] dw dx \end{aligned} \quad (5.39)$$

After integration by parts to remove partial derivatives of V , I , r^* , g^* , l , and c , we express the first variation of the augmented error integral as

$$\begin{aligned} \delta E = \int_0^d \int_{-\infty}^{\infty} \left(\delta V(x,w) [-\theta_x + (g^* - jw c) \phi] + \delta I(x,w) [-\phi_x + (r^* - jw l) \theta] \right. \\ \left. + \delta r^*(x) [I \theta - \lambda^r_w] + \delta g^*(x) [V \phi - \lambda^g_w] + \delta l(x) [-jw I \theta - \lambda^l_w] + \delta c(x) \cdot \right. \\ \left. [-jw V \phi - \lambda^c_w] \right) dw dx \\ + \int_{-\infty}^{\infty} \left(\delta V(d,w) [-w_2 (k_2 V_2 - V(d,w)) + \theta(d,w)] + \delta I(d,w) \phi(d,w) \right) dw \\ + \int_{-\infty}^{\infty} \left(\delta V(0,w) [-w_1 (k_1 V_1 - V(0,w)) - \theta(0,w)] - \delta I(0,w) \phi(0,w) \right) dw \\ + \int_0^d \left(\delta r^*(x) \lambda^r(x, \omega) + \delta g^*(x) \lambda^g(x, \omega) + \delta l(x) \lambda^l(x, \omega) + \delta c(x) \lambda^c(x, \omega) \right) dx \\ - \int_0^d \left(\text{same as the above integral changing } \omega \text{ to } -\omega \right) dx \end{aligned} \quad (5.40)$$

Interpretation of eq. 5.40 again leads to equations which describe the adjoint active transmission line shown in Fig. 47.

The internal behavior is described by

$$-\delta_x + (r^* - j\omega l)\theta = 0 \quad (5.41)$$

$$-\theta_x + (g^* - j\omega c)\delta = 0 \quad (5.42)$$

which are the coefficients of $\delta V(x, \omega)$ and $\delta I(x, \omega)$ for (x, ω) in D^w .

Thus, the adjoint line equations are analogous to the line equations (eqs. 5.34 and 5.35) when x and w are negative.

The boundary conditions arise from $\delta V(0, \omega)$ and $\delta V(d, \omega)$ coefficients as

$$w_1 \left[k_1 v_1 - V(0, \omega) \right] + \theta(0, \omega) - \delta(0, \omega)/Z_1(\omega) = 0 \quad (5.43)$$

$$w_2 \left[k_2 v_2 - V(d, \omega) \right] - \theta(d, \omega) - \delta(d, \omega)/Z_2(\omega) = 0 \quad (5.44)$$

since port variations are constrained by eqs. 5.36 and 5.37 to be

$$\delta V(0, \omega) + Z_1(\omega)\delta I(0, \omega) = 0 \quad (5.45)$$

$$\delta V(d, \omega) - Z_2(\omega)\delta I(d, \omega) = 0 \quad (5.46)$$

From the first variation of the parameters within and on the boundary, the following criteria is obtained,¹³

$$\int_{-\infty}^{\infty} \begin{bmatrix} \theta I \\ \delta V \\ -j\omega\theta I \\ -j\omega\delta V \end{bmatrix} dw = \begin{cases} < 0, & \underline{P}(x) = P_{\max} \\ = 0, & P_{\min} \leq \underline{P}(x) \leq P_{\max} \\ > 0, & \underline{P}(x) = P_{\min} \end{cases} \quad (5.47)$$

The iterative synthesis scheme in Fig. 46 is carried out as before by employing the local gradient of E to change parameter values in the direction of steepest descent as

¹³The same optimum condition $r^*(x)/l(x) = g^*(x)/c(x)$ results from these equations consistent with the previous result.

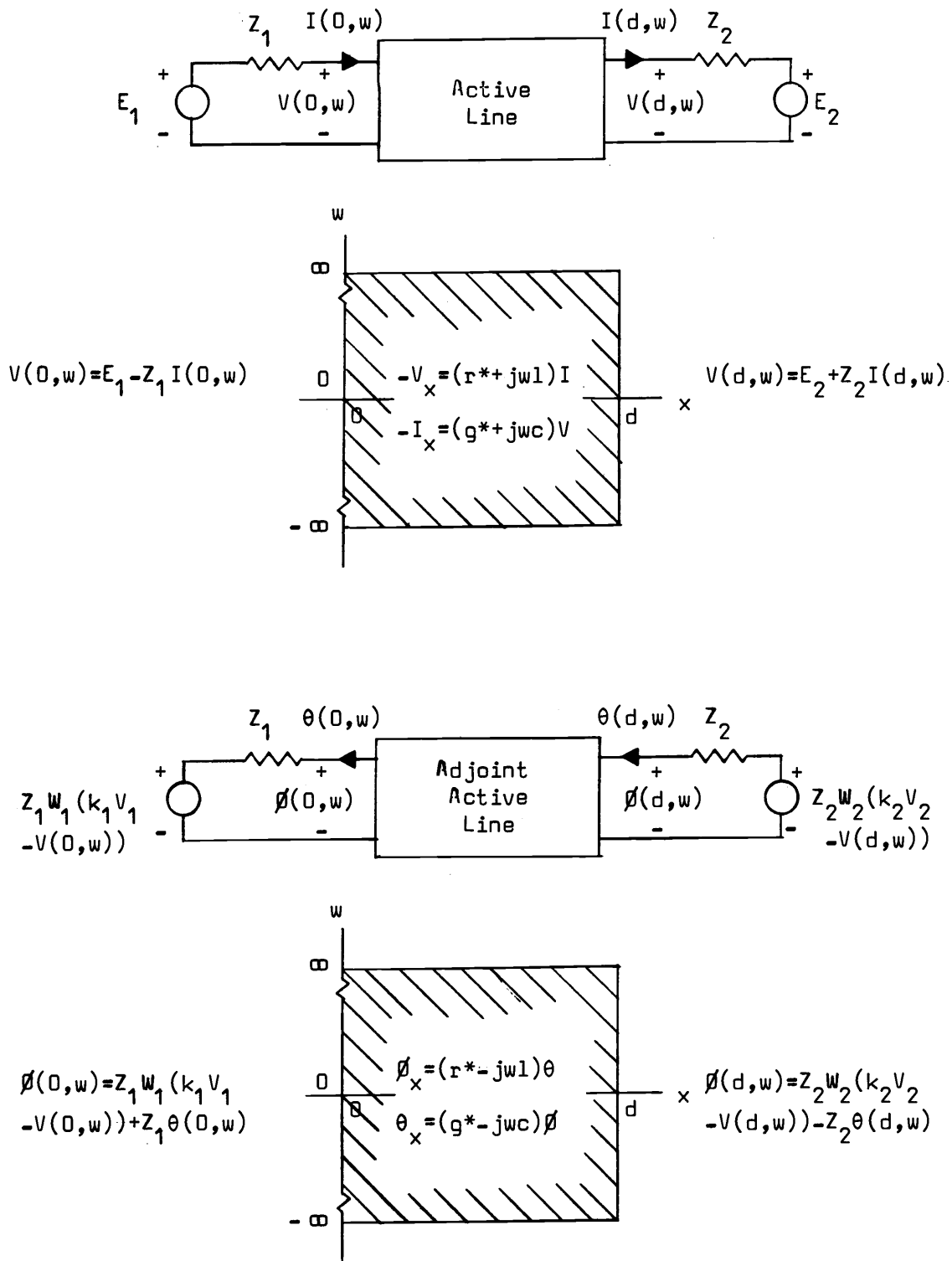


Fig. 47. Frequency domain synthesis requires frequency domain solution of the original active line and the adjoint line shown. Their constraints are labelled on the (x,w)-plane.

$$\begin{bmatrix} r_{n+1}^* \\ g_{n+1}^* \\ l_{n+1} \\ c_{n+1} \end{bmatrix} = \begin{bmatrix} r_n^* \\ g_n^* \\ l_n \\ c_n \end{bmatrix} - \begin{bmatrix} a_n^r \\ a_n^g \\ a_n^l \\ a_n^c \end{bmatrix} \int_{-\infty}^{\infty} \begin{bmatrix} \theta_n(x,w) I_n(x,w) \\ \phi_n(x,w) V_n(x,w) \\ -jw\theta_n(x,w) I_n(x,w) \\ -jw\phi_n(x,w) V_n(x,w) \end{bmatrix}^T dw \quad (5.48)$$

The only change is that frequency domain quantities are used rather than time domain quantities, and frequency runs from $-\infty$ to ∞ rather than time from 0 to ∞ .

Having presented the time and frequency domain synthesis of general type 1-3 active lines, the same methods are now used to synthesize type 2-4 active lines.

Time Domain Synthesis—Type 2-4 Active Lines

The minimization of the quadratic error integral must be consistent with the type 2-4 active line equations, port conditions, and parameter limitations. The active line equations are

$$-v_x = ri + li_t + Kv \quad (5.49)$$

$$-i_x = gv + cv_t + Li \quad (5.50)$$

for (x,t) in D^t . The port conditions as before are

$$e_1(t) = v(0,t) + R_1 i(0,t) \quad (5.51)$$

$$e_2(t) = v(d,t) - R_2 i(d,t) \quad (5.52)$$

The network is specified to be initially relaxed

$$v(x,0) = i(x,0) = 0 \quad (5.53)$$

The parameters are bounded as

$$\begin{bmatrix} r \\ g \\ l \\ c \\ K \\ L \end{bmatrix}_{\min} \leq \begin{bmatrix} r(x) \\ g(x) \\ l(x) \\ c(x) \\ K(x) \\ L(x) \end{bmatrix} \leq \begin{bmatrix} r \\ g \\ l \\ c \\ K \\ L \end{bmatrix}_{\max} \quad (5.54)$$

or, utilizing the parameter matrix, simply

$$\underline{P}_{\min} \leq \underline{P}(x) \leq \underline{P}_{\max} \quad (5.55)$$

Again the time-invariance of the parameter values is explicitly constrained,

$$r_t = g_t = l_t = c_t = K_t = L_t = 0 \quad (5.56)$$

The minimization of the error integral under the conditions of eqs. 5.49-5.56 is equivalent to minimizing the augmented error integral

$$E = E^* + \int_0^d \int_0^{\infty} \left(\theta \left[v_x + r i + l i_t + K v \right] + \phi \left[i_x + g v + c v_t + L i \right] + \lambda^r r_t + \lambda^g g_t + \lambda^l l_t + \lambda^c c_t + \lambda^K K_t + \lambda^L L_t \right) dt dx \quad (5.57)$$

consistent with eqs. 5.51-5.55. Again $\phi(x,t)$, $\theta(x,t)$, $\lambda^r(x,t)$, $\lambda^g(x,t)$, $\lambda^l(x,t)$, $\lambda^c(x,t)$, $\lambda^K(x,t)$, and $\lambda^L(x,t)$ are the Lagrange multipliers of the active line equations and time-invariance constraints. Performing integration by parts to remove partial derivatives of v , i , and the parameters, results in

$$E = \int_0^d \int_0^{\infty} \left(\left[-\theta_x v + \theta r i - \theta_t l i + \theta K v \right] + \left[-\phi_x i + \phi g v - \phi_t c v + \phi L i \right] - r \lambda_t^r - g \lambda_t^g - l \lambda_t^l - c \lambda_t^c - K \lambda_t^K - L \lambda_t^L \right) dt dx + \int_0^{\infty} \left(\frac{1}{2} W_1 \left[k_1 v_1 - v(0,t) \right]^2 + \frac{1}{2} W_2 \left[k_2 v_2 - v(d,t) \right]^2 + \left[\theta v + \phi i \right]_{x=0}^d \right) dt$$

$$+ \int_0^d \left(\left[\theta l i + \rho c v + \lambda^R r + \lambda^G g + \lambda^1 l + \lambda^C c + \lambda^K k + \lambda^L L \right]_{t=0}^{\infty} \right) dx \quad (5.58)$$

The first variation of the augmented error functional is

$$\begin{aligned} \delta E = & \int_0^d \int_0^{\infty} \left(\delta v(x,t) \left[-\theta_x + \theta k + \rho g - \rho_t c \right] + \delta i(x,t) \left[-\rho_x + \rho l + \theta r - \theta_t l \right] \right. \\ & + \delta r(x) \left[\theta i - \lambda^R_t \right] + \delta g(x) \left[\rho v - \lambda^G_t \right] + \delta l(x) \left[-\theta_t i - \lambda^1_t \right] + \delta c(x) \left[-\rho_t v - \lambda^C_t \right] \\ & + \delta k(x) \left[\theta v - \lambda^K_t \right] + \left. \delta L(x) \left[\rho i - \lambda^L_t \right] \right) dt dx \\ & + \int_0^{\infty} \left(\delta v(d,t) \left[-W_2(k_2 v_2 - v(d,t)) + \theta(d,t) \right] + \delta i(d,t) \rho(d,t) \right) dt \\ & + \int_0^{\infty} \left(\delta v(0,t) \left[-W_1(k_1 v_1 - v(0,t)) - \theta(0,t) \right] - \delta i(0,t) \rho(0,t) \right) dt \\ & + \int_0^d \left(\delta v(x, \omega) c(x) \rho(x, \omega) + \delta i(x, \omega) l(x) \theta(x, \omega) + \delta r(x) \lambda^R(x, \omega) \right. \\ & + \delta g(x) \lambda^G(x, \omega) + \delta k(x) \lambda^K(x, \omega) + \delta l(x) \lambda^L(x, \omega) + \delta l(x) \left[\lambda^1(x, \omega) \right. \\ & + \left. i(x, \omega) \theta(x, \omega) \right] + \left. \delta c(x) \left[\lambda^C(x, \omega) + v(x, \omega) \rho(x, \omega) \right] \right) dx \\ & - \int_0^d \left(\text{same as the above integral changing } \omega \text{ to } 0 \right) dx \quad (5.59) \end{aligned}$$

The adjoint active line equations result from $\delta v(x,t)$ and $\delta i(x,t)$ coefficients as

$$-\rho_x + r\theta - l\theta_t + \rho l = 0 \quad (5.60)$$

$$-\theta_x + g\rho - c\rho_t + \theta k = 0 \quad (5.61)$$

for (x,t) in D^t .

Boundary conditions result from $\delta v(0,d)$ and $\delta v(d,t)$ coefficients as

$$W_1(t) \left[k_1 v_1 - v(0,t) \right] + \theta(0,t) - \rho(0,t)/R_1 = 0 \quad (5.62)$$

$$W_2(t) \left[k_2 v_2 - v(d,t) \right] - \theta(d,t) - \phi(d,t)/R_2 = 0 \quad (5.63)$$

since the port variations are constrained from eqs. 5.51 and 5.52 as

$$\delta v(0,t) + R_1 \delta i(0,t) = 0 \quad (5.64)$$

$$\delta v(d,t) - R_2 \delta i(d,t) = 0 \quad (5.65)$$

"Initial" conditions along the adjoint line result from $\delta v(x, \omega)$ and $\delta i(x, \omega)$ coefficients as

$$\phi(x, \omega) = \theta(x, \omega) = 0 \quad (5.66)$$

while the final conditions are arbitrary since $\delta v(x,0)$ and $\delta i(x,0)$ are zero. The two lines with their boundary conditions are shown in Fig. 48. The partial differential equations describing the original line and adjoint line are analogous with sign reversal of x and t , where K and L are interchanged. Their initial conditions are identical and port conditions similar.

The parameter optimization follows as before as¹⁴

$$\int_0^\omega \begin{bmatrix} \theta i \\ \phi v \\ -\theta_t i \\ -\phi_t v \\ \theta v \\ \phi i \end{bmatrix} dt = \begin{cases} < 0, \underline{P}(x) = P_{\max} \\ 0, P_{\min} \leq \underline{P}(x) \leq P_{\max} \\ > 0, \underline{P}(x) = P_{\min} \end{cases} \quad (5.67)$$

When the adjoint line equations, and boundary and initial conditions are satisfied, the first variation of the augmented functional becomes

¹⁴ Differentiating eq. 5.67 once with respect to x and simplifying yields the result that $r(x)/l(x) = g(x)/c(x)$; differentiating twice results in $\frac{1}{2}(L-K) = (1_x / 1 - c_x / c)$ for the optimum active line.

Again, from eq. 4.65, the poles and zeros of the immittance parameters of the optimum line have constant negative real parts.

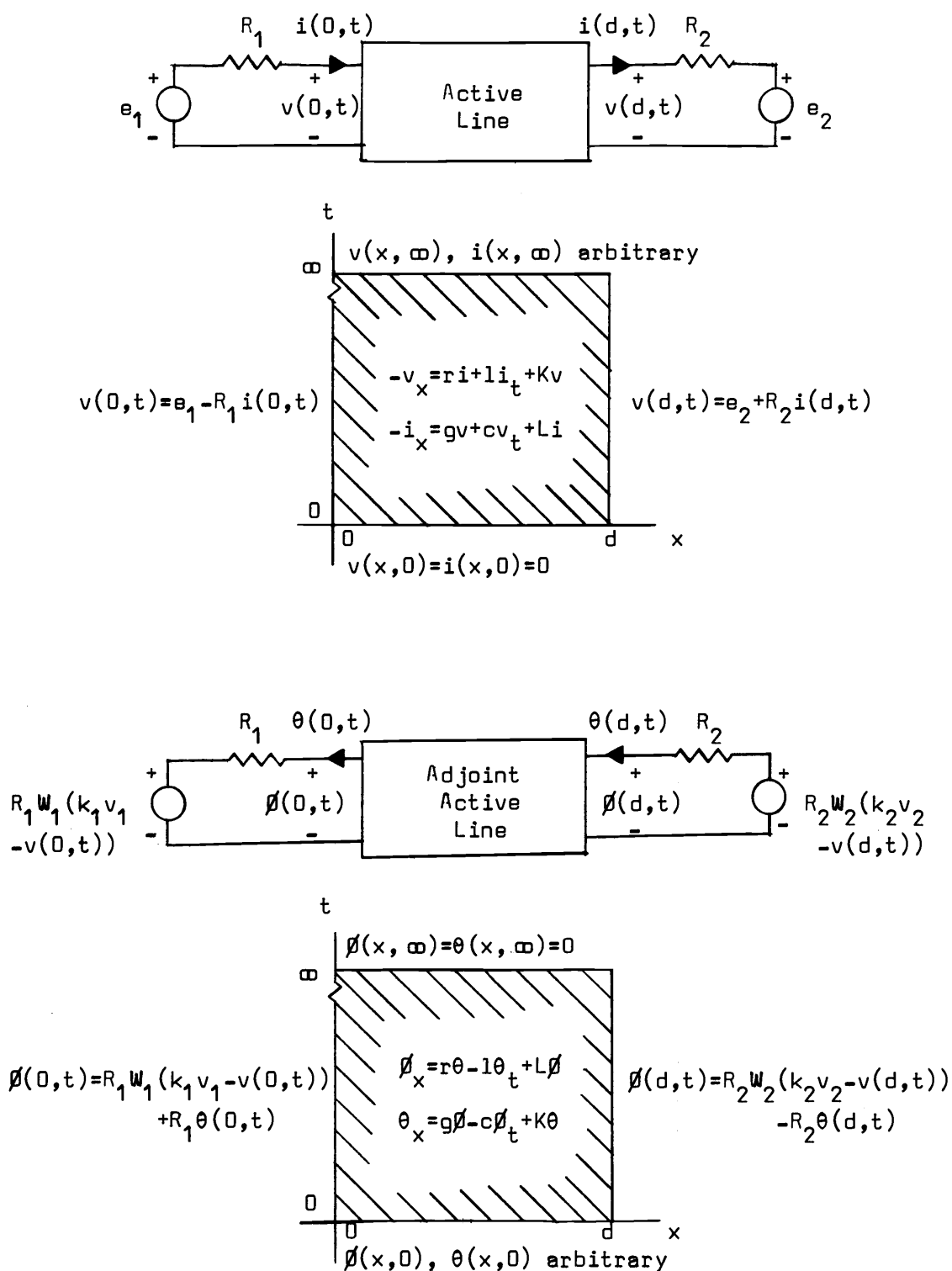


Fig. 48. Time domain synthesis requires time domain solution of the original line and the adjoint line shown. Their constraints are labelled on the (x,t) -plane.

$$\delta E = \int_0^d \int_0^{\infty} \begin{bmatrix} \theta_i \\ \phi_v \\ \theta_{t_i} \\ \phi_{t_v} \\ \theta_v \\ \phi_i \end{bmatrix} dt \begin{bmatrix} \delta r(x) \\ \delta g(x) \\ \delta l(x) \\ \delta c(x) \\ \delta K(x) \\ \delta L(x) \end{bmatrix}^T dx \quad (5.68)$$

Again forming the local gradient to alter parameter values in the direction of steepest descent to reduce the error, the iteration parameter matrix becomes

$$\begin{bmatrix} r_{n+1}(x) \\ g_{n+1}(x) \\ l_{n+1}(x) \\ c_{n+1}(x) \\ K_{n+1}(x) \\ L_{n+1}(x) \end{bmatrix} = \begin{bmatrix} r_n(x) \\ g_n(x) \\ l_n(x) \\ c_n(x) \\ K_n(x) \\ L_n(x) \end{bmatrix} - \int_0^{\infty} \begin{bmatrix} a_n^r \\ a_n^g \\ a_n^l \\ a_n^c \\ a_n^K \\ a_n^L \end{bmatrix} dt \begin{bmatrix} \theta_n(x,t) i_n(x,t) \\ \phi_n(x,t) v_n(x,t) \\ -\theta_{t_n}(x,t) i(x,t) \\ -\phi_{t_n}(x,t) v(x,t) \\ \theta_n(x,t) v_n(x,t) \\ \phi_n(x,t) i_n(x,t) \end{bmatrix}^T \quad (5.69)$$

for all x in D^t . If parameter bounds are exceeded, the appropriate bound in eq. 5.54 is chosen for the parameter value. It is interesting to note that the first four entries are identical to those of eq. 5.32 for type 1-3 active lines.

The basic flow chart for the synthesis procedure is identical to that for type 1-3 active lines (Fig. 46).

Frequency Domain Synthesis—Type 2-4 Active Lines

The frequency domain synthesis using phasor quantities follows that in the time domain. The active line equations are

$$-V_x = (r+j\omega l)I + KV \quad (5.70)$$

$$-I_x = (g+j\omega c)V + LI \quad (5.71)$$

for (x, ω) in D^W , with port conditions

$$E_1(\omega) = V(0, \omega) + Z_1(\omega)I(0, \omega) \quad (5.72)$$

$$E_2(\omega) = V(d, \omega) - Z_2(\omega)I(d, \omega) \quad (5.73)$$

The elements are bounded as before (eq. 5.54). The frequency invariance of the parameters is explicitly constrained as

$$r_w = g_w = l_w = c_w = K_w = L_w = 0 \quad (5.74)$$

Carrying out the minimization procedure leads to the first variation of the augmented error integral as

$$\begin{aligned} \delta E = & \int_0^d \int_{-\infty}^{\infty} \left(\delta v(x, \omega) \left[-\theta_x + \theta K + (g - j\omega c)\theta \right] + \delta I(x, \omega) \left[-\theta_x + \theta L + (r - j\omega l)\theta \right] \right. \\ & + \delta r(x) \left[\theta I - \lambda^r_w \right] + \delta g(x) \left[\theta V - \lambda^g_w \right] + \delta l(x) \left[-j\omega l \theta I - \lambda^l_w \right] \\ & + \delta c(x) \left[-j\omega c \theta V - \lambda^c_w \right] + \delta K(x) \left[\theta V - \lambda^K_w \right] + \delta L(x) \left[\theta I - \lambda^L_w \right] \Big|_{d\omega dx} \\ & + \int_{-\infty}^{\infty} \left(\delta V(d, \omega) \left[-W_2(k_2 V_2 - V(d, \omega)) + \theta(d, \omega) \right] + \delta I(d, \omega) \theta(d, \omega) \right) d\omega \\ & + \int_{-\infty}^{\infty} \left(\delta V(0, \omega) \left[-W_1(k_1 V_1 - V(0, \omega)) - \theta(0, \omega) \right] - \delta I(0, \omega) \theta(0, \omega) \right) d\omega \\ & + \int_0^d \left(\delta r(x) \lambda^r(x, \omega) + \delta g(x) \lambda^g(x, \omega) + \delta K(x) \lambda^K(x, \omega) \right. \\ & + \delta L(x) \lambda^L(x, \omega) + \delta l(x) \lambda^l(x, \omega) + \delta c(x) \lambda^c(x, \omega) \Big) dx \\ & - \int_0^d \left(\text{same as the above integral changing } \omega \text{ to } -\omega \right) dx \quad (5.75) \end{aligned}$$

Thus, the adjoint line equations are

$$-\theta_x + (r - j\omega l)\theta + L\theta = 0 \quad (5.76)$$

$$-\theta_x + (g - j\omega c)\theta + K\theta = 0 \quad (5.77)$$

for (x,w) in D^w , with boundary conditions

$$w_1 [k_1 V_1 - V(0,w)] + \theta(0,w) - \phi(0,w)/Z_1(w) = 0 \quad (5.78)$$

$$w_2 [k_2 V_2 - V(d,w)] - \theta(d,w) - \phi(d,w)/Z_2(w) = 0 \quad (5.79)$$

These conditions are summarized in Fig. 49. With the change in sign of x and w , the equations are analogous.

The parameter optimization criteria follows directly as,¹⁵

$$\int_{-\infty}^{\infty} \begin{bmatrix} \theta I \\ \phi V \\ -jw\theta I \\ -jw\phi V \\ \theta V \\ \phi I \end{bmatrix} dt = \begin{cases} < 0, \underline{P}(x) = P_{\max} \\ 0, P_{\min} \leq \underline{P}(x) \leq P_{\max} \\ > 0, \underline{P}(x) = P_{\min} \end{cases} \quad (5.80)$$

The flow graph of the synthesis procedure is the same as before except that frequency domain quantities replace time domain quantities.

The reiteration parameter matrix is

$$\begin{bmatrix} r_{n+1}(x) \\ g_{n+1}(x) \\ l_{n+1}(x) \\ c_{n+1}(x) \\ K_{n+1}(x) \\ L_{n+1}(x) \end{bmatrix} = \begin{bmatrix} r_n(x) \\ g_n(x) \\ l_n(x) \\ c_n(x) \\ K_n(x) \\ L_n(x) \end{bmatrix} - \begin{bmatrix} a_n^r \\ a_n^g \\ a_n^l \\ a_n^c \\ a_n^K \\ a_n^L \end{bmatrix} \int_{-\infty}^{\infty} \begin{bmatrix} \theta_n(x,w) I_n(x,w) \\ \phi_n(x,w) V_n(x,w) \\ -jw\theta_n(x,w) I_n(x,w) \\ -jw\phi_n(x,w) V_n(x,w) \\ \theta_n(x,w) V_n(x,w) \\ \phi_n(x,w) I_n(x,w) \end{bmatrix} dw \quad (5.81)$$

Variational Synthesis in Retrospect

Use of variational calculus has resulted in a direct and general synthesis procedure readily implemented by digital computers. It may

¹⁵The same optimum condition results from these equations consistent with the previous result.

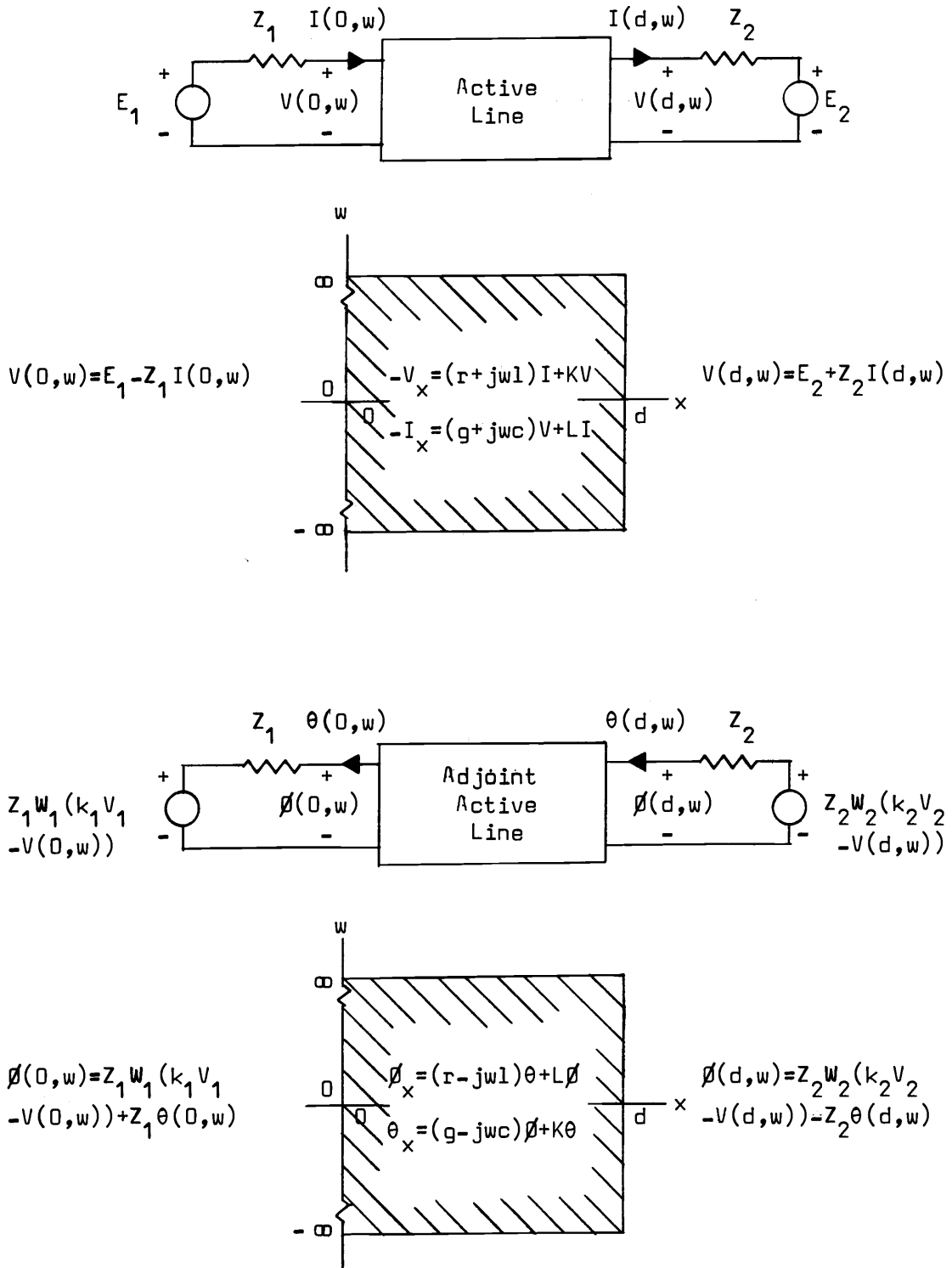


Fig. 49. Frequency domain synthesis requires frequency domain solution of the original active line and the adjoint line shown. Their constraints are labelled on the (x, ω) -plane.

well be that hybrid computers can carry out the necessary calculations with greater efficiency without loss of accuracy. An efficient general active line analysis program is required to solve for parameter generating functions v , i , θ , and β .

The necessary condition that the first variation of the error functional $\delta E \geq 0$ for a local minimum yielded the parameter generating expressions. The condition that the second variation $\delta^2 E > 0$ to insure a local minimum be attained was not employed. Likewise we tacitly assumed that the local minimum was also the global minimum of the error functional.

The analysis and synthesis of active lines has been fully developed and presented. In the next and concluding chapter, possible realizations for active transmission lines are proposed.

VI. REALIZATIONS OF ACTIVE TRANSMISSION LINES

Summary

The preceding chapter presented a synthesis method for general active transmission lines. Obviously such lines require fabrication techniques in which the various parameters can be independently controlled and distributed. This requirement is difficult to satisfy even today with passive rcg thin-film circuitry. This, however, does not pose any serious limitation to the synthesis technique since the original equations may be amended with appropriate additional constraints and an analogous procedure tabulated.

The fundamental problem at this time is the inability to distribute dependent or controlled sources along a passive transmission line. This is not the case for multiple lines. For example, two transmission lines actively (and passively) coupled appeared in Chapters 1 and 2. The simplified model of the traveling-wave transistor consisted of two delay lines, one unilaterally actively coupled to the other via g_m , the transconductance/unit length (see Fig. 10). Passive coupling complicated the analysis as noted by Jutzi (12). However this more general model represents many of the classical coupled mode devices such as the traveling-wave tube, etc. Semiconductor photodetectors and solid-state traveling-wave amplifiers also have coupled line models (see Fig. 15). Kawamura and Morishita considered a similar problem involving semiconductor bulk effects (14). Various higher order modes complicate the model as noted by Copeland (4).

These studies exemplify much of the research currently underway

in solid-state electronics. Through this research, new semiconductor effects leading to active materials are being discovered. Thin-film technology is also making rapid strides in miniaturization of existing devices and realization of new thin-film devices. It may well be that advances in the solid-state and thin-film areas will result in the ability to produce active transmission lines in the not too distant future.

At the present time, artificial active lines must be relied upon. In the following two sections, the topology and characteristics that the iterative two-port must possess are briefly outlined.

Artificial Type 1-3 Active Lines

The lumped network approximating a type 1-3 active line of length D is shown in Fig. 50. It is anticipated that an n -fold iterative structure made up of these two-ports will have low-pass characteristics approximating those of an active line of length $d = nD$. The lumped approximation of uniform active lines have parameters which are constant with section number, while the approximation network of nonuniform lines have parameters which depend upon section number.

Each controlled source of the approximation network of Fig. 50

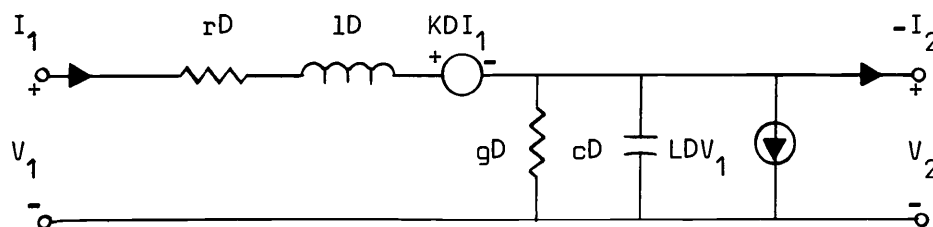


Fig. 50. Lumped approximation of the type 1-3 active line of length D .

must be realized by a two-port network. The two-port whose voltage output is controlled by input current is denoted as the KDI_1 voltage source, and the two-port whose current output is controlled by input voltage as the LDV_1 current source. Then, the approximation network can be realized by interconnecting the voltage source and current source two-ports as shown in Figs. 51 and 52. These realizations

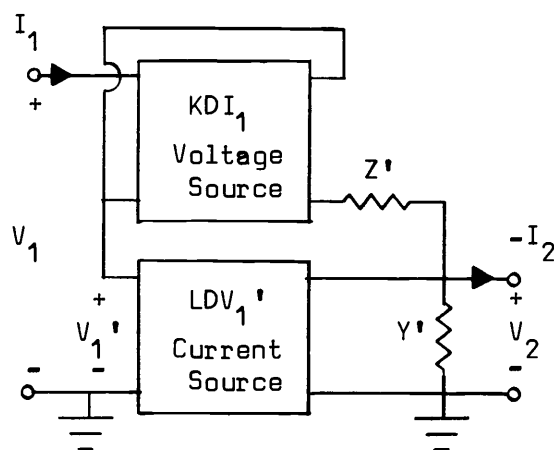


Fig. 51. First realization of the artificial type 1-3 active line.

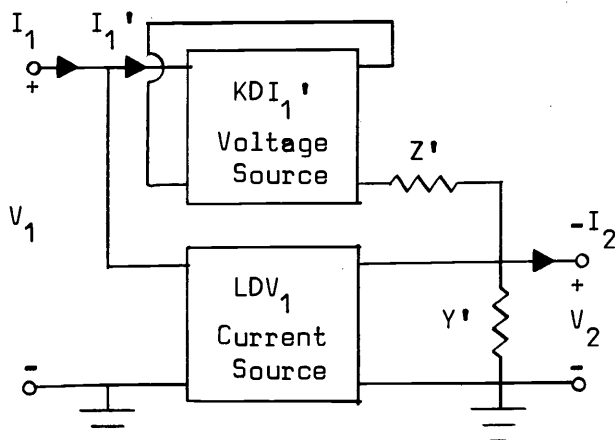


Fig. 52. Second realization of the artificial type 1-3 active line.

differ in that the first has the LDV_1 current source dependent on V_1' rather than V_1 (due to the voltage drop across the input to the KDI_1 voltage source); the second has the KDI_1 voltage source dependent on I_1' rather than I_1 (due to the current input into the LDV_1 current source). It is now shown that the latter realization leads to more flexible design requirements. It will be seen that impedance $Z' = (rD)' + s(lD)'$ and admittance $Y' = (gD)' + s(cD)'$ combine with two-port parameters to form impedance $Z = rD + s lD$ and admittance $Y = gD + s cD$, respectively.

The first realization has the equivalent circuit shown in Fig. 53, where the KDI_1 voltage source two-port is represented by its z equivalent circuit and the LDV_1' current source two-port by its y equivalent circuit. Clearly V_1 and V_1' differ by the voltage across the input to the KDI_1 voltage source two-port. From one point of view, this equivalent circuit consists of two cascaded networks which have series voltage sources controlled by series currents and shunt current sources controlled by shunt voltages. Thus, each section with appropriate parameters appears to realize the type 1-3 active line of Fig. 50. But the first section has sources controlled by quantities to its right rather than its left which is unsuitable. z_{12} and y_{12} are therefore

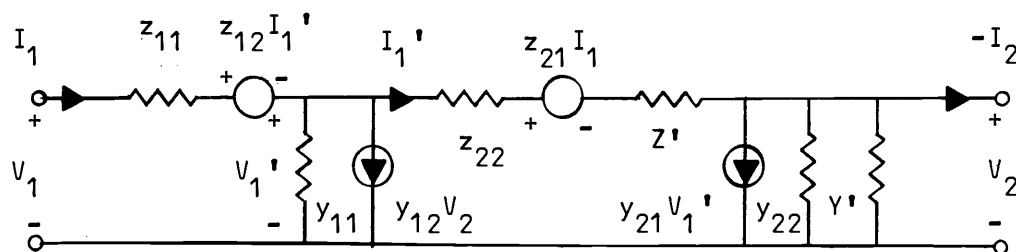


Fig. 53. Two-port equivalent of the first realization.

set equal to zero. Thus, to realize the type 1-3 active line with this topology, the two-port parameters must equal:

$$\begin{aligned}
 z_{11} &= y_{11} = 0 \\
 z_{12} &= y_{12} = 0 \\
 Z &= z_{22} + Z' \\
 Y &= y_{22} + Y' \\
 KD &= z_{21} \\
 LD &= y_{21}
 \end{aligned}
 \tag{6.1}$$

Again, the z parameters characterize the KDI_1' voltage source two-port and the y parameters characterize the LDV_1' current source two-port.

The type 1-3 active line may also be formed using the realization shown in Fig. 52. Its equivalent circuit is shown in Fig. 54 where as before, the KDI_1' voltage source two-port is represented by its z equivalent circuit and the LDV_1' current source two-port by its y equivalent circuit. Clearly I_1 and I_1' differ by the current entering the LDV_1' current source two-port. Since the $y_{12}V_2$ current source is dependent upon a voltage to its right, y_{12} is set equal to zero. Thus, we let

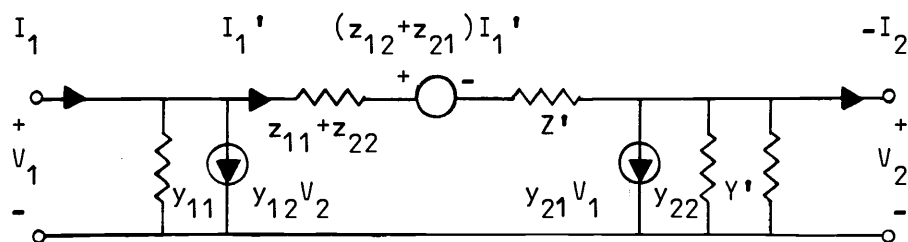


Fig. 54. Two-port equivalent of the second realization.

$$\begin{aligned}
 y_{11} &= 0 \\
 y_{12} &= 0 \\
 Z &= z_{11} + z_{22} + Z' \\
 Y &= y_{22} + Y' \\
 KD &= z_{12} + z_{21} \\
 LD &= y_{21}
 \end{aligned}
 \tag{6.2}$$

This set of design equations is more flexible than those of eq. 6.1 since z_{11} and z_{12} can be nonzero. It should be noted here that when the approximation networks are cascaded and viewed as cascaded L sections, adjacent admittances combine so $Y = y_{11} + y_{22} + Y'$. Therefore, y_{11} can be nonzero in Figs. 53 and 54, with corresponding y_{11} and Y changes in eqs. 6.1 and 6.2.

Thus, the problem of constructing an artificial type 1-3 active line consisting of cascaded sections shown in Fig. 50 becomes one of cascading the interconnected two-ports shown in Fig. 52 which have the respective properties listed in eq. 6.2.

Artificial Type 2-4 Active Lines

The lumped network approximating a type 2-4 active line of length D is shown in Fig. 55. Again it is expected that an n -fold iterative

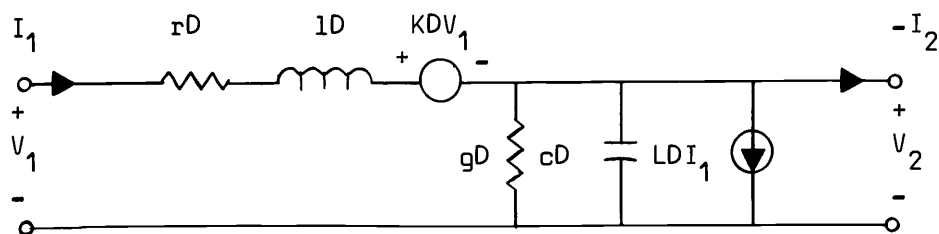


Fig. 55. Lumped approximation of the type 2-4 active line of length D .

structure made up of these two-ports will have low-pass characteristics that approximate those of an active line of length $d = nD$.

As before, each controlled source of Fig. 55 is realized by a two-port network. The two-port whose output voltage is controlled by the input voltage is denoted as the KDV_1 voltage source, and the two-port whose output current is controlled by the input current as the LDI_1 current source. Either of the two realizations of Figs. 56 and 57 may

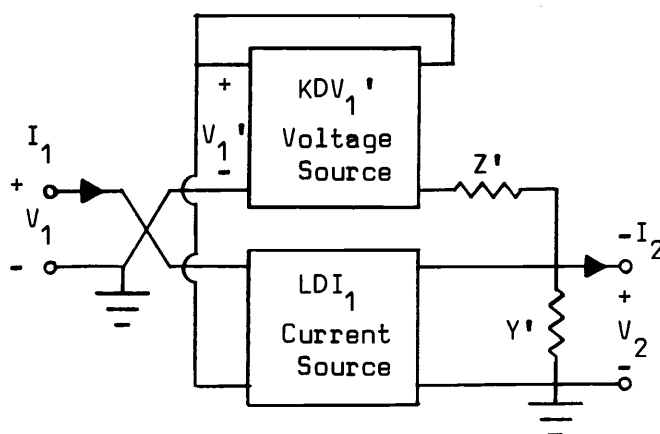


Fig. 56. First realization of the artificial type 2-4 active line.

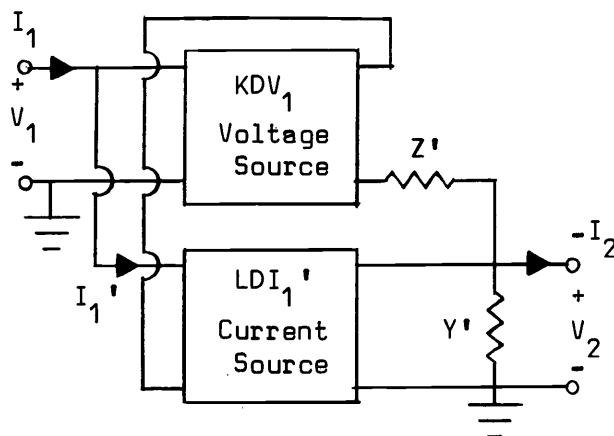


Fig. 57. Second realization of the artificial type 2-4 active line.

be used to realize the approximation network. Impedances Z and Z' admittances Y and Y' were previously defined. The voltages V_1 and V_1' and currents I_1 and I_1' differ in the same manner as before. The latter realization leads to more flexible design requirements as will now be shown.

The first realization has the equivalent circuit shown in Fig. 58, where the KDV_1' voltage source two-port is represented by its g equivalent circuit and the LDI_1 current source two-port by its h equivalent circuit. In the first half-section of the network, source values are dependent on voltage and current to their right which is unsuitable. Thus, this half-section is eliminated and the artificial type 2-4 active line realized by setting

$$\begin{aligned}
 h_{11} &= g_{11} = 0 \\
 h_{12} &= g_{12} = 0 \\
 Z &= g_{22} + Z' \\
 Y &= h_{22} + Y' \\
 KD &= g_{21} \\
 LD &= h_{21}
 \end{aligned}
 \tag{6.3}$$

Again, the g parameters characterize the KDV_1' voltage source two-port

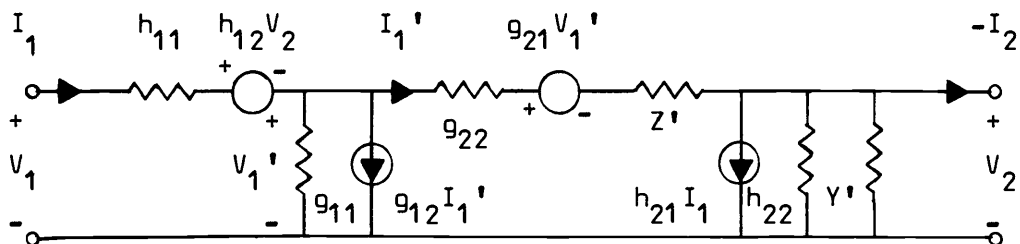


Fig. 58. Two-port equivalent of the first realization.

and the h parameters characterize the LDI_1' current source two-port.

The realization in Fig. 57 may also be used. Its equivalent circuit is shown in Fig. 59. As before, the KDV_1 voltage source two-port is represented by its g equivalent circuit and the LDI_1' current source two-port by its h equivalent circuit. The sources in the first half-section of the network have values depending on voltages and currents to their right which is unacceptable. g_{12} and h_{12} are therefore set equal to zero. The artificial type 2-4 active line is realized by adjusting the parameters as:

$$\begin{aligned}
 g_{11} &= 0 \\
 g_{12} = h_{21} &= 0 \\
 Z &= h_{11} + g_{22} + Z' \\
 Y &= h_{22} + Y' \\
 KD &= g_{21} \\
 LD &= h_{21}
 \end{aligned}
 \tag{6.4}$$

Comparing these values with those of eq. 6.3, the latter realization is more flexible since the input impedance h_{11} may be nonzero. It should again be noted that if cascaded L sections are considered, then g_{11} can be nonzero in which case $Y = g_{11} + h_{22} + Y'$.

Therefore, the problem of constructing an artificial type 2-4

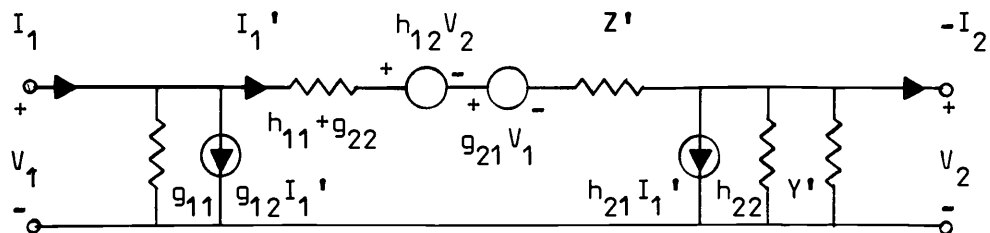


Fig. 59. Two-port equivalent of the second realization.

active line consisting of cascaded sections shown in Fig. 55 becomes one of cascading the interconnected two-ports shown in Fig. 57 which have the properties listed in eq. 6.4.

In the past, artificial distributed amplifiers were built with rather large discrete components. Parasitic elements limited high frequency operation. Today with the advent of thin-film and integrated circuit technology, iterated structures of minute size are manufactured with great precision. Accompanying size reduction is a corresponding decrease in parasitic element values. If the gain blocks of each stage are of sufficient magnitude, higher frequency operation appears possible. Redundancy may be beneficial to insure characteristics. However, the failure of several controlled voltage and current sources along the artificial active line composed of many sections should not significantly impair its performance.

Conclusion

In the preceding chapters, the active transmission line has been fully investigated. The active line was viewed in historical perspective and its current usefulness discussed. It was seen to be a useful device and to model many physical processes. The active line was fully analyzed and a general synthesis scheme was presented. Current investigations in high frequency devices were noted and the artificial active line was reviewed.

In concluding it should be pointed out that although this thesis has been concerned with the class of active distributed networks having an active transmission line equivalent, the considerations are readily

extendable to networks having other differential length models. Thus in a more general context, this thesis is concerned with developing methods for analyzing and synthesizing active distributed networks.

BIBLIOGRAPHY

1. Beam, W.R. Electronics of solids. New York, McGraw-Hill, 1965. 633 p.
2. Bolza, Oskar. Lectures on the calculus of variations. New York, Dover, 1961. 271 p.
3. Chrystal, G. Algebra. Part 1. London, Adam and Charles Black, 1886. 571 p.
4. Copeland, J.A. A new mode of operation for bulk negative resistance oscillators. Proceedings of the IEEE 54(10):1479-1480. 1966.
5. Courant, R. and D. Hilbert. Methods of mathematical physics. New York, Interscience, 1953. 2 vols.
6. Elmore, W.C. The transient response of damped linear networks with particular regard to wideband amplifiers. Journal of Applied Physics 19(1):55-63. 1948.
7. Elsgolc, L.E. Calculus of variations. Reading, Addison-Wesley, 1962. 178 p.
8. Ettenberg, M. and J. Nadan. Gain in solid-state traveling-wave amplifiers. Proceedings of the IEEE 56(4):741-742. 1968.
9. Ghauri, M.S. Principles and design of linear active circuits. New York, McGraw-Hill, 1965. 621 p.
10. Golembeski, John et al. A class of minimum sensitivity amplifiers. IEEE Transactions on Circuit Theory 14(3):69-74. 1967.
11. Gough, K.J. and R.N. Gould. Nonuniform rc and lossless transmission lines. IEEE Transactions on Circuit Theory 13(12):453-455. 1966.
12. Jutzi, W. Uniform distributed amplifier analysis with fast and slow waves. Proceedings of the IEEE 56(1):66-67. 1968.
13. Kamke, E. Differentialgleichungen, Lösungsmethoden und Lösungen. Vol. 1. J.W. Edwards, Ann Arbor, 1945. 642 p.
14. Kawamura, M. and S. Morishita. A new negative resistance of semiconductor bulk. Proceedings of the IEEE 56(7):1213-1215. 1968.
15. Kelly, J. and M.S. Ghauri. Network properties of distributed rc networks with arbitrary geometric shapes. New York, 1965. 172 p. (New York University. Dept. of Electrical Engineering. Technical Report 400-107)

16. Kelly, J., M.S. Ghausi and J.H. Mulligan, Jr. On the analysis of lumped-distributed systems. In: Circuit theory; information theory; basic sciences; electrostatic processes. IEEE International Convention Record Part 7. New York, Institute of Electrical and Electronic Engineers, 1966. p. 308-318.
17. Kohn, G. and R. Landauer. Distributed field-effect amplifiers. Proceedings of the IEEE 56(6):1136-1137. 1968.
18. Lindquist, C.S. A mathematical method of evaluating the reliability of electronic equipment. Master's thesis. Corvallis, Oregon State University, 1964. 84 numb. leaves.
19. _____ Transmission line response to independent distributed sources. Proceedings of the IEEE 56(8):1353-1354. 1968.
20. _____ Uniform transmission line response to independent distributed sources. Proceedings of the IEEE 56(10):1740-1741. 1968.
21. Linvill, J.G. and J.F. Gibbons. Transistors and active circuits. McGraw-Hill, 1961. 515 p.
22. McIver, G.W. A traveling-wave transistor. Proceedings of the IEEE 53(11):1747-1748. 1965.
23. Mooney, D.A. Introduction to thermodynamics and heat transfer. Englewood Cliffs, Prentice-Hall, 1953. 429 p.
24. Morse, P.M. and H. Feshbach. Methods of theoretical physics. New York, McGraw-Hill, 1953. 2 vols.
25. Pederson, D.O. and D.D. Thornton. Analysis of transistor distributed amplifiers. Berkeley, 1960. (University of California. Electronics Research Laboratory. Issue 312) (Cited in: Ghausi, M.S. Principles and design of linear active circuits. New York, McGraw-Hill, 1965. p. 349)
26. Roberts, G.E. and H. Kaufman. Table of Laplace transforms. Philadelphia, W.B. Saunders, 1966. 367 p.
27. Rohrer, R.A. Distributed network synthesis: a variational approach. Ithaca, 1965. 80 p. (Cornell University. Electrical Engineering Research Laboratory. Research Report EERL 45)
28. _____ Synthesis of arbitrarily tapered lossy transmission lines. In: Proceedings of the Symposium on Generalized Networks, Brooklyn, 1966. Brooklyn, Polytechnic Institute, 1966. p. 115-135.

29. Sneddon, I.N. Fourier transforms. New York, McGraw-Hill, 1951. 542 p.
30. Valley, G.E., Jr. and H. Wallman. Vacuum tube amplifiers. New York, McGraw-Hill, 1948. 743 p.
31. Weidner, R.T. and R.L. Sells. Elementary modern physics. Boston, Allyn and Bacon, 1960. 513 p.
32. Weinberger, H.F. Partial differential equations. New York, Blaisdell, 1965. 446 p.
33. Whittaker, E.T. and G.N. Watson. A course in modern analysis. 4th ed. Cambridge University, 1927. 608 p.
34. Wohlers, W.R. On electromagnetic gain mechanisms in solid-state plasmas. Proceedings of the IEEE 55(7):1230-1231. 1967.